

**RESEARCH
GRANTS**

STUDIES ON ICE FOG

U. S. ENVIRONMENTAL PROTECTION AGENCY

The APTD (Air Pollution Technical Data) series of reports is issued to report technical data of interest to a limited readership. Copies of APTD reports are available free of charge - as supplies permit - from the Office of Technical Information and Publications, Environmental Protection Agency, Research Triangle Park, North Carolina 27711.

This report was furnished to the Environmental Protection Agency by the Geophysical Institute of the University of Alaska in fulfillment of Research Grant No. AP-00449. The contents of the report are reproduced herein as-received from the contractor. The opinions, findings, and conclusions expressed are those of the author and not necessarily those of the Environmental Protection Agency.

Office of Air Programs Publication No. APTD-0626

GEOPHYSICAL INSTITUTE

of the

UNIVERSITY OF ALASKA

STUDIES ON ICE FOG

by

Takeshi Ohtake

Final Report

AP-00449

June 1970

This document has been approved
for public release and sale; its
distribution is unlimited.

Prepared for
National Center for Air Pollution Control
Public Health Service
Department of Health, Education and Welfare

Principal Investigator:

Takeshi Ohtake
Takeshi Ohtake *by Jimmy Kano*

Approved by:

K. B. Mather
Keith B. Mather
Director

STUDIES ON ICE FOG

Takeshi Ohtake
Geophysical Institute
of the
University of Alaska

ENVIRONMENTAL PROTECTION AGENCY
Research Triangle Park, North Carolina
July 1971

ABSTRACT

In order to clarify the mechanism of ice-fog formation, various atmospheric factors in ice fogs such as size and concentration of ice-fog crystals, condensation nuclei and ice nuclei, amount of water vapor, temperature profile near the sources of ice fog, etc. were measured.

Nuclei of the ice-fog crystals were studied by use of an electron microscope and electron-diffraction. The examination showed that most nuclei of ice-fog crystals were combustion by-products and many individual crystals collected near open water did not have a nucleus, especially at temperatures below -40°C . Dust particles or particles from air pollution are not essential for formation of ice fog; they merely stimulate freezing of water droplets at higher temperatures than the spontaneous freezing temperature. The essential factor is to first form many water droplets in the atmosphere through condensation of water vapor.

Based on these measurements and calculations of time required for water droplets to freeze, a physical mechanism of ice fog formation is proposed as follows: 1) Water vapor coming from open water which is exposed to a low temperature atmosphere, plus water vapor from various exhausts of combustion processes is released into the almost ice-saturated atmosphere and condenses into water droplets, 2) The droplets freeze very shortly after their formation and before entirely evaporating, 3) Such ice particles do not evaporate or grow much and stay in the atmosphere with insignificant fall out, and 4) These processes operate more efficiently in colder environments, which make ice fog more serious at lower temperatures.

Measurements of humidity and evaporation rates from open water at low air temperatures are described, as are some phenomena relating to ice crystals found in ice fog. The types of meteorological situations which are likely to cause ice fog, visual range in ice fog, and the electric properties and theoretical studies of size distribution of ice fog crystals are also described.

TABLE OF CONTENTS

	Page
ABSTRACT	i
PREFACE AND ACKNOWLEDGEMENTS	vii
LIST OF PUBLICATIONS	ix
LIST OF TABLES	x
LIST OF FIGURES	xi
1. INTRODUCTION	1
2. MEASUREMENTS OF ICE-FOG CRYSTALS	7
3. MEASUREMENTS OF CONDENSATION NUCLEI	20
4. MEASUREMENT OF ICE NUCLEI	25
5. RELATIONSHIP BETWEEN CONDENSATION AND ICE NUCLEI AND ICE-FOG CRYSTALS IN THEIR CONCENTRATIONS	32
6. ELECTRON MICROSCOPE STUDIES OF STEAM-FOG AND ICE-FOG CRYSTALS AND THEIR NUCLEI	34
a. Smoke Samples	35
b. Steam-Fog Nuclei	37
c. Ice-Fog Crystals and Their Nuclei	37
1. Method of Making Specimens	37
2. Size and Shape of Ice-Fog Crystals	41
3. Sizes and Composition of Ice-Fog Nuclei and Electric Conductivity of Melted Ice-Fog Crystals	41
4. Position of Nuclei in Ice-Fog Crystals	50
5. Spicules on Ice Fog Crystals	53
6. Sintering of Ice-Fog Crystals and Structure of Ice-Fog Crystals	55
d. Inactive Nuclei in Ice Fog	61

TABLE OF CONTENTS
(Cont'd)

	Page
7. OPTICAL MICROSCOPE STUDIES OF ICE-FOG CRYSTALS	62
A. THE EFFECT OF TEMPERATURE AND HUMIDITY ON ICE-FOG CRYSTALS	62
1. Sampling Method for Ice-Fog Crystals	62
2. Method of Analysis	63
a. Determination of the Diameters	63
b. Classification of the Shapes of Ice-Fog Crystals	63
3. Results and Discussion	64
a. Mean Diameters of Ice-Fog Crystals	64
b. Size Distribution and Percentage Distribution of Types of Ice-Fog Crystals	72
c. Numbers of Precipitated Ice-Fog Crystals	72
d. Precipitation Rate and Solid Water Content of Ice-Fog Crystals	78
e. The Effect of Ambient Humidity on Ice-Fog Crystals	83
f. Ice-Fog Crystals from an Unpolluted Area with a Moisture Source	85
B. UNUSUAL CRYSTALS IN ICE FOG (POLYHEDRAL ICE CRYSTALS)	87
8. MECHANISM OF ICE FOG FORMATION	97
a. Measurements of Humidity under Low Temperature Conditions	98
i. Data from Hair Hygrometers	99
ii. Absolute Method of Humidity Measurement	102
b. Visual Observations of Ice-Fog Sources	109

TABLE OF CONTENTS
(Cont'd)

	Page
c. Measurement of Evaporation of Water from the River or a Pan and the Formation of Water Droplets from the Vapor	117
d. Temperature Measurement above Water Surface	120
e. Derived Supersaturation Degrees, Compared with Supersaturations Required to Activate Condensation Nuclei	122
f. Time Required for Droplets to Freeze	123
1. Conductive Cooling	123
2. Radiation Cooling	124
g. Theoretical Study of the Size Distribution of Ice-Fog Crystals	129
h. Effects of Lower Air Temperature	130
i. Conclusions on the Mechanism of Ice-Fog Formation	132
9. SYNOPTIC METEOROLOGICAL STUDIES OF ICE FOG	135
a. Winter Pressure Systems and Ice Fog in Fairbanks, Alaska	135
b. Analysis of Air Mass Trajectories	136
c. Practical Ice Fog Prediction	137
10. VISUAL RANGE IN ICE FOG	139
11. ELECTRIC PROPERTIES OF ICE-FOG CRYSTALS	140
a. Experiments with Ice Fog Crystals in Electric Fields	141
i. Non-Uniform Electric Field	141
ii. Uniform Electric Field	144
b. Discussion	147
REFERENCES	154

TABLE OF CONTENTS
(Cont'd)

	Page
APPENDIX-THEORETICAL STUDY OF ICE FOG SIZE DISTRIBUTION	159
ABSTRACT	160
1. INTRODUCTION	161
2. THEORETICAL CONSIDERATIONS	163
3. COMPARISON WITH EXPERIMENT	169
4. CONCLUSION	174
ACKNOWLEDGEMENTS	176
REFERENCES	177

PREFACE AND ACKNOWLEDGEMENTS

In response to the rapidly increasing severity of the problem presented by ice fog in Fairbanks due to the recent increase in city activities and air traffic, the present research on ice-fog problems has been supported by the National Center for Air Pollution Control, Public Health Service, Department of Health, Education, and Welfare under Grant AP 00449, National Science Foundation, Grant GA-19475 and initially by State of Alaska funds. The project was also supported in part by the Department of Interior, Water Resources Research funds.

This report combines research done by the following persons:

Takeshi Ohtake: Principal Investigator

Sue Ann Bowling

Paul J. Huffman

George F. Lindholm

Teizi Henmi

Rudolf Suchanek

Carl S. Benson Consultant

Yosio Suzuki Consultant

Yoshiaki Toda Consultant

Gaishi Onishi Consultant

The researchers are indebted to Dr. Keith B. Mather and many staff members of the Geophysical Institute at the University of Alaska for their encouragement, to the above consultants and to Drs. Kenji Isono and Makoto Komabayasi of Nagoya University, Dr. Thomas E. Osterkamp of the

University of Alaska, Dr. Norihiko Fukuta of the University of Denver and Dr. Myron L. Corrin of the Colorado State University for their valuable discussions and comments, and to Messrs. Hiroshi Haramura and Akio Iwasaki who were working at the University of Alaska for their assistance in field work. The author wishes to thank Miss Sue Ann Bowling of the Geophysical Institute, University of Alaska for her assistance in preparing the manuscript. Also the author wishes to thank the management of the Municipal Utilities System of Fairbanks and the Industrial Air Products Company, Fairbanks, Alaska for providing locations and electric power for our instrumentation, and the meteorological staff at Eielson Air Force Base and the cooperative agencies at the Fairbanks International Airport, especially the Fairbanks Weather Bureau and Pan American World Airways, for providing various meteorological data as well as locations and electric power for taking micro-photographs. The Naval Arctic Research Laboratory, Pt. Barrow, Alaska, also provided support for the collection of data on condensation nuclei at Pt. Barrow. The researchers thank the Institute of Arctic Biology at the University of Alaska for giving us an opportunity to use their cold environmental room. Finally, we are grateful to the National Geographic Society for permission to reproduce Figure 61 from their book "Alaska".

LIST OF PUBLICATIONS RESULTING FROM PROJECT
ICE FOG RESEARCH SUPPORTED BY GRANT AP00449

- Ohtake T. : Alaskan Ice Fog, Physics of Snow and Ice, Proc. Intern'l Conf. Low Temp. Sci., 1966, Sapporo, Vol. 1, 105-118. (1967).
- Bowling S. : A Study of Synoptic-scale Meteorological Features Associated with the Occurrence of Ice Fog in Fairbanks, Alaska. University of Alaska, Master's Thesis, 141pp. (1967).
- Huffman P.J. : Size Distribution of Ice Fog Particles, University of Alaska, Master's Thesis, 93pp. (1968).
- Ohtake T. : Freezing of Water Droplets and Ice Fog Phenomena, Proc. Intern'l Conf. Cloud Physics, Aug., 1968, Toronto, (1968).
- Bowling S., T. Ohtake, and C.S. Benson : Winter Pressure Systems and Ice Fog in Fairbanks, Alaska, Journal of Applied Meteorology, Vol. 7, 961-968. (1968).
- Henmi T. : Some Physical Phenomena Associated with Ice Fog, University of Alaska, Master's Thesis, 90pp. (1969).
- Ohtake T. and P.J. Huffman : Visual Range in Ice Fog, Journal of Applied Meteorology, Vol. 8, 499-501. (1969).
- Ohtake T. and R. Suchanek : Electric Properties of Ice Fog Crystals, Journal of Applied Meteorology, Vol. 9, 289-293. (1970).
- Ohtake T. : Unusual Crystals in Ice Fog, Journal of Atmospheric Sciences, Vol. 27, 509-511. (1970).
- Ohtake T. : Studies on Ice Fog, University of Alaska, Geophys. Inst. Report UAG R-211, 179pp. (1970).
- Huffman P.J. and T. Ohtake : Formation and Growth of Ice Fog Particles at Fairbanks, Alaska, submitted to J.G.R.

LIST OF PUBLICATIONS IN PRESS

- Ohtake T. : Ice Fog and its Nucleation Process, Proceedings of Conf. on Cloud Physics, Ft. Collins, Colo., Aug., 1970.
- Ohtake T. and G. Lindholm : Electron Microscope Study of Ice Fog Crystals, Journal of Glaciology.
- Ohtake T. and T. Henmi : Ice Fog Crystals and Mechanism of their Formation. Journal of Glaciology or Quarterly Journal of the Royal Meteorological Society.

LIST OF TABLES

Tables

1. Mean size, concentration and solid water content vs. temperature at the MUS site.
2. Data of ice-fog crystals in various locations. Data other than the first two data were taken by the precipitation method (replicas). The temperature of stream water at Chena Hot Springs was 35C.
3. Concentration of condensation nuclei in and around the Fairbanks city and far from the city.
4. Average ice nuclei temperature spectrum.
5. Exposure time for vapor method of replication of ice crystals.
6. Percentage of composition of ice fog nuclei determined by electron microscope and electron microdiffraction. At the MUS site IC means ice crystal nuclei and IF means ice fog crystal nuclei.
7. Mean values of precipitation rates and solid water content of ice fog (by precipitation method).
8. Comparison of the data on humidities between the method used here and Assman type hygrometer.
9. Observation of evaporation rate of water from pans in low temperature.
10. Radiative temperature of various objects.

LIST OF FIGURES

Figures

1. The solid circles indicate the locations where counts of condensation nuclei were made.
2. Map showing locations in the Fairbanks area where data on ice-fog crystal size distributions, nuclei, humidities etc. were obtained and ice crystal samples were collected.
3. Comparison of size distributions of ice-fog crystals obtained simultaneously by two methods at the same location and time.
4. Three stage konimeter used for collecting ice-fog crystals.
5. Microphotographs of ice-fog crystals obtained with the ice-fog crystal sampler represented in Fig. 4.
6. Typical size distribution of ice-fog crystals in downtown Fairbanks, at -36.5°C . Total water content 0.23 mg l^{-1} , solid water content 0.12 mg l^{-1} , visibility 180 m. particle concentration 153 p cm^{-3} , at 1240 AST on 8 December 1968. Peaks A, B and C represent crystals from car exhausts, open water and heating plants (commercial and residential) respectively. Heights of the peaks are different from place to place owing to different moisture and temperature conditions.
7. Size distributions of ice-fog crystals at various locations on 2 January 1969, at temperatures between -47 and -50°C , excepting that of Chena H. S. At Chena Hot Springs, collection was made on 1 January 1969 at a temperature of -45°C . All distributions on this figure used the precipitation method.
- 8a. Concentrations of condensation nuclei at various places in Alaska using different expansion ratios.
- 8b. Concentration of condensation nuclei in terms of percentage of total nuclei to that of nuclei passing through Millipore filters. IF means the observations were made in ice fog.
9. Smoke from burning dry wood.
10. Smoke from heating plant.
11. Auto exhaust (English car MG).
12. Auto exhaust (Ford Falcon).

LIST OF FIGURES
(Cont'd)

13. Steam fog nucleus in fall season. The nucleus is presumed to be a combustion by-product.
14. Steam fog nucleus. The nucleus is identified as a sea salt particle.
15. Construction of sheet mesh for electron microscope examinations of ice-fog crystals.
16. Size distribution of ice-fog crystals examined under the electron microscope.
17. Size distribution of ice-fog nuclei examined under the electron microscope.
18. Ice-fog crystal without nucleus, collected at Chena Hot Springs on 31 December 1968. Temperature was -45C.
19. Ice-fog crystal with many dust particles only inside of the crystal. The crystal was sampled at the MUS site, on 2 January 1969. Temperature was -45C.
20. Ice-fog crystal with carbon black as a nucleus. The crystal was collected near the IAP site on 8 December 1968. The white part at upper right of picture seems to be a kind of spicule formed from the crystal.
21. Spherical ice-fog crystal with very small nucleus off center. The crystal was collected near the IAP site on 21 December 1965. Temperature was -36.4C.
22. Ice-fog crystal and its nucleus sampled at the Fairbanks International Airport on 1 January 1966. The nucleus is presumed to be a combustion by-product. The temperature was -43.2C.
23. A spherical ice-fog crystal with off center nucleus. The nucleus is presumed to be combustion by-product. The sample was taken near the Noyes slough in winter of January 1965. The temperature is unknown.
- 24a. Nuclei of ice-fog crystal. The nuclei were presumed to be combustion by-products, which may have been in the gas phase in temperate weather. Original outline of ice crystal also illustrated.
- 24b. Enlargement of the nuclei of Fig. 24a. The crystal was collected directly onto collodion film at the MUS site on 21 February 1966. The temperature was -32.9C.

LIST OF FIGURES
(Cont'd)

25. Ice-fog crystal with nucleus at center. The nucleus was also presumed to be soot. The crystal was sampled at the MUS site on 23 December 1965.
26. Ice-fog crystal with nucleus at the center. The nucleus was presumed to be a combustion by-product. The sample was taken near the University power plant on 6 January 1966. Temperature was -39.8C and visibility was 200 m.
27. Ice-fog crystal with spicule. The crystal was sampled on 16 January 1968 at the MUS site at a temperature of -38.2C.
28. Ice-fog crystal (replica) with boundaries or creases. The sampling was made at Chena Hot Springs on 31 December 1968 at a temperature of -45C.
29. Ice-fog crystal at Chena Hot Springs. The crystal has a line in the middle and was found on the same specimen mesh as the crystal shown in Fig. 28.
30. Optical microscope picture of ice-fog crystals at Chena Hot Springs. Temperature was -45C.
31. Sketch of two ice-fog crystals under a polarizing microscope. The crystals were collected at the MUS site at a temperature of -37C.
32. Nuclei which were not the ice-fog nuclei in ice fog.
33. Optical microscope picture of the types of ice-fog crystals taken at the MUS site. Temperature was -33.5C. H. P: Hexagonal Plates, Sp. : Sphericals, P.C. : Plain Columns, S. C. : Skeleton columns and Irr. : Irregular crystals.
34. Relationship between mean diameters of total ice-fog crystals and temperatures.
35. Relationship between mean diameters of hexagonal plates and temperatures.
36. Relationship between mean diameters of sphericals and temperatures.

LIST OF FIGURES
(Cont'd)

37. Relationship between mean diameters of plain columns and temperatures.
38. Relationship between mean diameters of skeleton columns and temperatures.
39. Relationship between mean diameters of irregular shaped crystals and temperatures.
40. Mean size distributions of various shaped ice-fog crystals for temperature range -31.0 to -32.9°C .
41. Mean size distributions of ice-fog crystals for temperature range of -35.0 to -36.9°C .
42. Mean size distributions of ice-fog crystals in various shapes for temperature range of -39.0 to -41.0°C .
43. Percentage distribution of the shapes of ice-fog crystals.
44. Numbers of ice-fog crystals precipitated versus ambient air temperatures.
45. Solid water contents and precipitation rates of ice fog.
46. Numbers of ice-fog crystals precipitated versus supersaturations over ice.
47. Ice-fog crystals at Chena Hot Springs, on 31 December 1968.
48. A polyhedral ice crystal found in ice fog at the temperature of -47°C . The crystal was collected at the MUS site on 3 January 1969. Three pictures show the crystal with different focusings. This crystal may be 14- or 20-faced polyhedral crystal. The crystal was suspended in silicone oil.
49. A polyhedral crystal looking from the exact top. The crystal was collected under the same condition as of Fig. 48.
50. Drawings of the crystals in Figs. 48 and 49.
51. Another polyhedral ice crystal in ice fog under same condition as of Fig. 48.

LIST OF FIGURES
(Cont'd)

52. An ice crystal similar to above polyhedral crystals under same conditions.
53. Ice-fog crystals collected under same conditions as Fig. 48. Mark A shows a thin plate with two half hexagonal thin plates. Marks B illustrate "block ice crystal". C_2 is a plate crystal which has another plate angled 60° or 90° .
54. Ice-fog crystals taken under same condition as above. C_1 shows a half plate and a vertical plate attached with it. The weather conditions were the same as above.
55. Drawings of the crystals A and C_1 of Figs. 53 and 54.
56. and 57. Block ice crystals. The crystal in Fig. 56 was collected under the same conditions as Fig. 48. The crystals of Fig. 57 were sampled on 23 December 1965 at the MUS site with temperature of -40°C . The crystals in Fig. 57 were suspended in formvar liquid.
58. Relationship between relative humidities provided by hair hygrometers and temperatures during the winter of 1967 to 1968 at various sites.
59. Arrangement of apparatus for humidity measurement.
60. Water vapor density versus temperatures under ice-fog conditions at the MUS site. The curves for water- and ice-saturation are according to Smithsonian Meteorological Table.
61. An aerial photograph of Fairbanks taken just before ice fog forms. (Photo by Mobley, National Geographic Society).
62. Relationship between temperatures and visibilities at the Fairbanks International Airport during December 1964 through February 1965.
63. Relationship between temperatures and visibilities at the Fairbanks International Airport during December 1968 through February 1969. Compare with the situation as of 4 years ago.
64. Temperature profiles above open water under the conditions of several ambient air temperatures.
65. Result of calculation of time for water droplet to cool from 0°C to -30°C through conduction cooling or radiation cooling.

LIST OF FIGURES (Cont'd)

66. A small impactor to check whether the water droplets have been frozen or not.
67. The parallel plates to produce a uniform electric field.
68. Drawings for the possible explanations of ice-fog crystal depositions on the parallel wires. The upper drawing (a) shows ice crystals which have induced dipole moments, (b) shows crystal which has dipole layer on the surface and (c) shows force exerted to the ice crystals near positive and negative electrodes.

APPENDIX LIST OF FIGURES

Figure

1. Typical examples of temperature of exhaust gases computed from equation (14). Curve A: automobile exhaust, $a = 5 \times 10^{-4} \text{ cm}^{-1} \text{ deg}^{-1}$, $b = 66.7 \text{ cm}^{-1}$, $v_o = 2000 \text{ cm sec}^{-1}$. Curve B: exhaust from heating plant, $a = 2 \times 10^{-4} \text{ cm}^{-1} \text{ deg}^{-1}$, $b = 667 \text{ cm}^{-1}$, $v_o = 200 \text{ cm sec}^{-1}$. Curve C: above open water, $a = 5 \times 10^{-4} \text{ cm}^{-1} \text{ deg}^{-1}$, $b = 6670 \text{ cm}^{-1}$, $v_o = 20 \text{ cm sec}^{-1}$.
2. Saturation ratio versus time for cooling rates of Fig. 1.
3. Computed size distributions for ice fog particles produced by cooling rates shown in Fig. 1.

1. INTRODUCTION

In arctic and subarctic continental cities, when the temperatures go down to about -30°C , a sort of fog appears. From theoretical considerations, this fog has been believed to be composed of many tiny ice crystals suspended in the air. This is ice fog, and it becomes increasingly dense as the air temperature continues to decrease. Since places away from cities do not normally have ice fog (except along heavily travelled roads), the ice fogs have been assumed to be associated with human activities such as home heating, car exhaust and power plant exhaust.

Ice fog causes many traffic and health problems to inhabitants, as well as hampering airport activities because of seriously reduced visibility. The recent discovery of oil in the north slope area of Alaska has been accompanied by more combustion exhaust from airport activities, more people working, and more ice fog. The ice fog normally develops only in a shallow layer (about 50 m thick) the exact thickness varying with the strength of the ground inversion, which may be extremely strong.

Investigations of ice fog problems, i.e., the causes of ice fog formation, various meteorological conditions associated with ice fog, and the ways to minimize ice fog have been carried out by many investigators. Most of the studies concerned with ice fog were primarily oriented towards Alaskan or Fairbanks ice fog as a local problem. However, a careful study would be a significant contribution to physical meteorology as ice-fog

phenomena are similar to those involved in the formation of ice crystals in the upper air in most parts of the world. Even though many investigators have studied ice fog, there are many aspects of the problem and much work to be done. The continuing study of ice fog will therefore provide an excellent approach to the physics of cloud formation, physical and synoptic meteorology and micrometeorology, as well as contributing to the practical problem of this type of air pollution during Alaskan winter conditions.

Recently Weller (1969) summarized the investigations of the Fairbanks ice fog which have been done and are being continued by many investigators. He gives an excellent bibliography on the subject. However, the purpose of Weller's paper was to give a better understanding of the Fairbanks ice fog to people who need information on it related to commercial or industrial purposes, rather than to provide physical information on ice fog in general or associated fundamental physical problems. As Weller stated, Benson's (1965) report can still be considered as the most comprehensive study of the overall problem of ice fog in Fairbanks and in the surrounding area. Benson reported the Fairbanks ice fog in detail using a different approach from that of other scientists.

Detailed introductions and references will be given in each chapter of this report rather than in this general introduction. The main purpose of the present research has been to clarify or confirm the mechanism of ice-fog formation. The conclusions are based upon substantial physical data observed by ourselves throughout the field and laboratory work, and synoptic and theoretical consideration.

Since Oliver and Oliver (1949) suggested that ice fog might be a form of air pollution, the Stanford Research Institute (Robinson et al., 1955), and Benson (1965) have emphasized that ice fog is a kind of air pollution. In particular, the report entitled "Ice fog: Low Temperature Air Pollution" by Benson described the ice fog as air pollution in the forms of water and pollution other than water at Fairbanks and compared it with the Los Angeles smog, which is probably the most widely known form of air pollution. Through the observations of concentrations of condensation nuclei in and around Fairbanks and the comparison of these values with the extent of ice fog, as well as through his pioneering study of ice-fog nuclei with an electron microscope Kumai (1964) also concluded that the ice fog covers the same area as do high concentrations of combustion by-products, even though he did not use the words "air pollution". However, he suggested that air pollution or condensation nuclei have relatively more important roles than water vapor in forming ice fog. It is a fact that hazardous gas and dust are considerably increased at the time that ice fog forms in a city, because at such a time an intense ground inversion normally develops and under such conditions hazardous gas and dust particles will be trapped near the ground together with water vapor, droplets and ice crystals, so it is necessary to study each component separately.

From these points of view, the main purposes of the present research were to clarify the following problems: 1) Which is the more critical ingredient for the formation of ice fog - dust (nuclei) or water,

2) what is the role of the air pollution other than water in ice-fog formation, and 3) how does water released from combustion processes, etc. make ice-fog crystals? The answers to these questions would clarify the nucleation process of ice-fog crystals. Since the ice fog is essentially the same phenomenon as the condensation trails (the so-called contrails) produced by airplanes flying in the higher troposphere, the research on ice fog also provides information about contrails.

During this research in an extremely cold environment, we have to expect some instrumental difficulties as well as the observers' physical problems. In the present project, many kinds of measurements such as the concentrations of ice-fog crystals, ice nuclei, condensation nuclei and their sizes and shapes etc., besides measurements of water vapor contents were made using several types of equipment and special techniques.

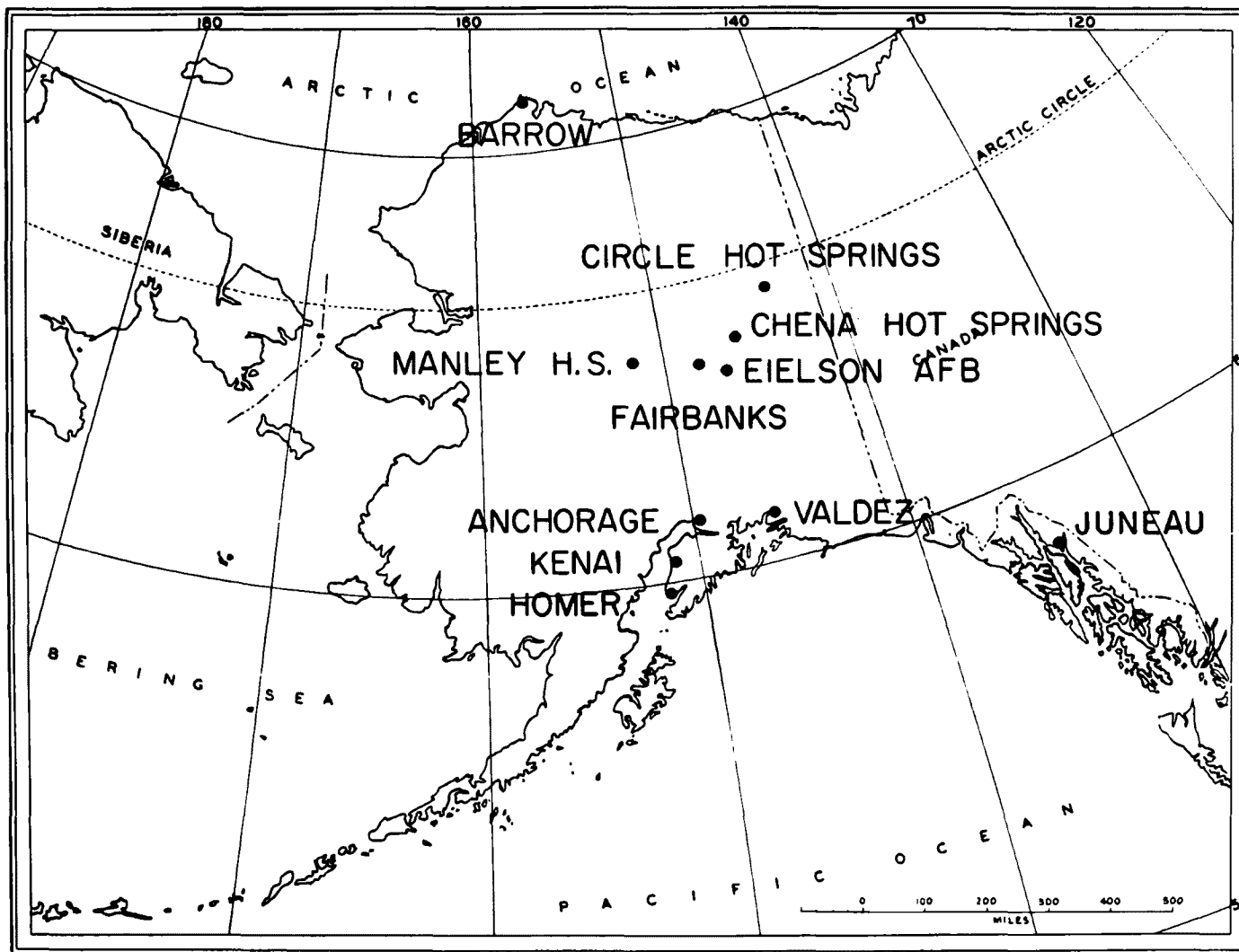


Fig. 1. The solid circles indicate the locations where the counts of condensation nuclei were made.

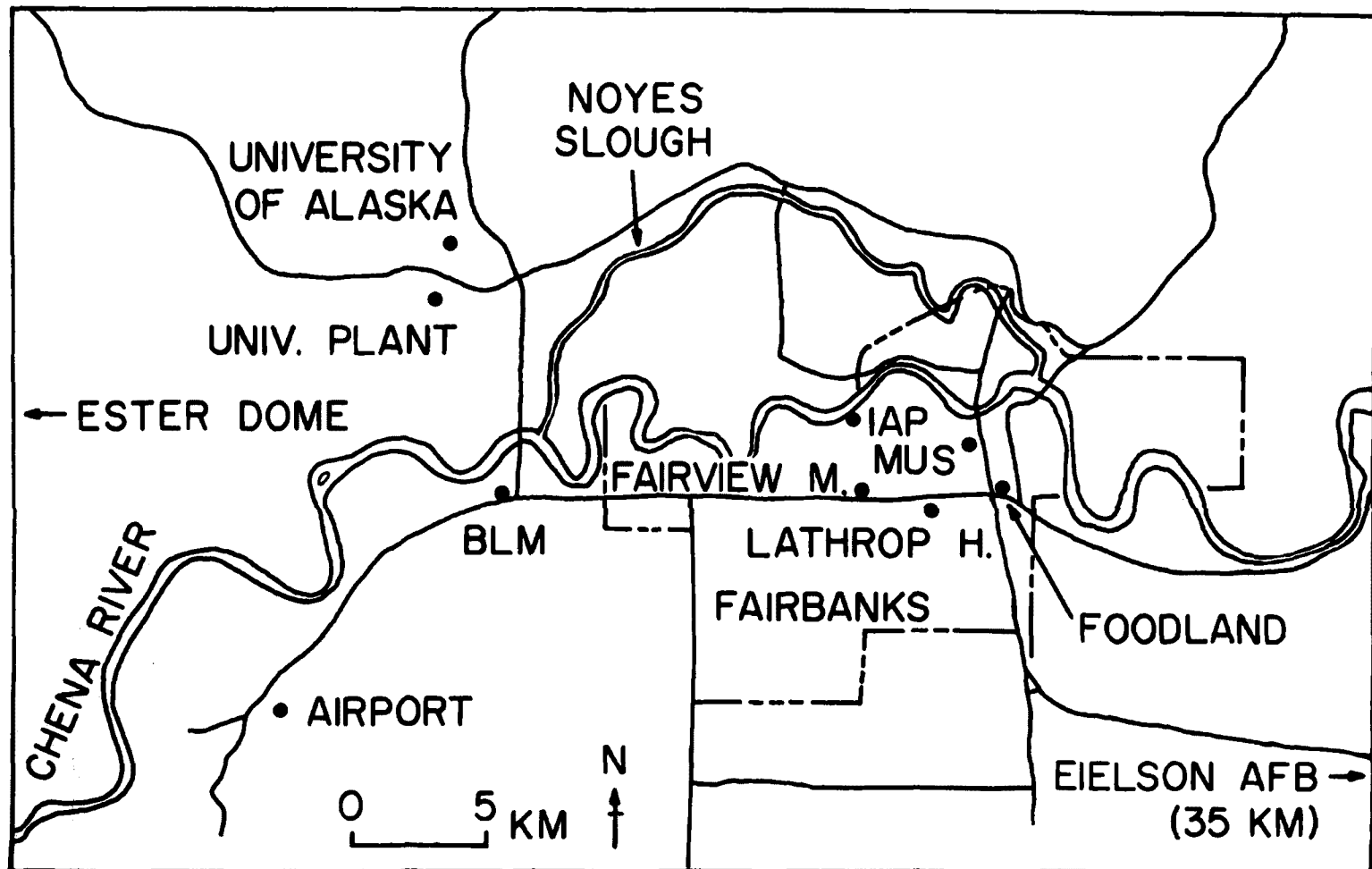


Fig. 2. Map showing locations in the Fairbanks area where the data on ice-fog crystal size distributions, nuclei, humidities, etc. were obtained and ice crystal samples were collected.

2. MEASUREMENTS OF ICE-FOG CRYSTALS

Thuman and Robinson (1954a) made the first observations of size distribution of ice-fog crystals at Eielson Air Force Base, 25 miles southeast of Fairbanks, Alaska. They found that the mean particle diameter of "droxtals*" (which was the predominant crystal type in ice fog at -44C) was 13μ at a temperature of -40C and the size increased with increasing temperature to 16μ at a temperature of -30C, although they did not show a complete size distribution in the paper. Later, Kumai (1964) showed size distributions of ice-fog crystals in terms of numbers of precipitated crystals including the spherical crystals (which are the same as "droxtals") with their sizes of 4 to 12μ (the peak was at 7μ) diameter for -39 and -41C in downtown Fairbanks and at the Airport, respectively. From these distributions Kumai figured out that the concentrations of crystals are $155 \text{ crystals cm}^{-3}$ and $96 \text{ crystals cm}^{-3}$ and that the solid water contents are 0.07 and 0.02 gm m^{-3} for the temperatures of -39 and -41C, respectively.

These size distribution studies carried out by Thuman and Robinson and by Kumai used a precipitation collection method in which particles are collected on a slide glass by gravitational precipitation or sedimentation at terminal velocity. Even though the precipitation method gives very consistent results, it normally produces an uncertainty in

* A droxtal, which is the term used by Thuman and Robinson, is a small-sized poorly-formed ice crystal. It is an equant solid particle with rudimentary crystal faces, and thus seems to have characteristics of both droplets and crystals, according to them.

concentration of such particles from the precipitation method, because we have to use the Stokes' fall speed for each size particle. However according to Ohtake (1964), small air turbulence disturbs such fall speeds and may give a lack or excess of smaller particles. The concentration of crystals is derived by dividing the numbers of crystals precipitated on a glass by Stokes' fall speed for corresponding sizes. The fall speeds for the smallest sized crystals are much smaller, for instance 0.1 mm sec^{-1} for 2μ diameter ice crystal, than the actual possible turbulent speeds. So the results from the precipitation method give variable concentrations, especially for less than 10μ diameters. Also Benson (1965) stated that updrafts in ice fog in the downtown Fairbanks area were likely to be greater than the falling velocity of the small particles. The error in size distributions introduced by turbulence or updrafts is demonstrated by Fig. 3, which shows the results obtained at the same time and location by a) the precipitation method, and b) the impaction method to be discussed below.

Considering these disadvantages of the precipitation method, we used the impaction method to obtain size distributions of ice-fog crystals. The method is similar to that used by Kozima et al. (1953) for collecting sea-fog drops. Figure 4 illustrates the three stage impactor, improved by K. Kikuchi (unpublished) of Hokkaido University, which we used. For the collection of ice-fog crystals we used only one of the three stages. As a measured volume of air (V) is drawn into the nozzle (Q) by rapidly pulling out the plunger (P), ice-fog crystals contained in the air sample are deposited in a thin film of silicone oil on the small microscope slide

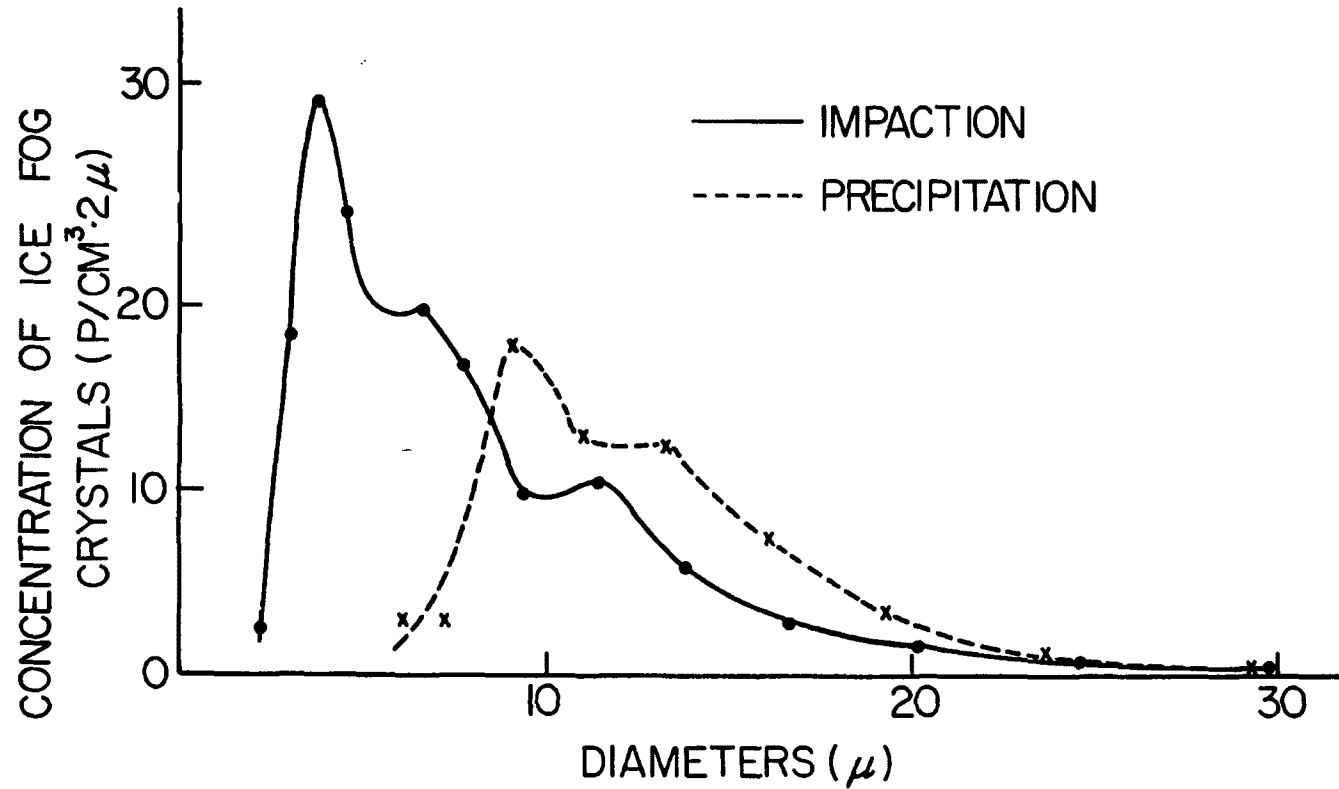


Fig. 3. Comparison of size distributions of ice-fog crystals obtained simultaneously by two methods at the same location and time.

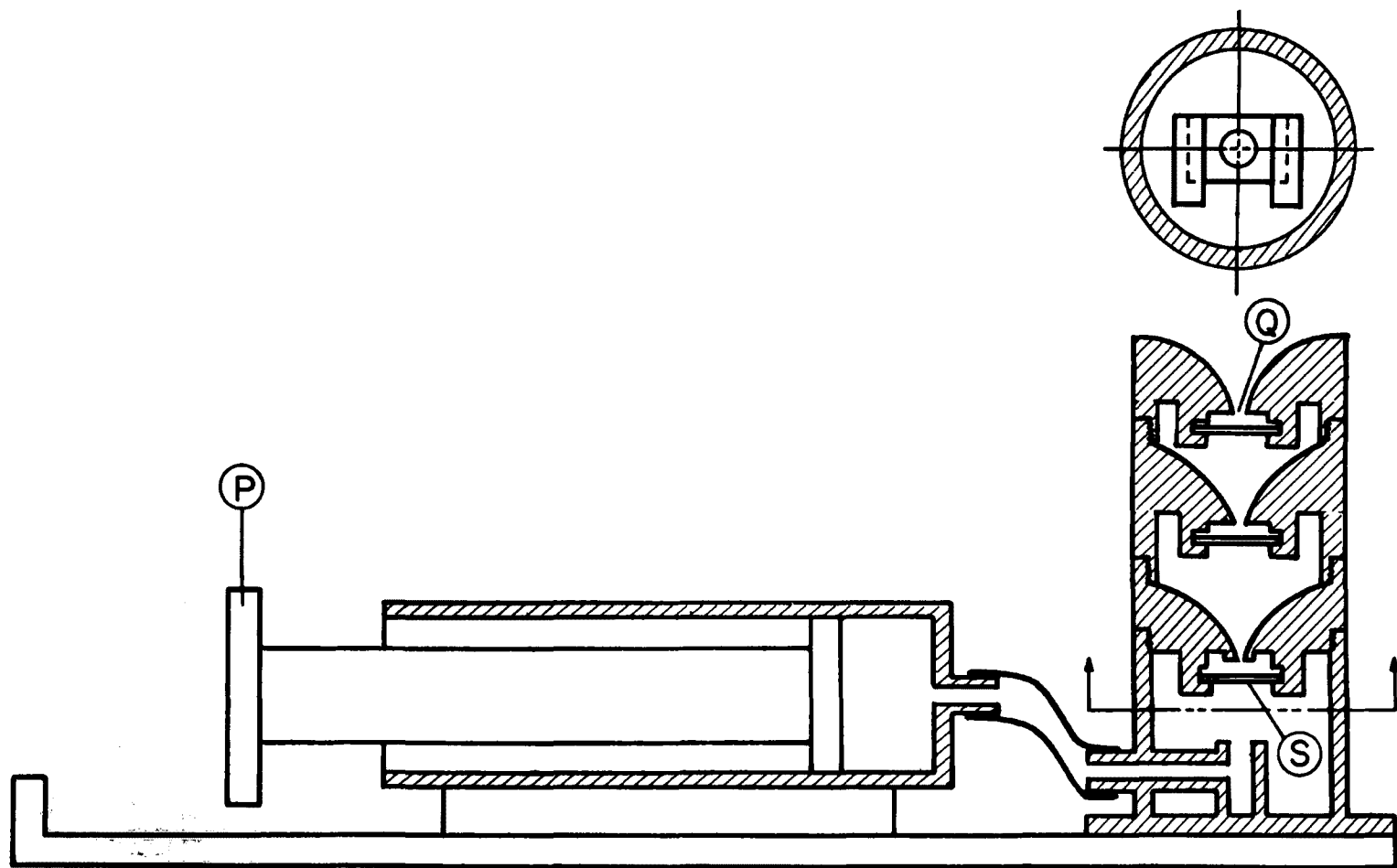


Fig. 4. Three stage konimeter used for collecting ice-fog crystals.

(S) (1.8 cm square). The area onto which the crystals are deposited depends on the nozzle diameter (Q), separation (y) between nozzle and slide, and the rate at which the plunger is pulled out. These parameters must be adjusted so that all particles are collected and are in the field of view of the microscope, or are concentrated at the center of the slide glass. This means that collection efficiency is 1.00 if the smallest crystals were circularly scattered around most of the other crystals deposited at the center. Two pictures are shown in Fig. 5 as examples. Some ice-fog crystals were falling onto the slide during the time the picture of the slide was being taken, but this introduces a negligible error. The values we used were $Q = 1.0$ mm and $y = 2.5$ mm. The volume of air sampled V was chosen according to ice fog density to give the largest possible numbers of crystals without overlapping, normally 8 c.c. The only disadvantage of this method is that any observer must practice to obtain good results in preventing overlapping without letting the smallest sized crystals escape from the slide. The difficulties are to choose an appropriate suction speed and volume as well as to select the correct thickness and kind of oil film on the slide.

An automatic sampler which was made and operated by Huffman (1968), who was a member of this project, was working well as long as he operated it. It needs some improvement. For further information about this refer to Huffman's thesis (1968).

Nevertheless we sometimes used the precipitation method to determine size distributions of ice-fog crystals, because this method gives consistent data by a very simple technique even though some errors in the

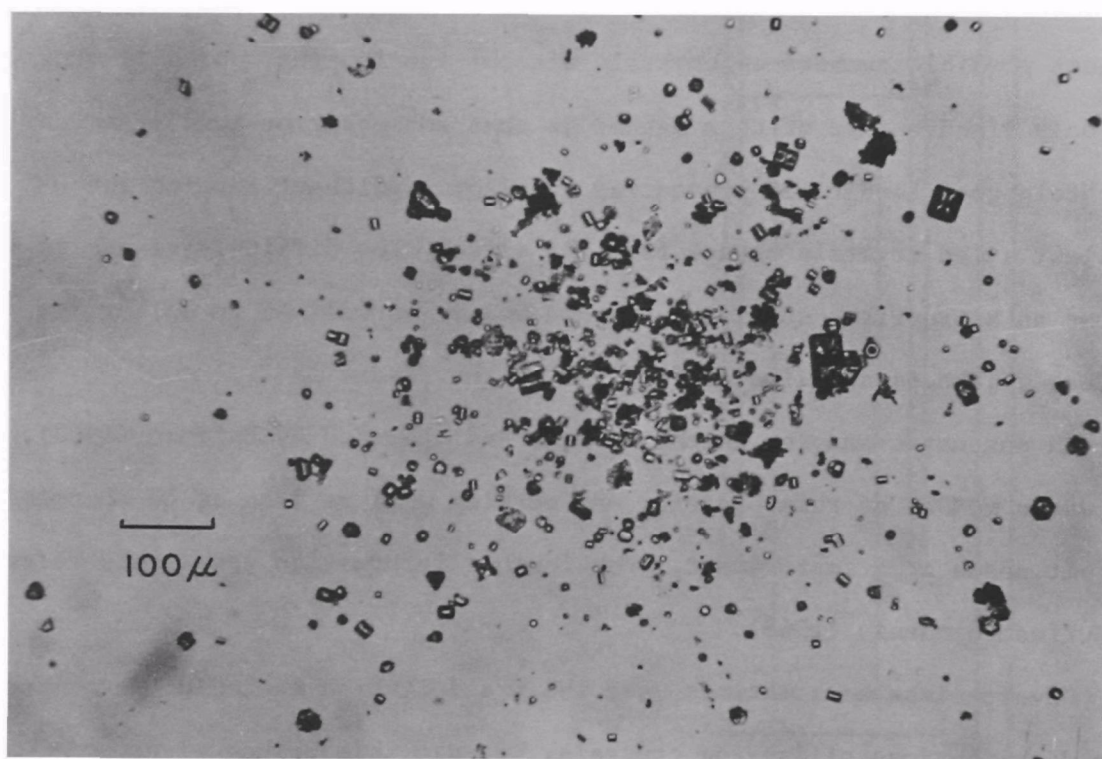
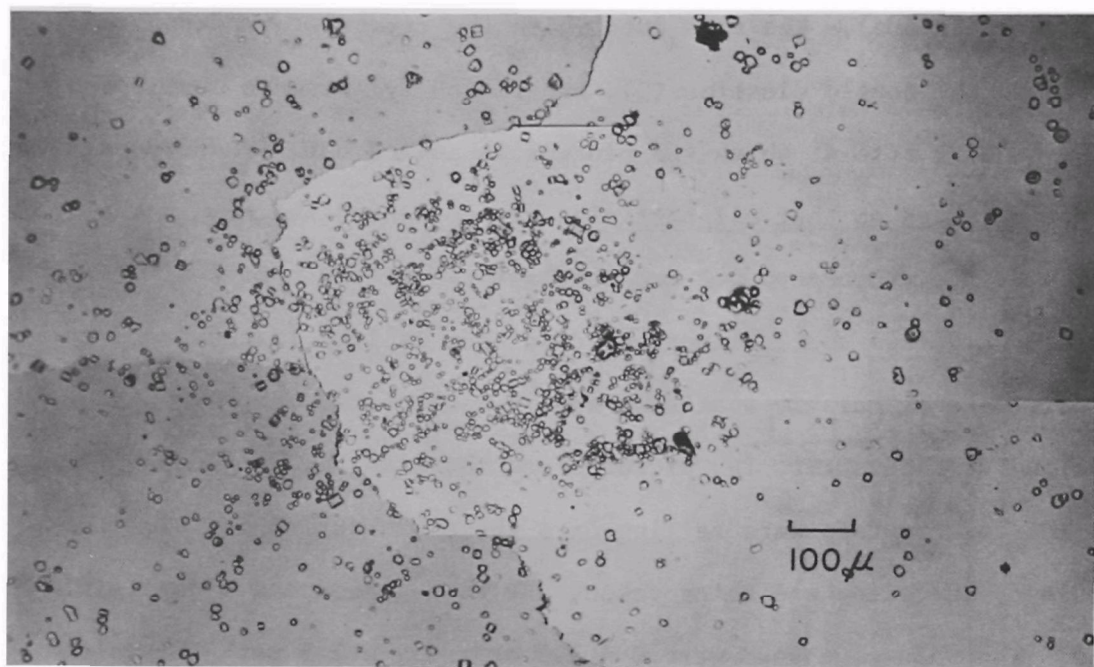


Fig. 5. Micro photographs of ice-fog crystals obtained with the ice-fog crystal sampler represented in Fig. 4.

smallest crystals are expected. Another advantage of this method is that it is possible to obtain formvar replicas of ice crystals or water droplets on a glass slide very easily, while the impact of crystals results in bouncing and the escape of crystals from a dry slide glass coated by formvar, even though it does not occur on a slide coated by oil. Procedures for making replicas of ice-fog crystals will be mentioned in a later chapter.

On the basis of the experimental data obtained, the following conclusions can be reached regarding the concentrations, size distribution, and solid water content of ice-fog crystals:

1. Mean diameters change from place to place, which implies that they depend upon temperature, humidity and the local supply rate of ice-fog crystals. Even at the same place, an increase of population, traffic, etc. produces thicker ice fog (more crystals per unit volume of air) and larger solid water contents, but normally the size distribution stays constant if the source(s) of the ice fog does not change.
2. During the winters of 1965 through 1969 the mean diameter of crystals in air traffic areas away from downtown Fairbanks (i.e. Fairbanks International Airport and Eielson Air Force Base) was about 5μ , in the downtown area (MUS) it was 3 to 4μ , and at the places adjacent to open water such as the Industrial Air Products parking lot (along the Chena River downstream from the MUS power plant), Chena Hot Springs, and Manley Hot Springs, the diameters of crystals were about 10μ . All values are for a temperature around -40°C or a little colder.

3. The distribution is usually bimodal or trimodal in downtown Fairbanks and unimodal at the other locations. The typical distribution in the downtown Fairbanks area is shown in Fig. 6.*

4. The concentration of ice-fog crystals also changes from place to place, and from time to time. For instance, the concentration is very high in the middle of downtown Fairbanks and almost zero outside of the city.

The mean value of concentration of ice-fog crystals was about 150 particles cm^{-3} which roughly agrees with Kumai's (1964) data although he observed the concentration only twice. The maximum value we got using the impaction method through 1968 was 227 p cm^{-3} and it is predicted that the maximum value would increase with lowering of temperature and with more increase in human activities in the town.

5. Concentration of ice-fog crystals should depend not only on temperatures but also on the supply rate of moisture to the air (or incoming and out-going water droplets or ice-fog crystals). The vapor supply is more important than the temperature at temperatures lower than -35°C . So observations of the temperature dependence of the concentration were made at definite locations (with nearly fixed conditions of moisture supply rate), but at different temperatures. The variation of concentration with temperature is based on observations using the precipitation method at the MUS site during the winters of 1967 through 1969.

* The datum of solid water content shown on page 26 of Weller's report (1969) (supplied from the author's result) was a misprint. It should be changed to "Total Water Content" and solid water content should have been 0.12 gm m^{-3} ; crystal concentration was 153 p cm^{-3} .

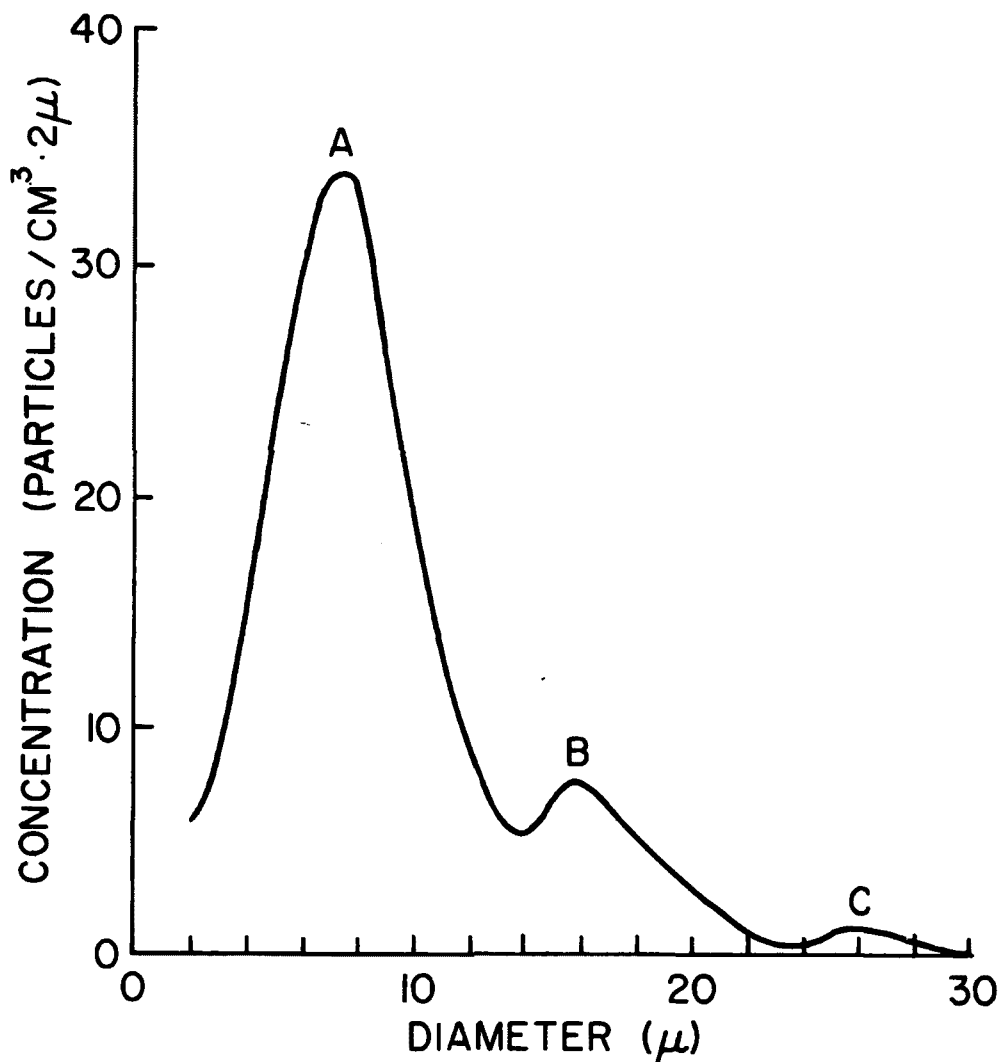


Fig. 6. Typical size distribution of ice-fog crystals in downtown Fairbanks, at -36.5°C . Total water content 0.23 mg l^{-1} , solid water content 0.12 mg l^{-1} , visibility 180 m, particle concentration 153 p cm^{-3} , at 1240 AST on 8 December 1968. Peaks A, B and C represent crystals from car exhausts, open water and heating plants (commercial and residential) respectively. Heights of the peaks are different from place to place owing to different moisture and temperature conditions.

TABLE 1

Mean Size, Concentration and Solid Water Content
vs. Temperature at the MUS Site

<u>Temperature</u> <u>°C</u>	<u>Mean Diameter</u> <u>μ</u>	<u>Concentration</u> <u>crystals cm^{-3}</u>	<u>Solid water</u> <u>content gm m^{-3}</u>
-47	3	715	0.05
-40	8	250	0.09
-35	22	9	0.05
-30	33	1	0.02

Despite the fact that the absolute numbers of concentration of ice-fog crystals may not be very accurate, because the data were derived from the precipitation method, the temperature dependence of the concentration is very clear in the table. The dependence of the solid water content on temperature was not clear.

From December 30, 1968, through January 6, 1969, the Alaskan interior experienced extremely severe cold weather with ice fog. During this time we obtained data on ice-fog crystals at various locations. Most of the data were obtained through the use of replicas of crystals collected by precipitation onto glass microscope slides. Table 2 shows the concentrations and solid water contents of ice-fog crystals and Fig. 7 shows the size distributions at all sites. In both the table and figure all samples except those of December 30, 1968, were collected by use of the precipitation method on slides as replicas to minimize the time spent.

Even though the values of concentration and size distribution are not entirely accurate because the precipitation method was used, comparison of the data at several sites may be valuable. In the concentration data

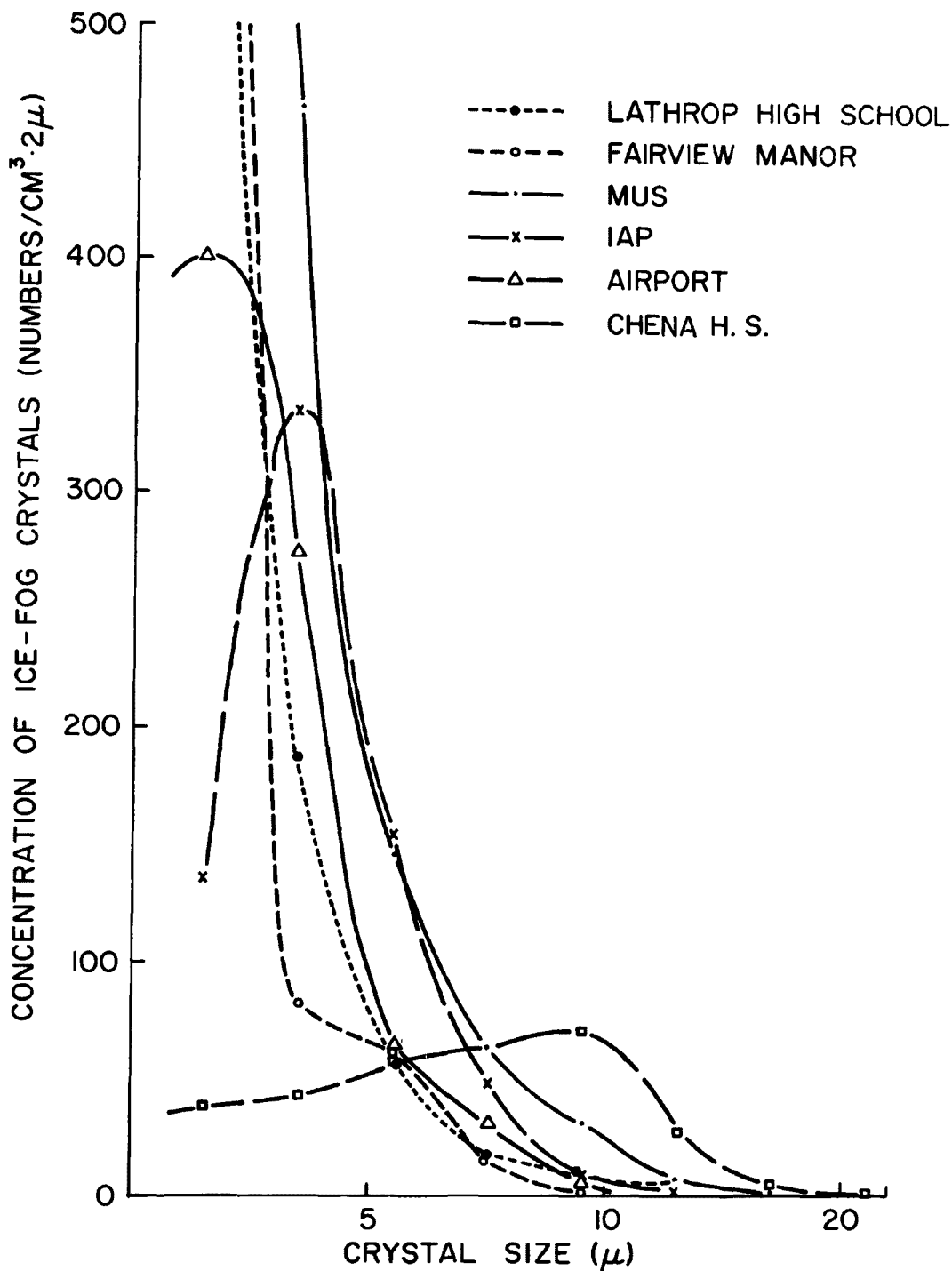


Fig. 7. Size distributions of ice-fog crystals at various locations on 2 January 1969, at temperatures between -47 and -50°C , excepting that of Chena H. S. At Chena H. S, collection was made on 1 January 1969 at a temperature of -45°C . All distributions on this figure used the precipitation method.

TABLE 2

Data of ice-fog crystals in various locations. Data other than the first two data were taken by the precipitation method (replicas). The temperature of stream water at Chena Hot Springs was 35C.

Date	Time exposed (AST)	Location	Temperature	Visibility	Concentration		Solid Water Content gm m ⁻³
			°C		>2.5 μ	<2.5 μ p.cm ⁻³	
Dec. 30, 1968	12:15(suction)	MUS	-38.0	60	210 (all together)		0.064
Dec. 30, 1968	12:47(suction)	MUS	-39.0	90	227 (" ")		0.131
Dec. 31, 1968	20:38-20:44	Chena Hot Springs	-43.9	?	266	39	0.073
Dec. 31, 1968	21:12-21:19	Chena Hot Springs	-42.2	?	724	32	0.179
Jan. 1, 1969	10:44-10:54	Chena HS (near stream)	-45.2	-	1780	465	0.127
Jan. 1, 1969	11:00-11:05	Chena Hot Springs	-44.8	-	373	506	0.042
Jan. 1, 1969	11:12-11:17	Chena HS (near stream)	-44.0	-	1231	691	0.074
Jan. 1, 1969	11:22-11:32	Chena HS (50m from ")	-44.5	-	77	68	0.022
Jan. 2, 1969	11:14-11:25	MUS	-47.0	60	715	889	0.055
Jan. 2, 1969	11:38-11:43	IAP	-48.0	70	549	136	0.036
Jan. 2, 1969	11:54-12:04	Fairview Manor Apt.	-47.2	60	163	660	0.012
Jan. 2, 1969	13:22-13:30	Lathrop High School	-47.0	60	260	1479	0.020
Jan. 2, 1969	13:51-14:17	Int'l Airport	-50.0	120	378	403	0.021
Jan. 2, 1969	14:37-14:46	College residential area	-48.5	100-300	185	25	0.009
Jan. 2, 1969	14:58-15:08	University campus	-48.5	80	350	546	0.019

in Table 2, crystals smaller than 2.5μ were too small to be counted accurately in the optical micro-photographs, but are listed separately to provide some possible findings.

Under similar conditions, both concentration and solid water content were highest in the center of downtown Fairbanks (the MUS site) excluding the data observed at Chena Hot Springs. The next highest values can be seen at the IAP site which is near the open water of the Chena River and has some automobile traffic nearby. The high solid water contents at both sites were associated with higher concentrations of ice-fog crystals in the size range larger than 5μ than those of other stations, as can be seen in Fig. 7. The other four sites (except the College site which had almost no traffic or open water) had similar features. For all stations, very high concentrations of crystals smaller than 2.5μ seemed to occur in ice fog associated with automobile traffic. Only the MUS site might have over-lapping of ice-fog crystals formed from open water and car exhaust. At Chena Hot Springs both concentration and solid water content were remarkably high near the hot spring stream (about 2m away) but rapidly decreased with distance from the stream. This is probably due to some evaporation in a dryer environment than in the city area. It was noticed that all particles were frozen at a distance of about 5m from the stream. (The method for this observation will be mentioned in a later chapter).

3. MEASUREMENTS OF CONDENSATION NUCLEI

Many reports have been published of condensation nuclei counters using various degrees of supersaturation. Especially, Kocmond (1965) and Radke and Hobbs (1969) tried to observe condensation nuclei active at the low supersaturations which occur in cloud formation associated with updrafts in the free atmosphere. This is the most desirable way to observe the real concentration of condensation nuclei for the natural clouds. Normally less than 1 percent of supersaturation is expected in nature (Houghton, 1951) and sometimes even when the humidity is only 75 to 80 percent, in the cities along the ocean coast, we can easily find droplets as haze or smog (Yamamoto and Ohtake, 1955). However, as will be described later, in the case of ice fog we have much higher supersaturations than the above values at the source of the fog. The supersaturation is approximately 300 to 400 percent or more in the vicinity of ice-fog sources.

Because of this, we used a traditional condensation nuclei counter, the Gardner Small Particle Detector, which counts Aitken nuclei (measurable size ranges are larger than 1×10^{-7} or larger than 1.3×10^{-5} cm) and which has supersaturations of 300% to 400%. The values provided by the counter are not useful for natural clouds and normal fogs but valid for condensation nuclei for the fog near open water and exhausts because of similar degrees of supersaturation.

Table 3 shows the data we obtained in and around the city of Fairbanks and other locations including Manley Hot Springs, Chena Hot Springs,

Pt. Barrow, Anchorage, Juneau, etc. Most of these observed values are similar to Landsberg's results (1938), but the data in Fairbanks (essentially same as "town" in Landsberg's data) are higher, especially in the ice-fog season. The observed maximum concentration of condensation nuclei was $6 \times 10^6 \text{ p cm}^{-3}$ in the middle of the downtown area. This value is much higher than the absolute maximum value for towns in Landsberg's data. Also the values at Manley, Chena and Big Delta were nearly the same as the absolute minimum values for country inland data.

Sometimes, to get a size spectrum of the nuclei, several kinds of Millipore filters such as 14, 8, 5, and 0.45μ pore sized filters were used. However, more than 98 percent of the total nuclei (larger than $1.3 \times 10^{-5} \text{ cm}$ in radius) were captured by the 8μ filter. Figure 8b shows the ratios of the concentration without filters to that with filters. From the figure it can be said that the nuclei at the MUS site consisted of smaller particles than at the other sites. These nuclei must come from automobile exhausts. Using smaller expansion ratios of 15 inch Hg and 5 inch Hg of the instruments pressure gauge reading, instead of 26 inch Hg (the value of pressure suggested by the maker to measure nuclei larger than $1.3 \times 10^{-5} \text{ cm}$ radius), gave ratios similar to those of Fig. 8b. Figure 8a shows that the nuclei in areas of heavy traffic decrease in number with decreasing expansion ratios, while the nuclei in clean air areas such as Circle, Manley and at sea shore sites such as Kenai and Anchorage do not change much with changing pressure gauge readings. Unfortunately, the absolute values of the expansion ratio is not known for these data. However, these data show the same tendency as the Millipore filter method.

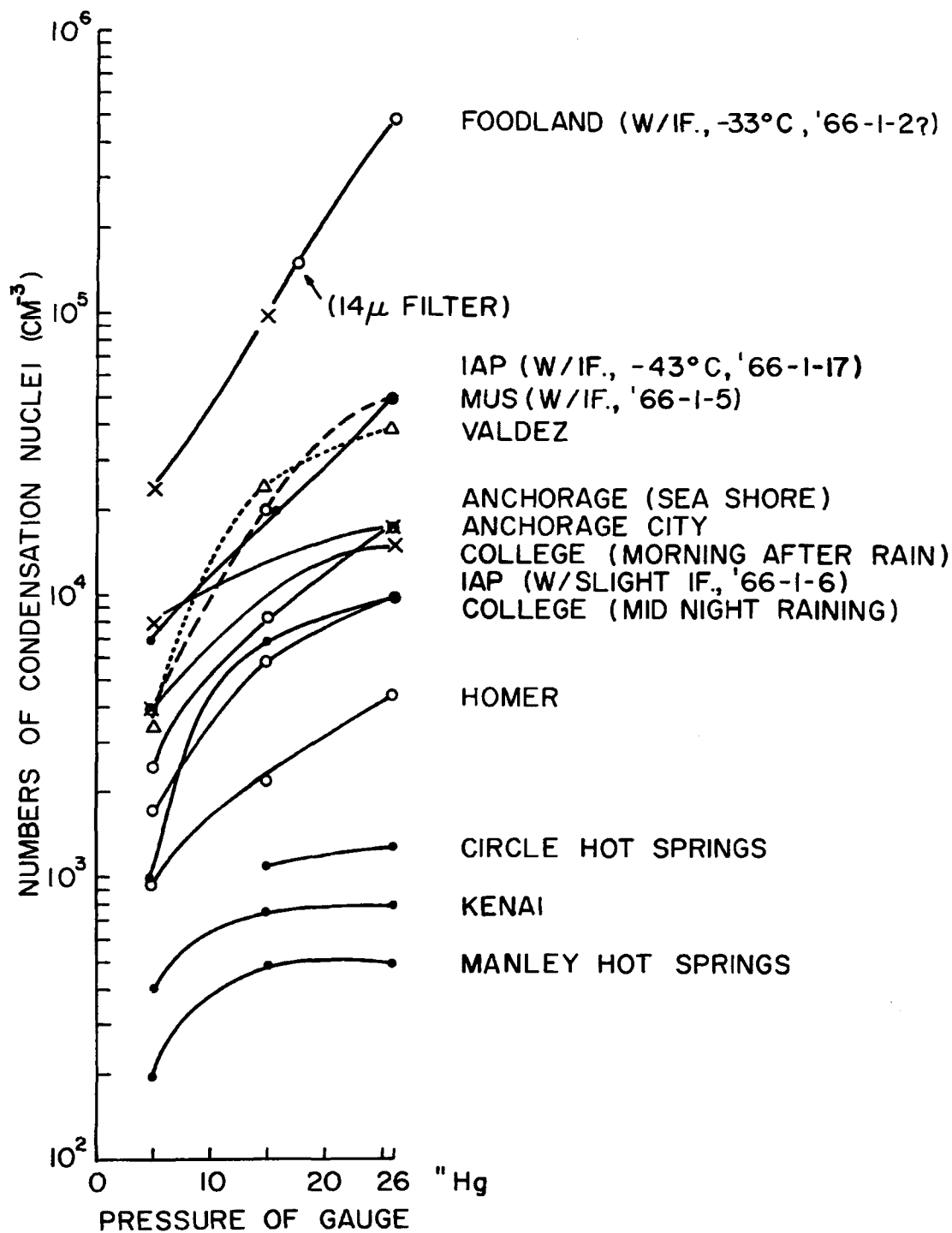


Fig. 8a. Concentrations of condensation nuclei at various places in Alaska using different expansion ratios.

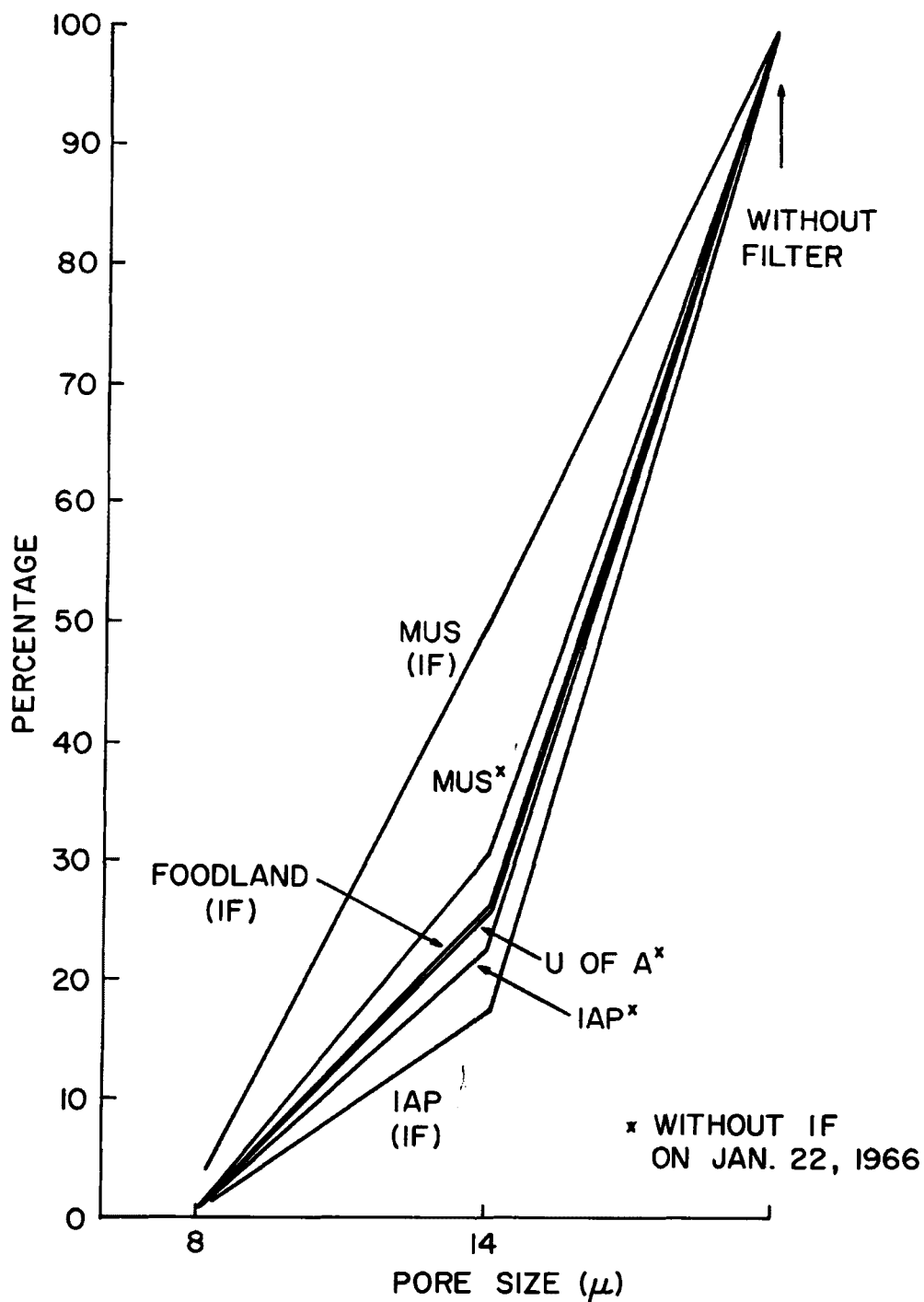


Fig. 8b. Concentration of condensation nuclei in terms of percentage of total nuclei to that of nuclei passing through Millipore filters. IF means the observations were made in ice fog.

Obviously, the observed concentrations of condensation nuclei shown in Table 3 are much greater than those of ice-fog crystals even under -50C conditions. These observations imply that only a very small fraction of the condensation nuclei act as real ice-fog nuclei, and the remaining large numbers of condensation nuclei are floating in the air co-existing with the ice-fog crystals. Huge numbers of dry, unactivated nuclei or dust particles including lead compounds resulting from car exhaust as well as carbon monoxide, carbon dioxide, gaseous sulfur compounds and other gases hazardous for our health are also associated with ice-fog crystals.

Another interesting point is that even though the concentration of condensation nuclei is only about 300 p. cm^{-3} at Chena Hot Springs under ice-fog conditions, we found about twice that concentration of ice-fog crystals. From the electron microscope study, which will be mentioned in more detail in a later chapter, we found many ice-fog crystals without any nuclei. This means that a high concentration of condensation nuclei is not a very important factor for the formation of steam fog or the final ice fog when temperatures are lower than about -40C, although it is an indication of the action of combustion which produces water vapor and condensation nuclei or dust and gases.

4. MEASUREMENT OF ICE NUCLEI

The definition of an ice nucleus is, according to Wegener (1911), a nucleus necessary to form an ice crystal in the atmosphere; Wegener assumed that a sublimation nucleus was involved. However, Fournier d'Albe (1949) and Weickmann (1949) made some experiments and both of them concluded that ice crystals can be formed only under conditions of water saturation or supersaturation over water, and they suggested that a thin water film might first condense on the surface of a solid particle, and the film would then freeze. From this point of view they called the ice nucleus a freezing nucleus. Houghton (1951) criticized their term of freezing nucleus and stated that there is certainly a clear physical difference between ice crystals formed in such a way and those which are formed by the freezing of a liquid drop which has already attained cloud drop size. In the latter case it is evident that a freezing nucleus is involved. Until more information is available it would seem preferable to call all nuclei on which ice forms below water-saturation sublimation nuclei. Most recently, Isono (1969) suggested that an ice nucleus is a particle which accelerates the formation of an ice crystal from water vapors regardless of the exact process of ice crystal formation. This definition includes both sublimation nuclei and freezing nuclei as defined by Fournier d'Albe and Weickmann. A freezing nucleus is then a particle which accelerates the formation of an ice crystal in a water droplet. These definitions seem to be reasonable. Analogously, a condensation nucleus is a particle which accelerates the formation of a water droplet in air.

Sometimes an ice nucleus or freezing nucleus is confused with a condensation nucleus especially in the study of the ice fog. However, an active condensation nucleus such as NaCl is not effective as an active freezing nucleus, at least at temperatures higher than -15°C . And active ice nuclei such as AgI are not active condensation nuclei. Under ice-fog conditions, since the temperature is very low, any kind of particles contained in water drops may accelerate freezing of the drops at a higher temperature than would be observed for pure water drops. To form a water fog some condensation nuclei are needed under normal atmospheric conditions. These nuclei, after acting as condensation nuclei, may act as freezing nuclei at lower temperatures. On the other hand, ice nuclei may form ice-fog crystals even under sub-water saturation conditions. Up to the date, no measurement of ice nuclei at effective temperatures lower than -30°C has been published.

A temperature spectrum of ice nuclei concentration was obtained at Ester Dome using the same diffusion-type ice nuclei counter with a sugar solution detector which had been used by the author at Tohoku University, Japan (Ohtake and Isaka, 1964), as can be seen in Table 4. In the author's experience (unpublished) and also that of others (e.g. Fletcher, 1966), the concentration of ice nuclei in the atmosphere rises an order of magnitude with every 4°C decrease in temperature. Applying this temperature dependence to the concentrations at Ester Dome for a temperature of -21°C , we derive 25,000 nuclei L^{-1} (or 25 cm^{-3}) of ice nuclei concentration at effective temperature of -35°C .

TABLE 3

Concentration of Condensation Nuclei in and around
the Fairbanks city and far from the city

	Nuclei cm^{-3} 26 inch Hg without filter	Date	Size Range
Juneau Airport	750	December 2, 1965	$r > 1.3 \times 10^{-5} \text{ cm}$
Mendenhall Glacier	1,500	December 2, 1965	$r > 1.3 \times 10^{-5} \text{ cm}$
Juneau City	160,000	December 2, 1965	$r > 1.3 \times 10^{-5} \text{ cm}$
Douglas Marine Station	14,000	December 2, 1965	$r > 1.3 \times 10^{-5} \text{ cm}$
Clear Air Force Base	2,500	June 18, 1965	$r > 1 \times 10^{-7} \text{ cm}$
Ester Dome	500~5,000	June 21, 1965 (and many times)	$r > 1 \times 10^{-7} \text{ cm}$
University of Alaska	20,000~60,000	June 21, 1965 (and many times)	$r > 1 \times 10^{-7} \text{ cm}$
Airport - Fairbanks	5,000	June 21, 1965	$r > 1 \times 10^{-7} \text{ cm}$
Eielson Air Force Base Base Operation	12,000	July 30, 1965	$r > 1.3 \times 10^{-5} \text{ cm}$
Cooling Pond	30,000	July 30, 1965	$r > 1.3 \times 10^{-5} \text{ cm}$
Power Plant	70,000	July 30, 1965	$r > 1.3 \times 10^{-5} \text{ cm}$
Airport Road w/water fog	2,000~100,000	June 21, 1965	$r > 1.3 \times 10^{-5} \text{ cm}$
Richardson Highway Black Rapid Glacier	500	August 11, 1965	$r > 1.3 \times 10^{-5} \text{ cm}$
Anchorage (sea shore)	18,000	August 11, 1965	$r > 1.3 \times 10^{-5} \text{ cm}$
Anchorage (city)	20,000	August 23, 1965	$r > 1.3 \times 10^{-5} \text{ cm}$
Circle Hot Springs	1,300	August 14, 1965	$r > 1.3 \times 10^{-5} \text{ cm}$
Manley Hot Springs	200~1,000	August 17, 1965	$r > 1.3 \times 10^{-5} \text{ cm}$
Chena Hot Springs	300~700	December 31, 1968	$r > 1.3 \times 10^{-5} \text{ cm}$
Chena Hot Springs Road	200	January 1, 1969	$r > 1.3 \times 10^{-5} \text{ cm}$

TABLE 3
(Cont'd)

	Nuclei cm ⁻³ 26 inch Hg without filter	Date	Size Range
Valdez	40,000	August 30, 1965	$r > 1.3 \times 10^{-5}$ cm
Kenai	700	August 29, 1965	$r > 1.3 \times 10^{-5}$ cm
Homer	5,000	August 26, 1965	$r > 1.3 \times 10^{-5}$ cm
Birch Hill	700	November 8, 1965	
	1,500	October 29, 1967	$r > 1.3 \times 10^{-5}$ cm
Hamilton Acres, Fairbanks	120,000	October 29, 1967 (and many times)	$r > 1.3 \times 10^{-5}$ cm
MUS	50,000~180,000 6,000,000 (max)	December 4, 1967 (and many times)	w/I.F. $r > 1.3 \times 10^{-5}$ cm
IAP	26,000~100,000	(many times)	$r > 1.3 \times 10^{-5}$ cm
2nd Street	5,000,000	December 4, 1967	w/I.F. $r > 1.3$
Foodland	500,000	January 2, 1966	w/I.F. $r > 1.3 \times 10^{-5}$ cm
Big Delta(near river)	200~500	January 2, 1966	- no I. F. along Highway but I.F. above river. $r > 1.3 \times 10^{-5}$ cm

TABLE 4
Average ice nuclei temperature spectrum

Type of Counter	Temperature							
	-15	-20	-25	-30	-35	-40	-45	
Diffusion	0.6	5	7	8	-	-	-	nuclei ℓ^{-1}
Acoustical	-	-	0.3	-	2	6	100	nuclei ℓ^{-1}
Expansion	-	-	0.3	-	2	25	300	nuclei ℓ^{-1}

However this value was not determined by direct measurement. After obtaining an NCAR acoustical ice nuclei counter (Langer, et al., 1967), we also obtained the temperature spectrum of ice nuclei concentration with it, as shown in Table 4. From the Table we see 100 nuclei ℓ^{-1} for -35C, which is a much smaller concentration than that of actual ice-fog crystals. Also we recognized miss-counting of ice crystals formed in the chamber of the counter due to smaller size of ice crystals than could be detected with the acoustical sensor of the counter. This appears to be a problem with this machine at temperatures lower than -25C.

An expansion type counter which is called the Bigg-Warner counter (Warner, 1957) and was developed by ESSA (Kline and Brice, 1961) was available at Colorado State University. Using this, another temperature spectrum of ice nuclei was measured at the HAO station at Climax, Colorado. As can be seen in Table 4, 300 n. ℓ^{-1} for -35C was obtained. Even though the detection of ice crystals by this counter seems to be much better than

by the NCAR acoustical counter, this number is still a very small number compared to the concentration of the ice-fog crystals. Also 300 n.l^{-1} is the maximum detectable number by the expansion type counter. The concentrations of ice nuclei for various effective temperatures varied by a factor of 10 per 4°C in the temperature range between -20°C and -35°C in the case of the expansion chamber. Assuming that this relation is valid to -39°C , we may expect $3,000 \text{ n.l}^{-1}$ for a temperature of -39°C , which is still almost negligible in comparison to observed ice crystal concentrations in ice fog at a temperature of -39°C .

However, these observations were made at places where the air is relatively clean (where condensation nuclei numbers are 200 to $2,000 \text{ n.cm}^{-3}$) and it is expected that the air which contains a lot of condensation nuclei might produce many more ice crystals in the expansion chamber, because the condensation nuclei which made water droplets in the chamber may act as freezing nuclei in the water droplets under the lower temperature conditions. In fact, adding some combustion by-products to the air to be tested before the expansion obviously resulted in the formation of many more ice crystals in the chamber under the same temperature conditions. In the chamber of the expansion counter, the degree of supersaturation appears to be very high, even though only momentarily. Thus it is suggested such condensation nuclei are very important for the formation of many ice crystals in high supersaturation environment in the temperature range between $\sim -20^\circ\text{C}$ and $\sim -37^\circ\text{C}$. In other words, many condensation nuclei in the air must act as freezing nuclei under ice-fog conditions.

In the air at temperatures lower than -37°C (diameter of water droplets is assumed about 10μ) some droplets would freeze spontaneously. In clean air with a very high moisture content, combination of homogeneous condensation and spontaneous freezing must result in a threshold temperature between -37 and -40°C . In polluted air in the same temperature range, such a threshold would not be recognized because the crystals can be formed by both homogeneous and heterogeneous nucleation on pure and polluted water droplets.

5. RELATIONSHIP BETWEEN CONDENSATION AND ICE NUCLEI AND ICE-FOG CRYSTALS IN THEIR CONCENTRATIONS

Although we obtained some data on the concentrations of ice nuclei in the air at a temperature of -35°C , we had better compare the concentration of ice-fog crystals to that of condensation nuclei (including nuclei acting as freezing nuclei), as discussed above. We can assume maximum value for the concentration of the condensation nuclei of $5 \times 10^6 \text{ p cm}^{-3}$ in the downtown area* and 10^4 p cm^{-3} in the outlying areas during ice-fog conditions, while the concentration of ice-fog crystals at a temperature of about -35°C in downtown Fairbanks is around 200 p cm^{-3} , at most 1000 p cm^{-3} . As was mentioned before, the temperature inversion during ice fog keeps all water vapor, solid dust, gases, and possibly liquid aerosols as well as cold air near the ground.

There is then no problem in finding sufficient nuclei for the observed ice-crystal concentration in the air of Fairbanks at low temperatures, especially temperatures below -37°C . In fact it seems that only 1/1000 of the dust particles in the city act as nuclei regardless of whether the nuclei are condensation or freezing-nuclei. We may ask what happens to the remaining 999/1000 of the dust particles which may be considered air pollution in the normal meaning. Apparently these dust particles are co-existing with ice-fog crystals. Benson (1965) stated

* This number will increase with the further development of human activity, and may become a serious problem for human health. The city council or members of city development planning group are urged to consider seriously such high contents of dust as well as hazardous gases, not only for the effect on ice fog directly, but also for the general health of the residents.

"The small ice crystals which make up ice fog are often associated with impurities. This is especially true of those formed from combustion products." He collected ice fog and snow crystals precipitated on polyethylene sheets at various places in and around Fairbanks. After melting those into water, he measured electrical conductance and also filtered particles suspended in the melted water precipitated. In these observations he found much heavily polluted water at the center of the city, while the outlying area was clear of pollution. He pointed out that "the electric conductance is, of course, due to free ions in the melt water." Furthermore he stated "They could be associated with the crystal nuclei which are found in each crystal, or they could have been concentrated on the crystal surfaces." However, according to our observations of concentration of dust particles (or condensation nuclei) using 14 μ pore sized Millipore filters to remove all ice-fog crystals and larger dust particles, we still had as many as about 10^5 p dust particles per cm^3 . This shows that huge numbers of particles are still co-existing with the ice-fog crystals. Also from the electron microscope study of ice-fog crystals we could not find many crystals which had much dust either on the inside or their surfaces. In other words, such dust or pollution must have been precipitated on the polyethylene sheets independently of ice-fog crystals.

6. ELECTRON MICROSCOPE STUDIES OF STEAM-FOG AND ICE-FOG CRYSTALS AND THEIR NUCLEI

Kumai (1964) was the first to try an electron microscope study of ice-fog nuclei in the Fairbanks area. The main purpose of an electron microscope study of such fog or cloud droplets, ice crystals, and snow crystals is to separate the nuclei of hydrometeor particles from unactivated dust particles which co-exist with the hydrometeors. Historically, Köhler (1925) concluded that most cloud nuclei must be sea salt particles. He collected bulk samples of cloud droplets or rime on a high mountain, chemically analyzed the collected water and found high concentrations of NaCl. However, in the electron microscope studies of cloud and fog nuclei by Kuroiwa (1951), Ogiwara and Okita (1952), and Yamamoto and Ohtake (1953 and 1955) it has been possible to inspect the nuclei of individual droplets separately from airborne particles other than water droplets. This work has led to the conclusion that most cloud or fog nuclei are very small combustion by-products, although a few large sea salt particles also have been found. Salinity of bulk water is controlled by the small numbers of sea salt particles. Measurements of bulk water could not have shown this. It is tedious work, but electron microscope studies are essential in the field of nucleation processes.

Kumai (1964 and 1965*) tried this for ice-fog nuclei after his successful work (1951 and 1963) on snow-crystal nuclei. He reported that most of the ice-fog nuclei were combustion by-products and 10 to 21% were clay particles. He also reported that all the ice-fog crystals he

* Co-authored by O'Brien.

collected had nuclei. However, in order to inspect such very small nuclei as residues of micron size ice crystals which were evaporated without melting, we must be certain we have a very clean film as the ice crystal support. If not, we can not distinguish between contamination due to poor preparation and true nuclei. Also the technique of identifying nuclei on the electron microscope screen with crystals on optical photomicrographs taken earlier of the same sample grids is difficult and time consuming even with a special grid having a finder pattern. In the present project, we tried to use the replication method for ice-fog crystals in the electron microscope, so that crystals and nuclei were both visible on the electron micrographs.

a) Smoke Samples:

Some samples of smokes which were considered to be possible sources of fog nuclei were taken and examined in the electron microscope. The specimens included car exhausts, smoke from oil - and coal-burning furnaces, exhaust smoke from a power plant, and smoke of burning dry grass or dead trees. The electron micrographs for them are shown in Figs. 9 to 12. Generally speaking, combustion for heating and power plants produced soot or carbon black only as solid particles, while car exhausts showed various shapes. Gasoline for cars includes lead compounds and other additives to prevent knocking. Also the characteristics of the exhaust vary from car to car, and as a function of motor adjustment, age of the car, etc. Sometimes car exhausts showed a granular structure as shown in Fig. 12. Smoke of dead plants showed very thin and semi-transparent structures on fluorescent screen in electron microscope.

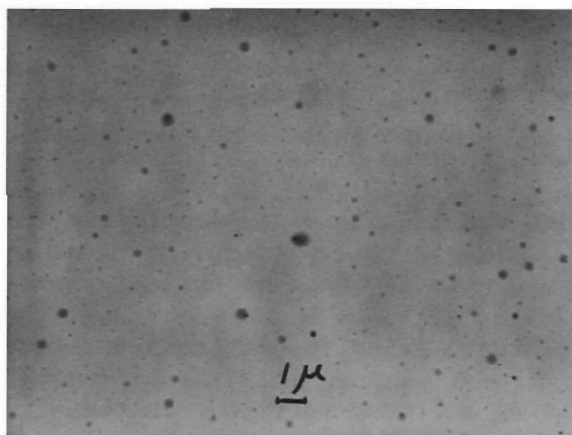


Fig. 9. Smoke from burning dry wood.

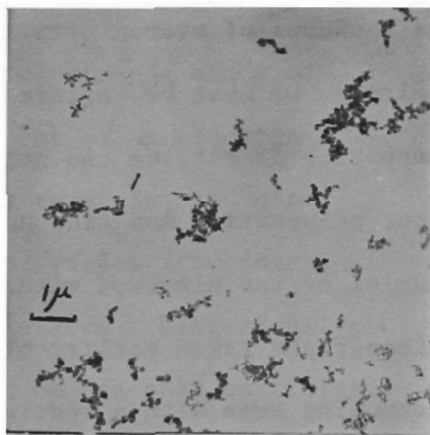


Fig. 10. Smoke from heating plant.

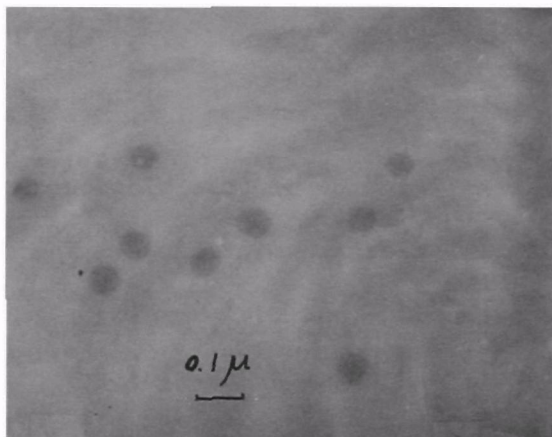


Fig. 11. Auto exhaust (English car MG).

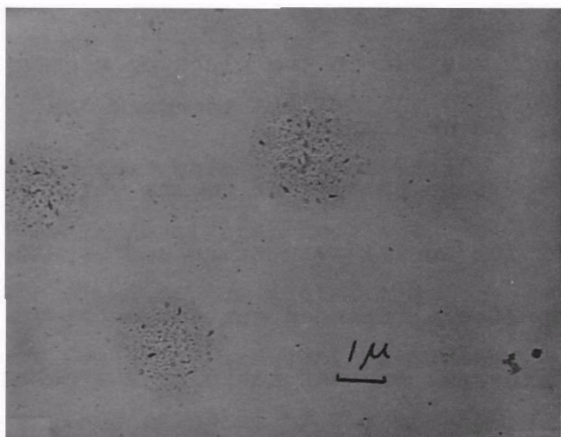


Fig. 12. Auto exhaust (Ford Falcon).

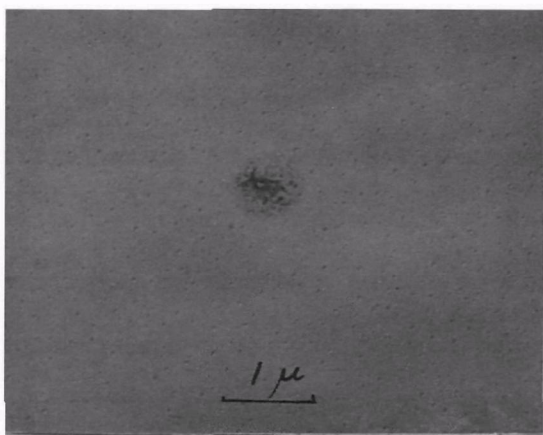


Fig. 13. Steam fog nucleus in fall season. The nucleus is presumed to be a combustion by-product.

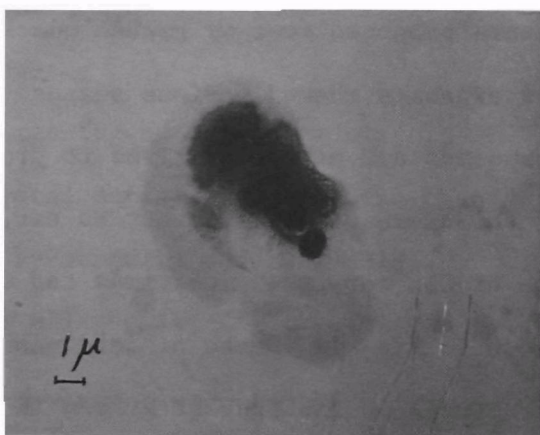


Fig. 14. Steam fog nucleus. The nucleus is identified as a sea salt particle.

b) Steam-Fog Nuclei:

On clear nights during the summer and fall seasons, steam fog usually develops due to radiative cooling of the air near the ground and the constant warm temperature of water surfaces especially near lakes. The mechanism of formation of steam fogs seems to be similar to that of ice-fog formation above open water except for absolute temperature. Under such conditions, fog can be seen above and around lakes or damp ground even in unpopulated areas or areas far from traffic. Steam-fog droplets were collected on electron-microscope grids and their nuclei were examined with the electron microscope. Most of the nuclei were identified as combustion by-products (see Fig. 13 as an example). In addition to the combustion nuclei, a few sea-salt particles have been detected as shown in Fig. 14. These nuclei were identified as in the report by Yamamoto and Ohtake (1953).

c) Ice-Fog Crystals and Their Nuclei:

1. Method of Making Specimens:

To prepare the ice-fog samples for electron-microscope examination, the vapor replication method was used instead of the liquid method. The liquid method has two main disadvantages: (i) the ice-fog crystals will be displaced and concentrated into a small portion of the slide glass because of the surface tension of the liquid, and (ii) the film is thicker than desired for use with the electron microscope. The vapor method, which was developed by Schaefer (1962), prevents any displacement of ice particles and produces good replicas for the electron beam. The exposure times for a slide glass coated with 0.5% formvar solution to be

in contact with chloroform vapor were determined by means of saturation vapor pressure over chloroform for various temperatures. On this matter, the only exposure time Schaefer (1962) gives is 20 seconds for -20C. The exposure times for chloroform vapor at various temperatures are shown in Table 5.

TABLE 5

Exposure Time for Vapor Method of Replication of Ice Crystals								
Ambient Temperature	(°C)	0	-10	-20	-30	-40	-45	-50
Exposure Time	(sec)	8	13	20	40	80	120	160

To prepare a specimen sheet mesh (grid) for the electron microscope, according to Tanaka and Isono's (1966) method, a collodion film and a layer of carbon were deposited between a formvar film and metal sheet mesh (see Fig. 15). The films can be made at room temperature and the carbon layer is deposited in a vacuum evaporator. These meshes with an outer layer of formvar were then cooled to ambient temperature and exposed to the ice fog. After the ice-fog crystals were allowed to deposit on the grids (which were normally on slides) for several minutes, the mesh was exposed to chloroform vapor in a closed petri dish for the time shown in Table 5. The exposure of the formvar film with ice crystals on it to chloroform vapor allows the film to soften, and because of surface tension the softened formvar covers the ice crystals. After exposing the film to the vapor, the slide glass is waved in the air to remove excess chloroform vapor from the slide. The slide glasses (or grids) should be kept cold and dry during the sublimation of the ice crystals after the replica

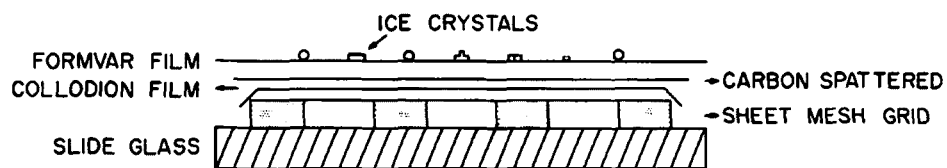


Fig. 15. Construction of sheet mesh for electron microscope examinations of ice-fog crystals.

is formed. The specimens made in this way are ready to be examined by regular electron microscope techniques including chromium shadow casting. Laboratory tests for permanency of replicas and for migration of nuclei were made prior to the ice-fog season. Under an optical microscope the real ice-fog crystals and their replicas deposited on a slide glass in a specially made glass container were observed during evacuation of the container. The results of the test were quite satisfactory.

To make a plain slide glass with replica, a simple formvar film can be coated on a slide glass rather than the three layers of film, and further procedures will be similar to those for grids. For thicker or larger crystals an increased thickness of formvar will be needed.

Direct collections of ice-fog crystals on specimen grids coated with formvar film without replication were also made during the 1965-1966 winter. An ice-fog crystal or any kind of hydro-particle, such as a steam fog droplet, will evaporate in an electron microscope because of the high vacuum inside. So we cannot see the outlines of the original ice-fog crystals and steam-fog droplets on a specimen grid. Up to date, the original positions of particles on the grids had been deduced from pictures taken with an optical microscope. Using these pictures, the exact positions of the ice-fog crystals or steam-fog droplets, even to the exact outline of ice particles, could be determined with accuracy as great as 1 to 2 μ by means of the "Specimen Position Indicator" built in the JEM-electron microscope. This method has also been used for checking the displacement of nuclei or other effects during the replication of ice-fog crystals.

Many specimens of ice-fog crystals and ice crystals for electron microscopic examinations were collected at different places and times. It was expected that the ice-fog crystals would have different kinds of nuclei according to their conditions of formation.

2. Size and Shape of Ice-Fog Crystals:

As was mentioned previously, the size distribution and shape of ice-fog crystals change with variations of temperature. Since ice-fog crystals have been collected only by the precipitation method for electron microscopy, the deduced size distributions and average shapes of ice-fog crystals may be different from the real ones. However, we tried to take electron micrographs of randomly sampled ice-fog crystals from sheet mesh grids. Even though the total number of pictures of ice-fog crystals at each station or total stations is not enough to allow construction of an accurate distribution, we can find average sizes of ice-fog crystals and compare them with the average sizes of ice-fog nuclei. Figures 16 and 17 show size distributions of both ice-fog crystals (including normal sized well shaped ice crystals) and their nuclei measured by electron microscopy, regardless of temperature, location and other conditions.

3. Sizes and Composition of Ice-Fog Nuclei and Electric Conductivity of Melted Ice-Fog Crystals:

The sizes of ice-fog nuclei are quite small in comparison with those of normal fog in cities of the temperate region, but similar to mountain fog or cloud nuclei. Figure 17 shows the size distribution of ice-fog nuclei. These sizes are almost in agreement with Kumai's result. However,

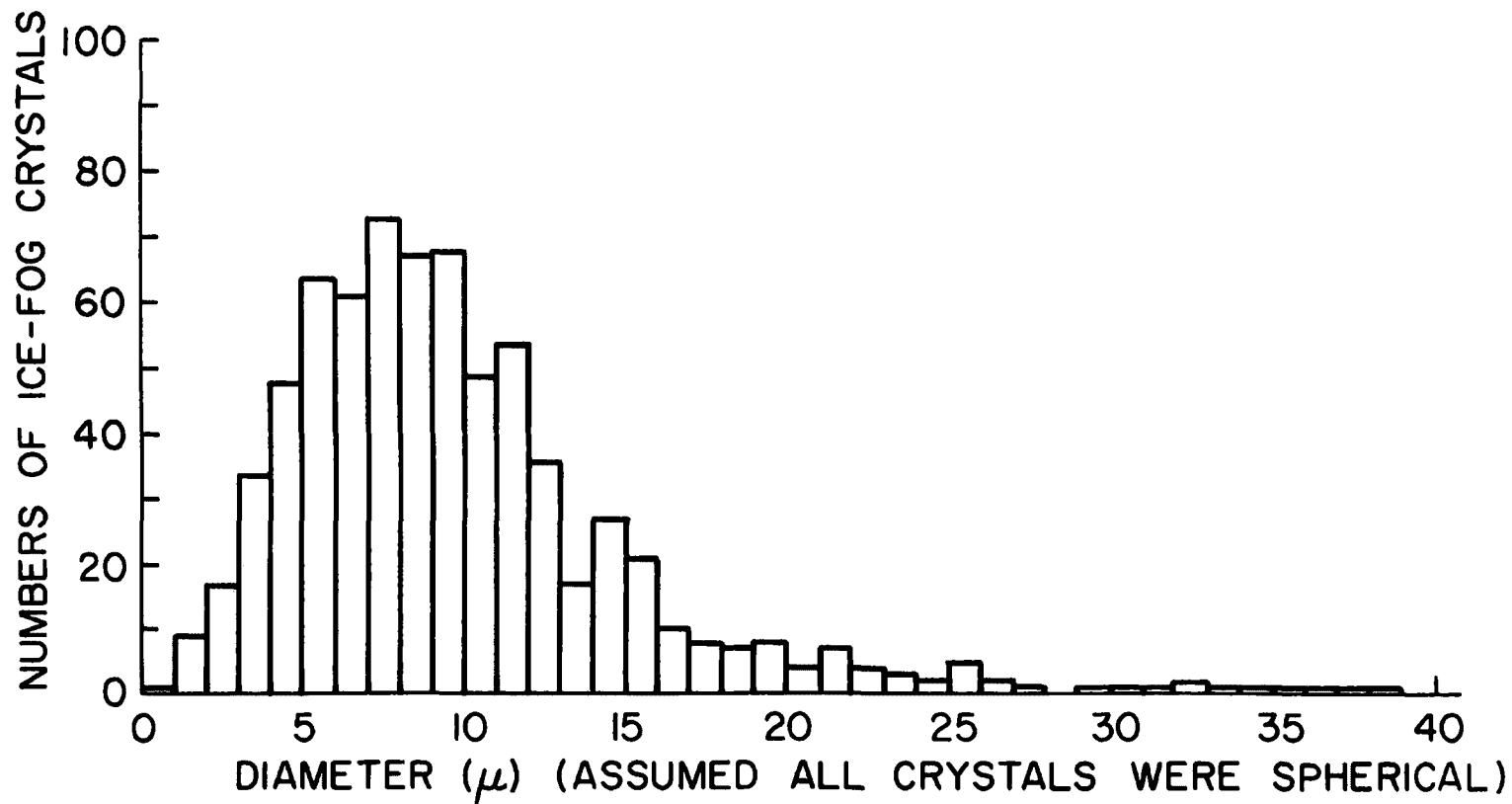


Fig. 16. Size distribution of ice-fog crystals examined under the electron microscope.

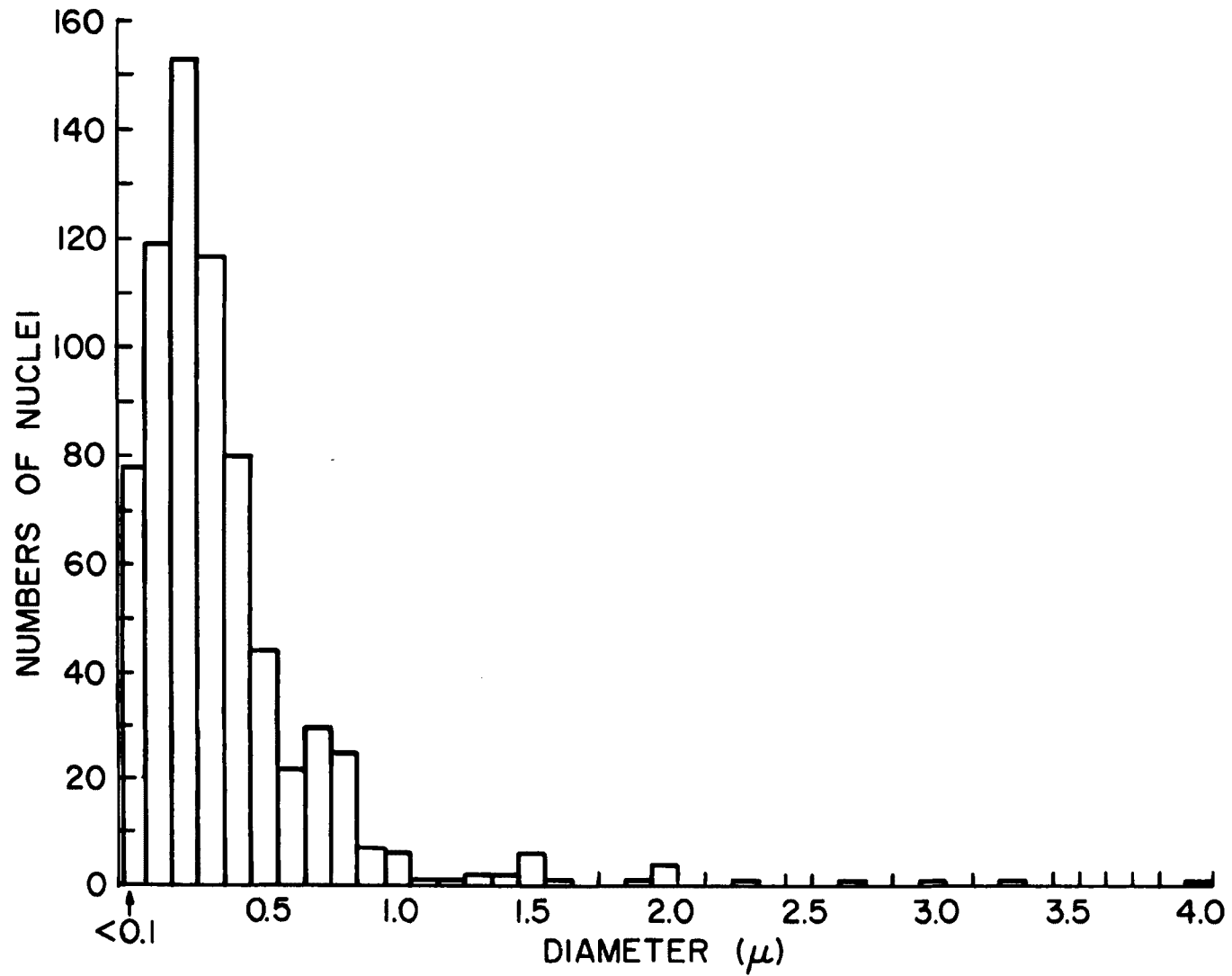


Fig. 17. Size distribution of ice-fog nuclei examined under the electron microscope.

generally speaking, it is difficult to determine whether a particle is a nucleus of an ice-fog crystal or a contamination particle in or on the collodion and formvar films. Even though we tried to make the films on sheet mesh (grid) as clean as possible, sometimes many minute particles could be found outside and inside the replicas of crystals. Based on the author's experience of electron-microscope study of fog and cloud nuclei, the nuclei of ice-fog crystals were distinguished from the contamination particles by aid of replication and shape of particles. However, since identification was difficult in some cases, we measured the most probable and the largest particle inside the replica. After improving our technique we found many ice-fog crystals containing no particles inside the crystal replica. The crystals with no particle inside of them show that the crystals were frozen spontaneously from supercooled water droplets which had homogeneously condensed from water vapor or sublimed onto small fragments of ice particles, although the last mechanism is not likely in the case of ice fog. If any small particle was found in the crystal we assumed it was a nucleus. This means that we might have underestimated the possibility of spontaneous nucleation in the formation of ice-fog crystals. However any particles outside of the replicas of ice-fog crystals were disregarded as contamination or as dusts which co-existed with ice fog in the air. Generally speaking, taking pictures of nuclei of ice-fog crystals with the electron microscope without replicas and referring to optical micrographs as Kumai (1964) did would give errors in the original locations of ice-fog crystals by as much as 5μ . This is dangerous, especially for the smallest sized crystals.

As can be seen in Table 6, 71 out of 713 crystals inspected by the electron microscope did not have any nucleus in the crystal replicas. Most of these were found in ice fog at Chena and Manley Hot Springs at temperatures lower than about -40°C . An example of ice-fog crystals is shown in Fig. 18. At the IAP site which is located near the open water area along the Chena River, we found no nuclei in about 12 percent of 110 ice-fog crystals we collected when the temperature was below -39°C . At other places such as on the University of Alaska campus we could sometimes find only very small nuclei or contaminations in the crystal replicas. At the center of city only 1.7 percent of 236 ice-fog crystals had no nuclei, and a few ice-fog crystals had many particles inside of the replicas and few or none outside. An example is shown in Fig. 19. These crystals were probably frozen from dirty droplets formed directly from some kind of exhaust such as car exhaust. On the other hand many ice-fog crystals even in the center of the city did not have large dust particles. These ice-fog crystals must have formed initially from the process of water vapor condensation under conditions of high supersaturation which are available from car, power and heating plant exhausts and from steam coming from open water.

Although we tried to identify the composition of the nuclei by use of the electron microscope and electron diffraction, we could not determine the composition very well, especially for the smallest size nuclei. Some nuclei were presumed to be only carbon black (Fig. 20) resulting from combustion. Using a morphological determination which was essentially the

TABLE 6

Percentage of composition of ice fog nuclei determined by electron microscope and electron microdiffraction. At the MUS site IC means ice crystal nuclei and IF means ice fog crystal nuclei.

Site	Total	Combustion by-product%		Soil Particle %		No nuclei %		Undertermined %	
MUS site IC	10	5	50	5	50	0	0	0	0
IF	236	222	94	6	3	4	2	4	2
IAP and slough	120	96	80	5	4	13	11	6	5
MUS power plant	52	50	96	2	4	0	0	0	0
U. of Alaska	84	73	87	3	4	2	2	6	7
BLM (along Highway)	32	27	85	2	6	2	6	1	3
Int. airport	59	54	92	1	2	3	5	1	2
Manley H. S.	32	22	70	0	0	9	28	1	3
Chena H. S.	88	50	57	0	0	38	43	0	0
Total	713	599	84	24	3	71	10	19	3

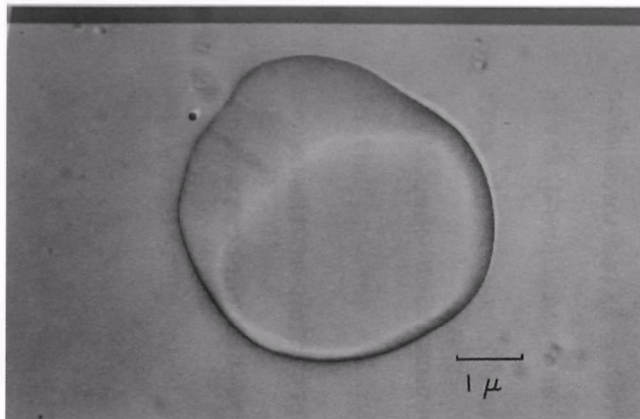


Fig. 18. Ice-fog crystal without nucleus, collected at Chena H. S. on December 31, 1968. Temperature was -45C.

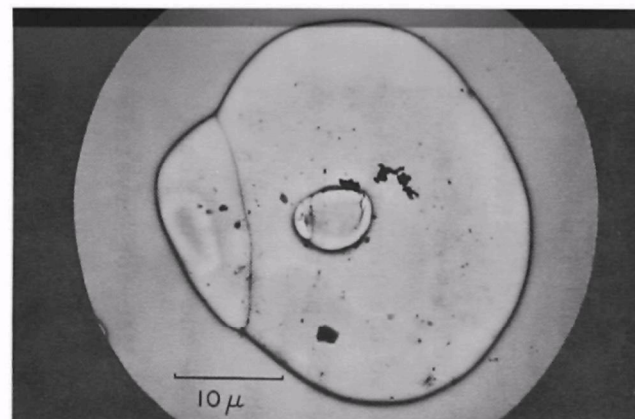


Fig. 19. Ice-fog crystal with many dust particles only inside of the crystal. The crystal was sampled at the MUS site, on January 2, 1969. Temperature was -45C.

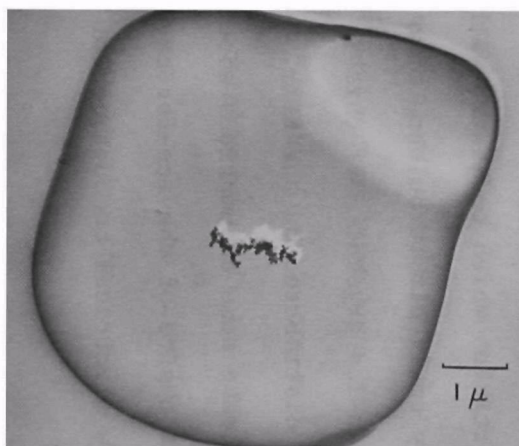


Fig. 20. Ice-fog crystal with carbon black as a nucleus. The crystal was collected near the IAP site on December 8, 1968. The white part at upper right of picture seems to be a kind of spicule formed from the crystal.

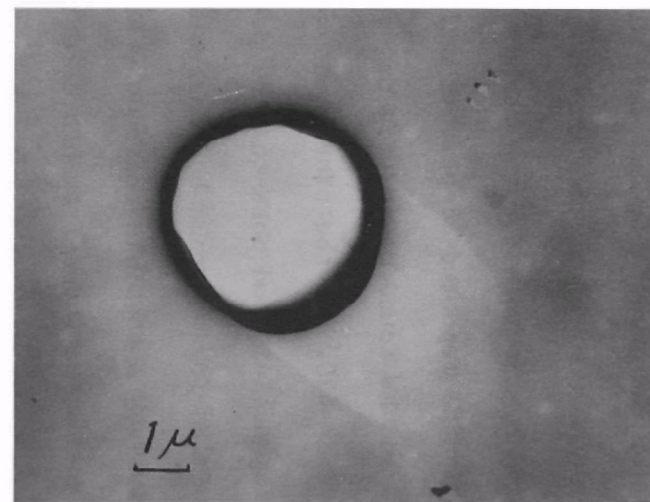


Fig. 21. Spherical ice-fog crystal with very small nucleus off center. The crystal was collected near the IAP site on December 21, 1965. Temperature was -36.4C.

same as Yamamoto and Ohtake's (1953), we found that most (more than 90 percent) of the ice-fog nuclei were classified as combustion by-products. Kumai (1964) found 74 percent and 90 percent of the ice-fog nuclei were combustion by-products for the temperatures of -37°C and -41°C , respectively. In addition he reported 21 percent and 10 percent of the nuclei were clay minerals and he found no ice-fog crystals without nuclei at the temperatures of -37°C and -41°C . On the other hand we found only a few soil particles as ice-fog nuclei, and more than 80 percent and 10 percent of the total number of ice-fog crystals had combustion by-product nuclei and no nucleus, respectively. A possible reason why Kumai did not find any ice-fog crystals without nuclei may come from his direct sampling on collodion film without replication. He might have missed the exact original positions of the ice-fog crystals on the collodion film under the electron microscope.

With our electron-microscope studies, there was no evidence of many chance dust particles or solid phase "air pollution" (other than ice fog) deposited on the surfaces of the ice-fog crystals. It is quite possible that the particles considered as contamination on the formvar films were the dust particles which coexisted with ice-fog crystals and were precipitated by small air turbulence onto the film and in rare cases on a replica of an ice crystal. If this is correct, then the particles should be randomly distributed on the film.

If we make some assumptions about the size and composition of the nuclei and the size of the ice-fog crystals, we can derive the concentration and thus the electrical conductance of the melted ice-fog crystals. If we

assume the composition of the nuclei to be KCl or H_2SO_4 , normalities of these solutions should be $4.16 \times 10^{-4}\text{N}$ ($= 3.1 \times 10^{-2} \text{ gm } \ell^{-1}$) and $5.83 \times 10^{-4}\text{N}$ ($= 2.9 \times 10^{-2} \text{ gm } \ell^{-1}$) for KCl and H_2SO_4 , respectively, assuming the average diameters of ice-fog crystals are 8μ and of ice-fog nuclei are 0.2μ , which were the estimated peaks of the size distributions of Figs. 16 and 17. Using these values we get the specific electrical conductance of melted ice-fog crystals as $54 \mu\text{mho cm}^{-1}$ and $225 \mu\text{mho cm}^{-1}$ for all the nuclei assumed to be KCl and H_2SO_4 , respectively. These values are of the same order of magnitudes as Benson's (1965) results from melted and filtered snow pack in the city. He reported the electric conductances were about $100 \mu\text{mho cm}^{-1}$ in the city and $10 \mu\text{mho cm}^{-1}$ in the outlying area; he also reported that a lot of water insoluble particulate matter was concentrated at the center of the city. In our data, however, all nuclei were assumed to be water soluble KCl or H_2SO_4 and their apparent diameters were measured as an equivalent circular area, after which we calculated the volume of the particles as spheres. Also the aqueous solution of H_2SO_4 was selected as the possible chemical material which gives the highest value of equivalent conductance of an aqueous solution. From this point of view, even though the present result agreed with Benson's (1965) observation, all the above mentioned values must have been overestimated in the present estimation due to the many assumptions in our reduction and the many water soluble and insoluble dust particles precipitated separately from ice-fog crystals in the case of Benson's. On the other hand, our analysis considered only visible nuclei, neglecting the possibility of

ions adsorbed on the crystals. For crystals on the order of 8μ , absorption effects would be negligible.

4. Position of Nuclei in Ice-Fog Crystals:

The positions of the nuclei of ice-fog crystals were examined by means of the replica technique and the Specimen Position Indicator which was previously described. Many nuclei of ice-fog crystals smaller than about 10μ diameter were found not in the center but rather away from the center of the crystals, especially in ice-fog crystals which had been collected when the air temperature was lower than -35°C . Figures 21 through 24b show some examples. Of course ice-fog crystals with no nucleus are excluded. In contrast the nuclei of ice crystals larger than 10μ diameter (which normally have well developed crystal faces) were at the exact centers of the ice crystals. Examples are shown in Figs. 25 and 26. This was also confirmed by direct collection with the aid of the Specimen Position Indicator. The probable explanations for these positions of nuclei may be as follows: The smaller ice-fog crystals must result from the freezing of supercooled water droplets. The supercooled water droplets are formed on condensation nuclei through water vapor condensing onto the nuclei. When the condensation nucleus grew into a water droplet, the nucleus could move by Brownian motion anywhere inside of the water droplet, because the water droplet is in the liquid phase. At the moment the water droplet freezes under temperatures lower than -30°C there is no reason for the center to be a preferential position for the nucleus. This explanation

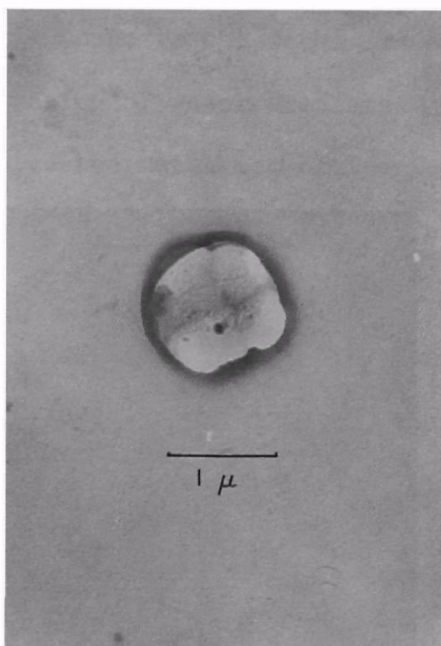


Fig. 22. Ice-fog crystal and its nucleus sampled at the Fairbanks International Airport on Jan. 1, 1966. The nucleus is presumed to be a combustion by-product. The temperature was -43.2°C .

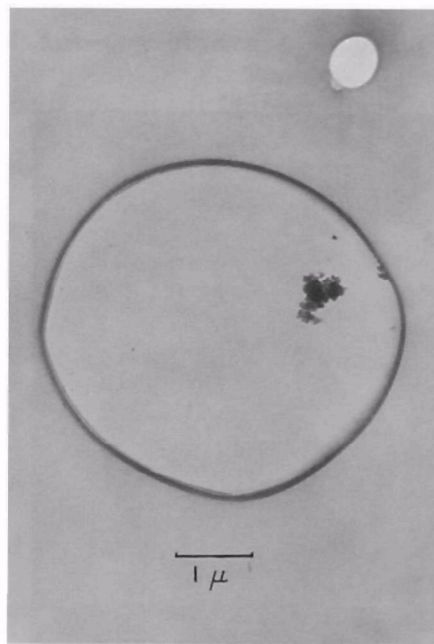


Fig. 23. A spherical ice-fog crystal with off center nucleus. The nucleus is presumed to be combustion by-product. The sample was taken near the Noyes slough in winter of Jan. 1965. The temperature is unknown.

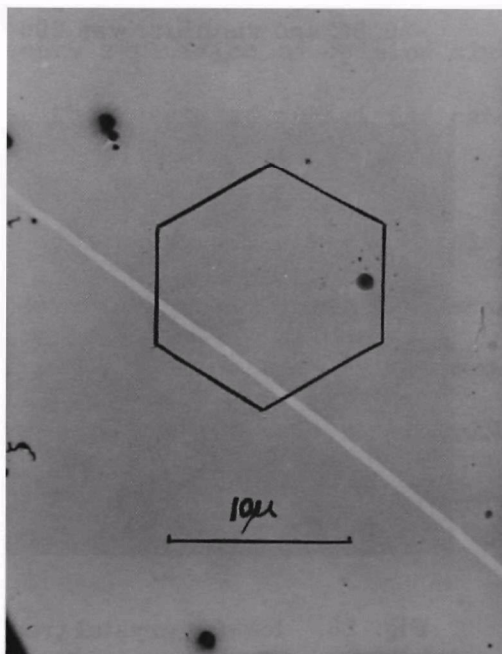


Fig. 24a. Nuclei of an ice-fog crystal. The nuclei were presumed to be combustion by-products, which may have been in the gas phase in temperate weather. Original outline of ice crystal also illustrated.

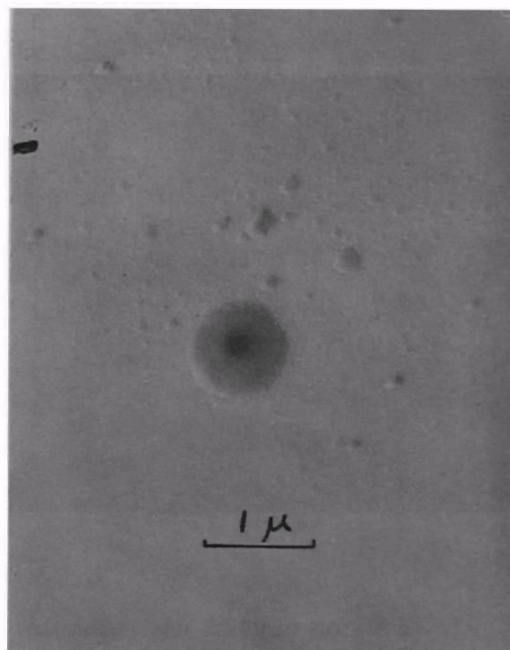


Fig. 24b. Enlargement of the nuclei of Fig. 24a. The crystal was collected directly onto collodion film at the MUS site on Feb. 21, 1966. The temperature was -32.9°C .

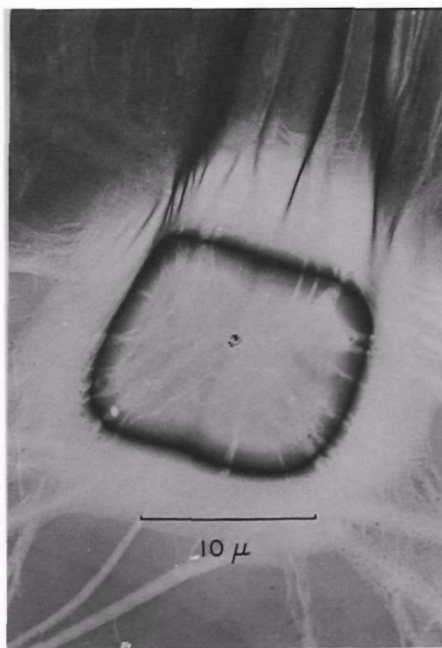


Fig. 25. Ice-fog crystal with nucleus at center. The nucleus was also presumed to be soot. The crystal was sampled at the MUS site on December 23, 1965.

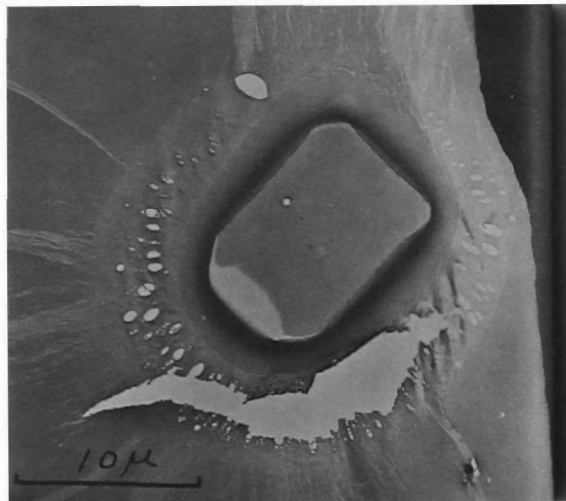


Fig. 26. Ice-fog crystal with nucleus at the center. The nucleus was presumed to be combustion by-product. The sample was taken near the University power plant on Jan. 6, 1966. The temperature was -39.8°C and visibility was 200 m.

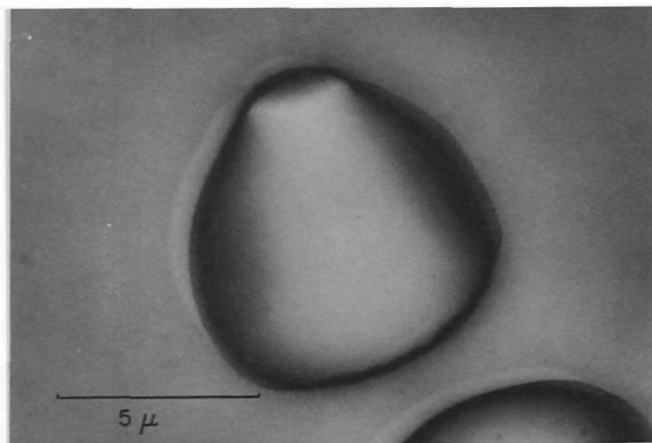


Fig. 27. Ice-fog crystal with spicule. The crystal was sampled on January 16, 1968 at the MUS site at a temperature of -38.2°C .

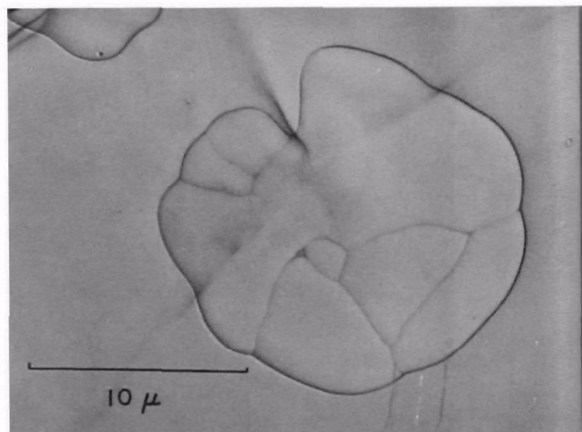


Fig. 28. Ice-fog crystal (replica) with boundaries or creases. The sampling was made at Chena H. S. on 31 December 1968 at a temperature of -45°C .

strongly supports the mechanism of formation of ice-fog crystals as being the freezing of water droplets. So far most ice-fog investigators have suggested the mechanism of ice-fog crystal formation to be the freezing of water droplets, but they did not have any strong observational evidence.

Another possible explanation for the off-center nuclei observed in many crystals would be general contamination of formvar films with many homogeneously nucleated crystals. However, the density of contamination on the portion of the formvar films not covered by crystals is too low to account for more than a small fraction of the observed off center nuclei.

Larger well formed crystals which have nuclei at their centers may have grown by sublimation onto very small ice-fog type crystals which probably passed through a liquid phase rather than directly sublimating onto nuclei. If the droplet was small enough, the displacement of the nucleus from the center of the final large crystal would be undetectable. This concept represents a revision of opinion since Ohtake (1967), in which it was assumed that centered nuclei indicated initial crystal formation by sublimation.

5. Spicules on Ice Fog Crystals:

Many nearly spherical or columnar ice-fog crystals appeared to have a sort of projection when viewed under the electron microscope (Henmi, 1969). Because there was some possibility that the projections were formed only on replicas of ice-fog crystals, it was confirmed under the optical

microscope that many ice-fog crystals suspended in silicone oil had such projections or spicules. Figure 27 is an example of a crystal with a spicule which was probably produced by the Bally-Dorsey effect (Dorsey 1948, Blanchard 1951). Concerning the spicules, Dorsey stated as follows: "As freezing proceeds, the pressure of the enclosed water rapidly increases, the temperature changing but little. The pressure may rupture the surface ice at some weak spot. A jet of very slightly supercooled water then issues through the break, its surface freezes promptly, forming a tube which grows at its tip, and through which water continues to flow until the pressure is sufficiently relieved or the tube has become blocked with ice." In the case of small droplets, say 10μ , at -40°C temperature the surface tension is strong and the blocking of the tube rapid so that the spicules may not grow as large as for the case of larger drops. All the fog particles found at large enough distances from the water source were solid ice (see chapter 8), which effectively rules out the possibility that the spicules were formed on unfrozen droplets hitting the slides.

Spicules thus appear to be an excellent indicator that particles carrying them have frozen from a supercooled liquid phase. The crystals shown in Figs. 20 and 27 were almost certainly formed from supercooled droplets. On the other hand, the crystals shown in Figs. 25 and 26 do not have spicules, and may have grown by sublimation after initial freezing. This phenomenon also supports the idea that the ice-fog crystals originate from freezing of supercooled water droplets. The size and shape of ice-fog crystals near open water are essentially the same as those of water droplets

very near the open water, although near open water in the city we can find other sizes and shapes of crystals which have drifted from beyond the open water.

6. Sintering of Ice-Fog Crystals and Structure of Ice-Fog Crystals:

Some electron photomicrographs of ice-fog crystal replications had a line or several lines as can be seen in Figs. 19 and 28. The crystal of Fig. 28 was collected in replica at Chena Hot Springs, and has many lines on the picture. These lines are likely to be boundary lines of ice-crystal grains, because the ends of the lines seem to separate the crystal into several parts. Another crystal which was also taken at Chena Hot Springs and has no nucleus is shown in Fig. 29. This crystal has a line in the middle which appears to divide the crystal into two coagulated parts. Under an optical microscope we could not find many of these lines because of the poor resolving power compared with that of an electron microscope. The explanation of this appearance has not been clarified.

Kumai (1964) reported 65.5% of the ice-fog crystals sampled at -39°C in Fairbanks were combined crystals (formed by sintering of two or more spherical crystals) and 8.5% of those were columnar crystals with a boundary (formed by sintering of two spherical ice crystals). Hobbs (1965) supported Kumai's observation by theoretical considerations. However the photomicrograph in Fig. 7a of Kumai's paper seems to show that the slide glass had been exposed to ice fog for too long a time and probably many ice-fog crystals stuck together on the slide rather than in the air. In fact in Kumai's Fig. 7b which was taken at the temperature of -41°C such a

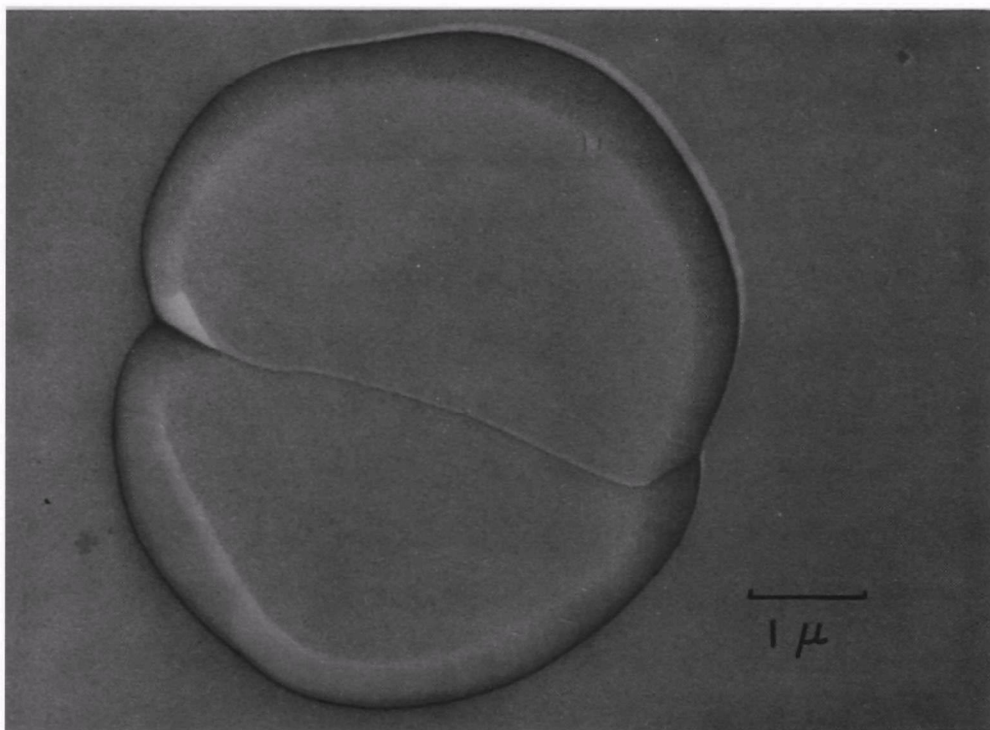


Fig. 29. Ice-fog crystal at Chena H. S. The crystal has a line in the middle and was found on the same specimen mesh as the crystal shown in Fig. 28.

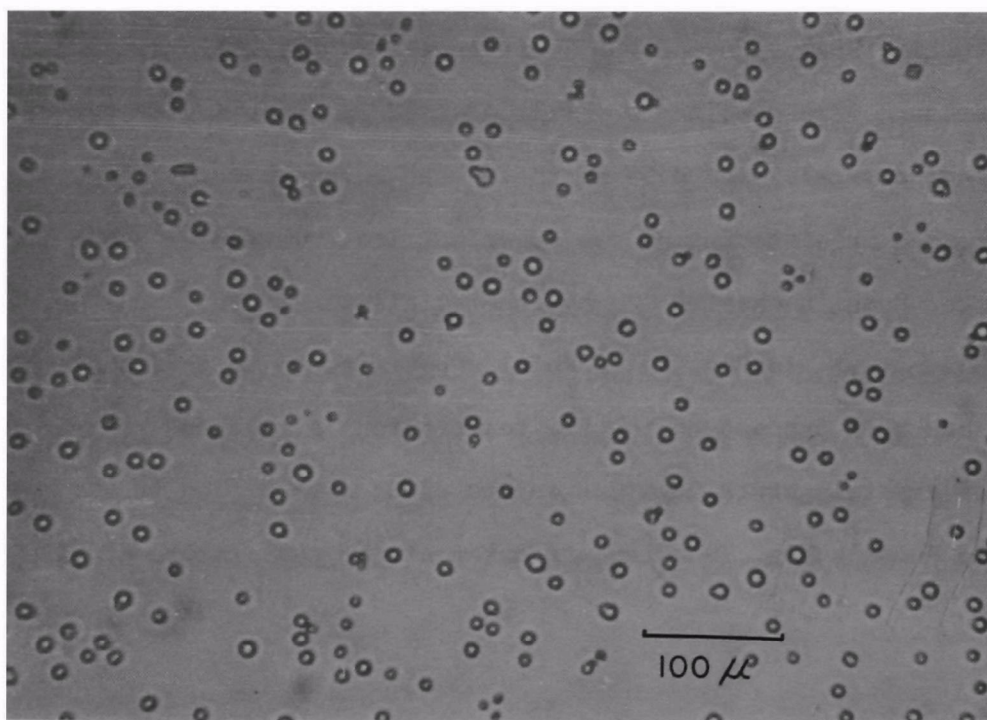


Fig. 30. Optical microscope picture of ice-fog crystals at Chena H. S. Temperature was -45°C .

high percentage of "aggregated crystals" does not appear. This must result from the collection of an appropriate number of crystals by precipitation on the glass slide. According to the present observations (see next chapter), irregular shaped crystals were only 6% and columnar crystals with a boundary on each crystal were less than 8% for the temperature range of -38 to -40°C . One might attribute the scarcity of the aggregated crystals of Kumai's Fig. 7b to the lack of a water film between ice particles to be bounded at the "critical temperature -41°C as spontaneous freezing".

Kumai considered that the combination of two small spherical ice-fog crystals through the sintering process resulted in a column crystal with a boundary, and if three crystals were sintered, the aggregation would produce a three pointed bullet crystal. Such sintering of crystals will occur even at -40°C as Hobbs stated if the crystals collide. Hobbs estimated that the time needed for sintering to occur between two ice-fog crystals of 5μ radius each at -40°C must be 760 seconds. Furthermore, according to him, this time of 760 seconds is easily expected in ice fog in which crystals fall in the 10 m thickness (height) of usual ice fog. Even though the available travel time of ice-fog crystals is much more than 760 seconds because the ice fog is normally 50 m thick and crystals are usually drifting almost horizontally, in order to sinter two ice-fog crystals, they should contact or almost contact each other for as long as 760 seconds. This is almost impossible in the actual ice fog.

Thus now we have arrived at the point of checking the possibility of collision of two ice-fog crystals. Since the average falling speed of ice-fog crystals is less than the turbulent velocity of air in ice fog as was described in the previous chapter, their relative motion should be controlled by Brownian random motion of each ice-fog crystal rather than aerodynamical motion due to differences of falling speeds. Fletcher (1966) summarized the theory for coagulation of aerosols, using the development of a basic equation by Smoluchowski for liquid suspension and their application to aerosols by Whytlaw-Gray and Patterson, and to give an idea of numerical magnitudes gave an equation for reasonably homogeneous aerosols as follows:

$$-\frac{1}{n} \frac{dn}{dt} \approx 10^{-6} n \left(1 + \frac{10^{-5}}{r}\right).$$

Here r is the radius of an average particle in cm, n is the particle concentration in particles cm^{-3} and t is time in hours. From this equation if we assume a particle diameter of 10μ and initial concentration of 1500 particles cm^{-3} , we find that it takes about 220 hours for the concentration to decrease to 1000 particles cm^{-3} (after coagulation, 50% of the particles are two-particle aggregates). 220 hours is far beyond the lifetime of a fog particle, or even of most ice fogs. Also Fletcher (1966) remarked on the coalescence of water droplets:

"In a typical cloud there may be perhaps 300 droplets cm^{-3} , all roughly 10μ in diameter. Equation (4.12) (same as the above equation) then states that the collision efficiency is only $0.1 \text{ cm}^{-3}\text{hr}^{-1}$ or $30 \text{ m}^{-3}\text{sec}^{-1}$. This represents a completely

negligible proportion of the cloud droplets during the life of an ordinary cloud, so that second collisions with these larger droplets virtually never occur. Collisions due to Brownian motion can thus be neglected as a mechanism for the production of appreciable numbers of larger droplets. With Brownian motion neglected and the effect of gravity considered, the problem now becomes an aerodynamic one".

The microscope picture (Fig. 30) of ice-fog crystals which was taken at Chena Hot Springs at -45°C , not only fails to show many aggregated crystals, but also has no columns with boundaries. Thus we arrive at the conclusion that the sintering of ice crystals may be neglected in the case of ice fog. The columnar crystal with a boundary at the middle is considered to be a twin crystal rather than a crystal formed through the sintering process.

Even though we had a narrow monotonic peak in the size distribution of ice-fog crystals at Chena Hot Springs, which indicates the infrequency of aggregation in both the liquid and solid states of water, we found lines similar to grain boundaries in the smallest sized ice crystals, as can be seen in Figs. 28 and 29. Considering the points discussed above, it is suggested that these grain boundaries may be attributed to abnormal thermal distribution in the water droplets or ice crystals at the time of their freezing. This concept would also cover the mechanism of formation of twin or poly-crystalline crystals. An attempt was made to look at such crystals under a polarizing microscope. All columnar crystals showed mono-orientation. However, a few irregular crystals showed a brilliant portion and one or more dark portions with different angles of rotation of the microscope stage. Figure 31 shows a sketch of such ice-fog crystals. The three different parts were brilliant alternately with rotation of the stage. This crystal was presumed to be composed of three differently oriented

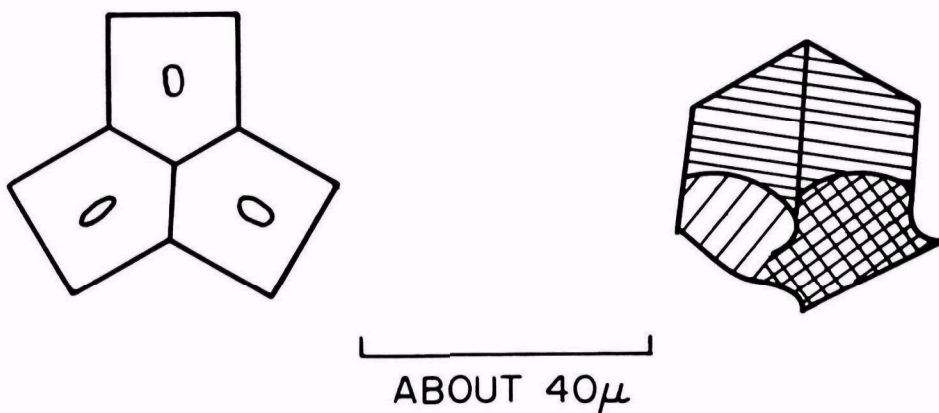


Fig. 31. Sketch of two ice-fog crystals under a polarizing microscope. The crystals were collected at the MUS site at a temperature of -37°C .

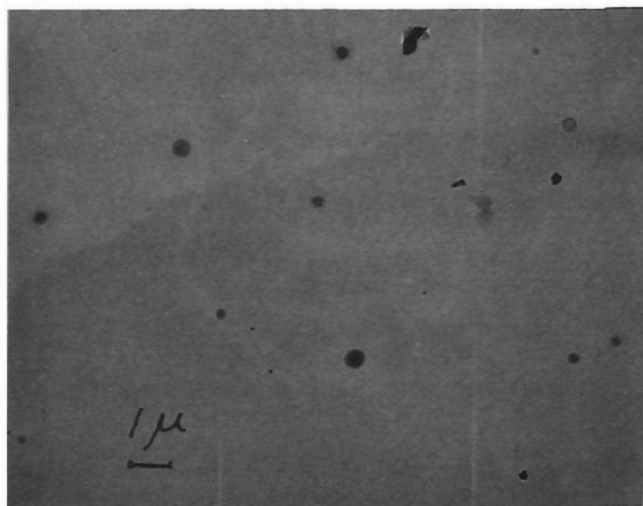


Fig. 32. Nuclei which were not the ice-fog nuclei in ice fog.

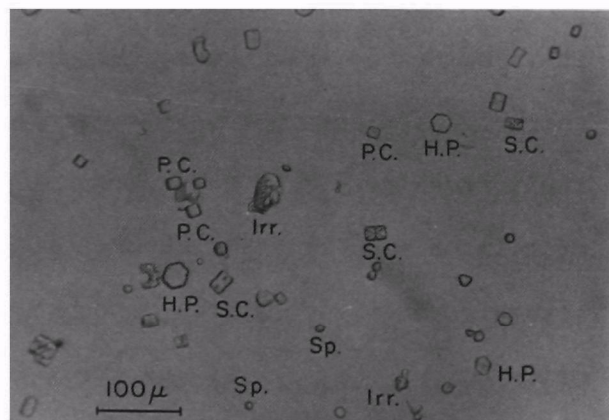


Fig. 33. Optical microscope picture of the types of ice-fog crystals taken at the MUS site. Temperature was -33.5°C . HP. : Hexagonal Plates, Sp. : Sphericals, P.C. : Plain Columns, S.C. : Skeleton Columns and Irr. : Irregular Crystals.

crystal grains. The approximate fraction of these crystals was only a few percent of the total ice-fog crystals at -37°C . On two occasions we found that the bright portion continuously moved from one side to another as the stage was rotated. Those must have been wedge-shaped column crystals. Unfortunately, there was no chance to use a good polarizing microscope, especially for taking a picture at high magnification. Another possible explanation is that the formvar film may have developed wrinkles during the replication process, even though Fig. 29 does not seem to support this idea. Further study is needed. The question might be solved by use of a scanning electron microscope.

d. Inactive Nuclei in Ice Fog:

As was previously mentioned, we have about 10^6 particles cm^{-3} of total condensation nuclei in the atmosphere of Fairbanks city. However, the concentration of ice-fog crystals during ice fog was about 200 crystals cm^{-3} . The role of the inactivated nuclei is of interest. For this reason, the inactive nuclei during ice fog in the air filtered by a Millipore filter, pore size 14μ , have been taken on specimen grids for examination by electron microscope. The use of the Millipore filter to restrict ice-fog crystals from coming into the specimen grid also removes some of the nuclei as mentioned before. Although we have only three electron micrographs for them, the inactivated nuclei were presumed, from their shape, to be combustion by-products from car exhaust or other hygroscopic materials. And such nuclei seemed to be essentially of the same composition as ice-fog nuclei. See Fig. 32 as an example.

7. OPTICAL MICROSCOPE STUDIES OF ICE-FOG CRYSTALS

A. The Effect of Temperature and Humidity on Ice-Fog Crystals

1. Sampling Method for Ice-Fog Crystals:

In order to study the size distributions, the mean diameters, the precipitation rates and the concentrations of ice-fog crystals, the crystals were collected on microscope slides covered by a thin film of silicone oil. A box of size 10 cm x 10 cm x 10 cm was used to shelter the slides from surface winds. In most cases, exposure times were 20 minutes, after which the ice fog crystals collected on the slides were immediately photomicrographed. This was a use of the precipitation method which has many disadvantages compared with the methods previously mentioned.

According to our pre-observations, there was apparently a temperature dependence of the solid water content of ice fog, i.e. we had no ice fog, slight and heavy ice fog at the temperatures of -20, -30 and -40C, respectively (refer to later chapter). Thus, it is necessary to know the temperature dependence of concentrations, precipitation rates and solid water content of ice fog. By the precipitation method, it is impossible to obtain the absolute values as indicated previously, but it may be possible, if we use a large amount of data, to obtain approximate average values.

Ambient temperatures were measured by means of a bimetallic thermometer whose accuracy was better than $\pm 0.2^{\circ}\text{C}$. Temperatures and most humidities were observed simultaneously when ice-fog crystals were sampled, so that the effect of ambient humidity on ice-fog crystals could be studied.

2. Method of Analysis:

a. Determination of the Diameters:

The diameters of ice-fog particles were measured from the photomicrographs enlarged to a magnification of 300. The Carl Zeiss TGZ3 Particle Size Analyzer was used to determine the diameter of each crystal. To obtain mean diameters for each sampling time, 500-2000 ice-fog crystals were measured.

b. Classification of the Shapes of Ice-Fog Crystals:

Thuman and Robinson (1954c) classified ice-fog crystals into the following three types: Hexagonal plates, prismatic columns, and droxtals (equant solid particles with rudimentary crystal faces). Kumai (1964) studied the size distributions of two types of ice-fog crystals, hexagonal plate and spherical.

It is, however, necessary to classify ice-fog crystals more precisely in order to study their growth process. Therefore, in the present work, ice-fog crystals are classified into the following five types:

1. Hexagonal plates
2. Plain columns
3. Skeleton columns (columns with inner designs or a boundary)
4. Sphericals
5. Irregulars

"Irregular" means that the particles cannot be classified into any of the four preceding types. In Fig. 33, a photograph of typical representatives of each type is shown.

3. Results and Discussion:

a. Mean Diameters of Ice-Fog Crystals:

Sixty-five samples were taken in the temperature range -30 to -41°C under ice-fog conditions. The relationships between the mean diameters of different types of ice-fog particles and temperatures are shown in Figs. 34 to 39. From these figures, the following facts may be inferred:

1. Although data are scattered, the mean diameter of ice-fog crystals is obviously a linearly increasing function of temperature.
2. The dependence on temperature of sphericals, however, is much less than that of other types of crystals.
3. The mean diameters of skeleton columns are larger than those of plain columns.
4. Hexagonal plates show the largest mean diameters.
5. Above the temperature of -35°C , the mean diameters of each type are more scattered than below -35°C .

It is probable that the scattering of the mean diameters is mainly due to the variation of wind direction at the sampling time, because there are many sources of ice-fog crystals.

According to Thuman and Robinson (1954a), the mean diameters of ice-fog particles are statistically logarithmic functions of temperature. The mean diameters obtained here are slightly smaller than those obtained by them. In addition, their results show that generally the largest crystals are columns and the second largest are hexagonal plates. On the contrary, our results show that the largest are hexagonal plates, and the second largest are skeleton columns. For purposes of comparison, their results are shown in Figs. 35 and 38.

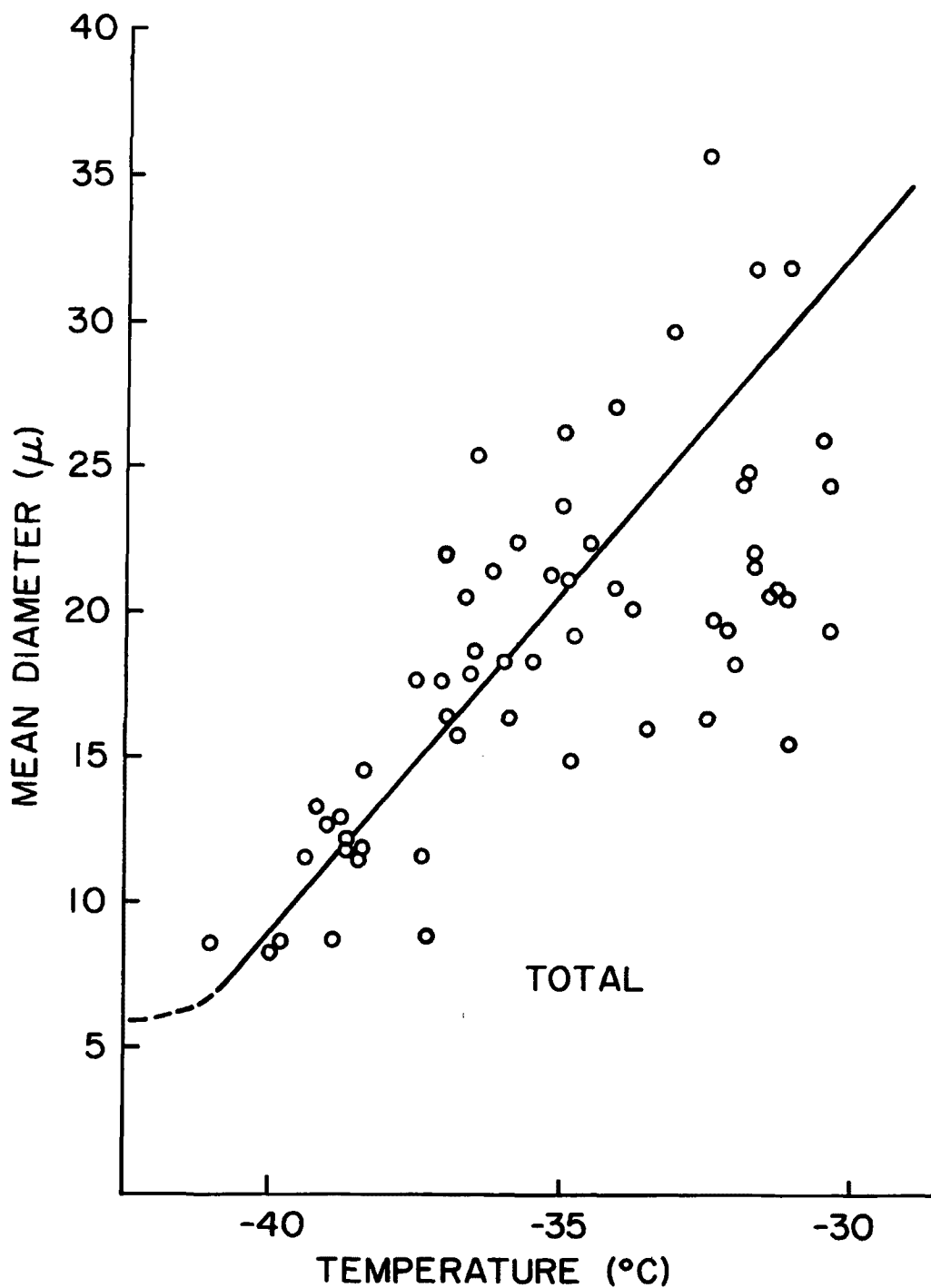
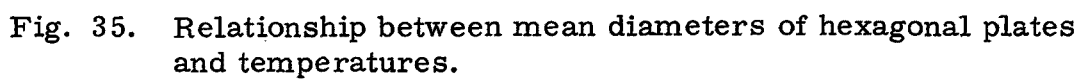


Fig. 34: Relationship between mean diameters of total ice-fog crystals and temperatures.



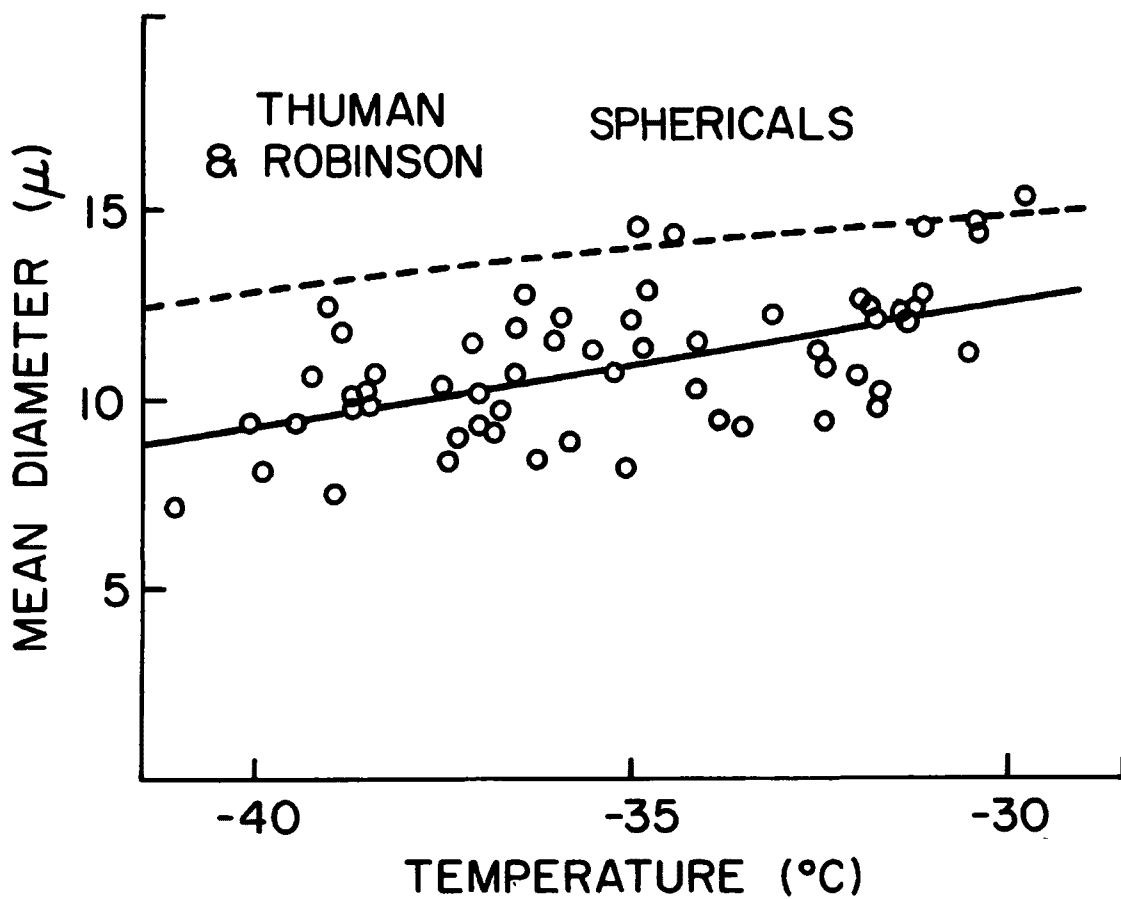


Fig. 36. Relationship between mean diameters of sphericals and temperatures.

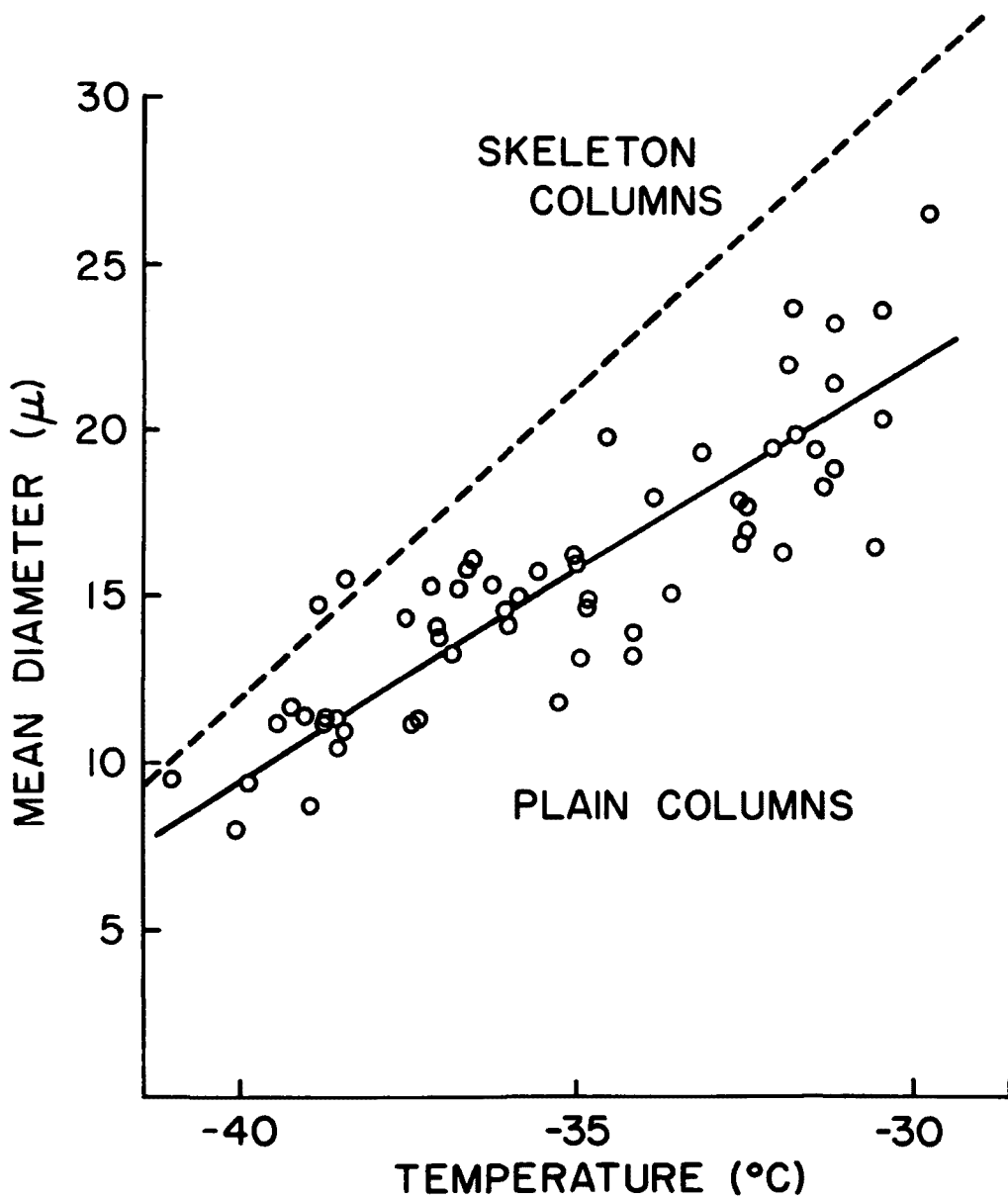


Fig. 37. Relationship between mean diameters of plain columns and temperatures.

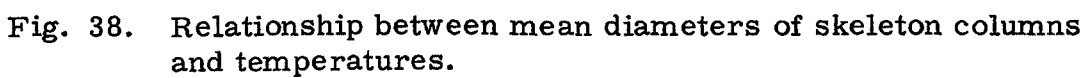


Fig. 38. Relationship between mean diameters of skeleton columns and temperatures.

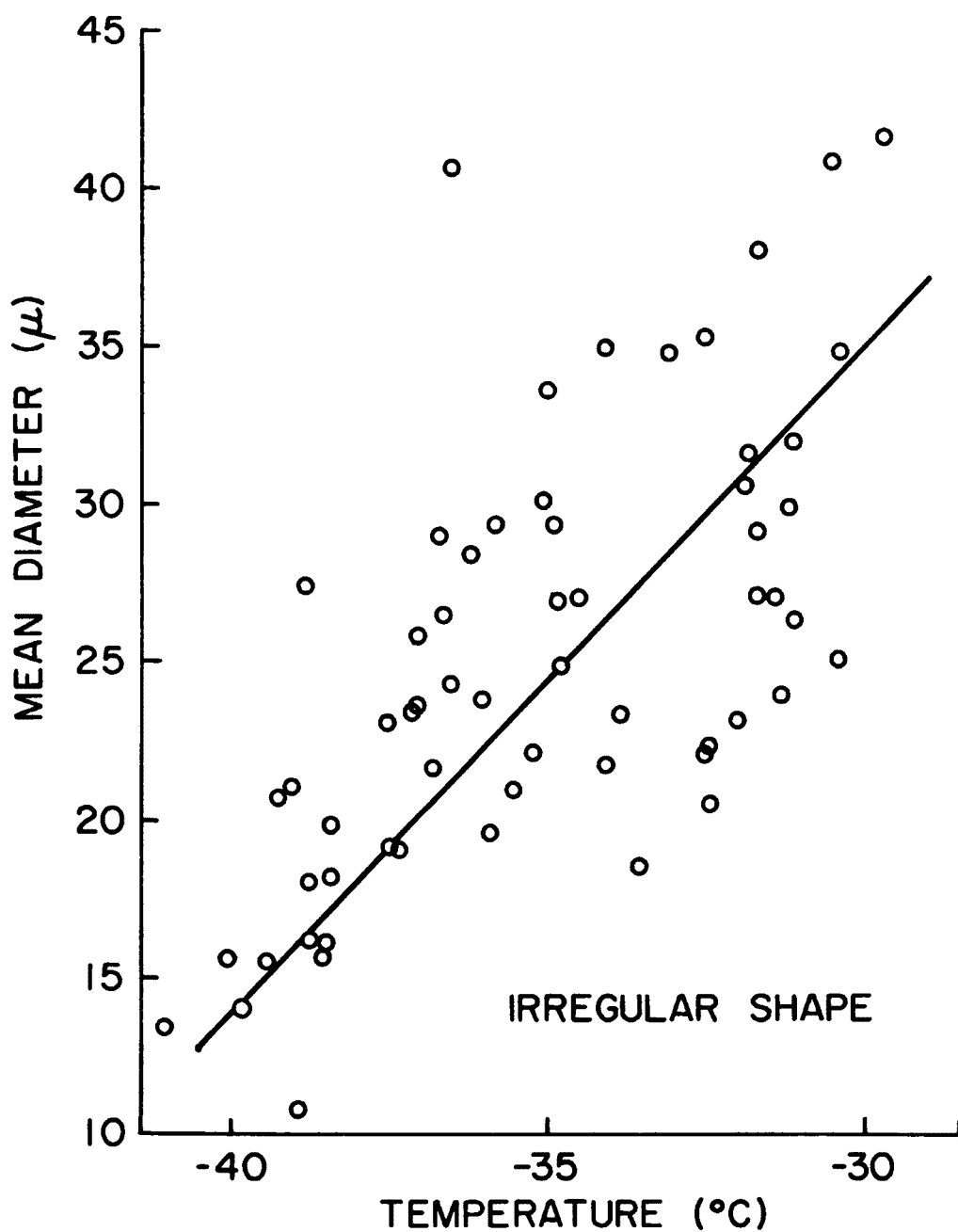


Fig. 39. Relationship between mean diameters of irregular shaped crystals and temperatures.

The differences between their results and ours are probably due to the following reasons: 1) Different location for sampling, 2) different classification of types, and 3) different scaling methods. Thuman and Robinson defined the diameter as the mean length of a line which approximately bisected the area of the profile of an ice-fog crystal. The bisecting line is taken parallel to a fixed direction, irrespective of the orientation of each crystal. However, in our case, the diameter is defined as that of a circle whose area is equal to that of the profile of an ice-fog crystal.

In an experiment using a diffusion cloud chamber, Kobayashi (1956) observed the following successive changes in shape of the precipitating ice crystals after silver iodide seeding:

Droxtals and hexagonal columns (or plain columns)

—————> Hexagonal simple plates

—————> Hexagonal simple plates with skeleton structure

—————> Sector forms and droxtals.

The interesting point is that hexagonal simple plates with skeleton structure are formed after hexagonal simple plates. This seems to suggest that the skeleton columns are formed by the growth of plain columns, which explains the fact that the mean diameters of skeleton columns are larger than those of plain columns. Furthermore, from the change of ice crystal shapes observed by Kobayashi and the fact that the mean diameters of sphericals are almost independent of temperature, it is inferred that the sphericals represent the initial stage of growth.

b. Size Distribution and Percentage Distribution of Types of Ice-Fog Crystals:

Figures 40, 41 and 42 show the mean size distributions of ice-fog particles in the temperature ranges -31.0 to -32.9°C , -35.0 to -36.9°C and -39.0 to -41.0°C , respectively. Each figure is obtained by averaging 7 to 10 different sets of data. From the figures it is obvious that the lower the temperature becomes, the narrower is the breadth of distribution of crystal size.

From the percentage distribution of five ice-fog crystal types, which is shown in Fig. 43, it is evident that the percentage of sphericals becomes suddenly predominant below -37 or -38°C . Such spherical crystals must be formed near the observation site through the freezing of supercooled water droplets which then undergo very little further growth. The temperature of -37 or -38°C may be considered as a threshold temperature of the small nuclei being active as freezing nuclei in the supercooled water droplets or that of the spontaneous nucleation (homogeneous freezing) of 10μ diameter water droplets which do not have any nucleus. Furthermore, the ratio of the percentage of skeleton columns to that of plain columns decreases with decreasing temperature, which seems to imply that the probability of the growth from plain column to skeleton column decreases with decreasing temperature.

c. Numbers of Precipitated Ice-Fog Crystals:

Using the data obtained by the precipitation method, the number of precipitated ice-fog crystals N_H is plotted against temperature in Fig. 44. It can be seen that although the data are scattered, there is a definite tendency for N_H to increase exponentially with decreasing

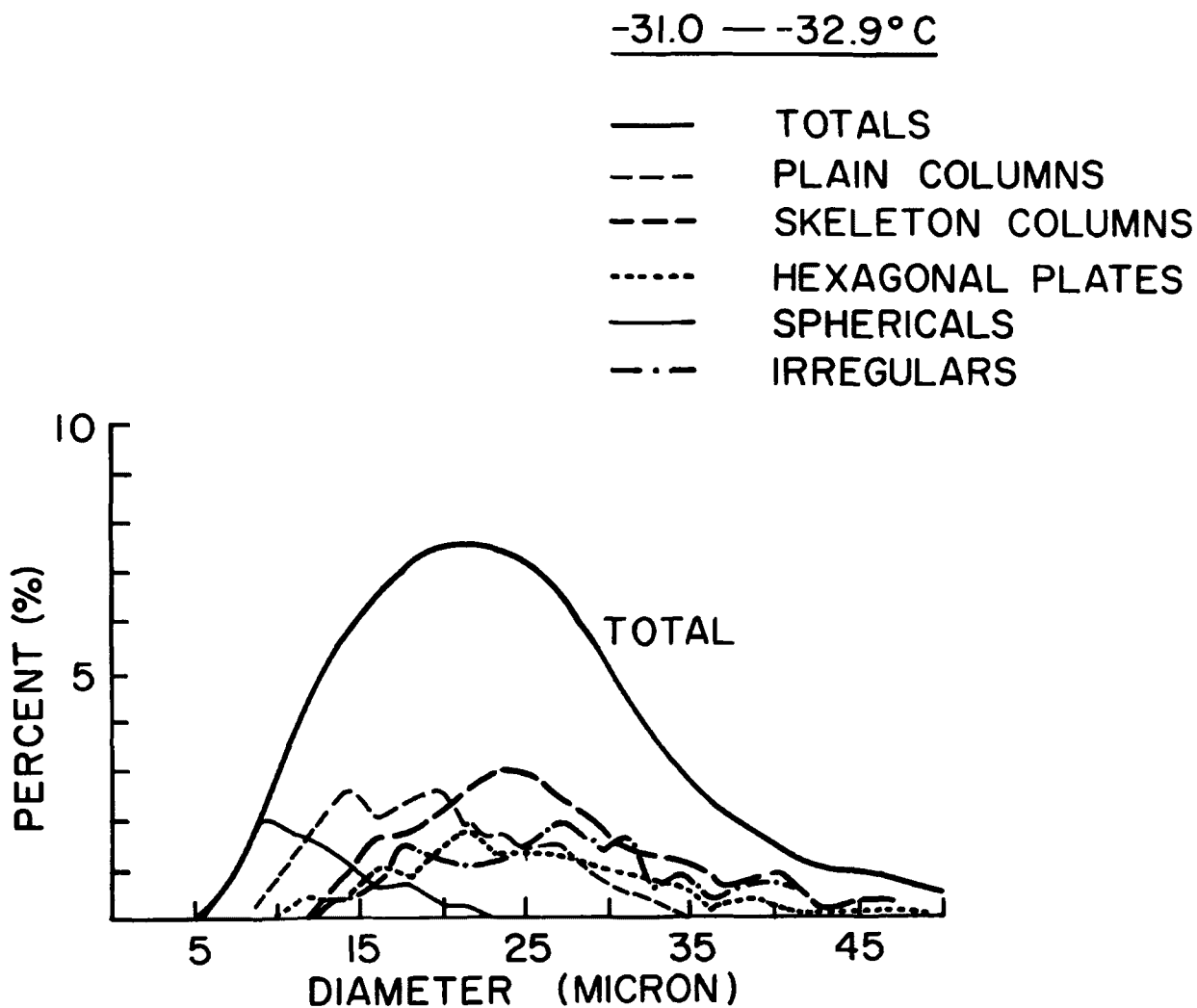


Fig. 40. Mean size distributions of various shaped ice-fog crystals for temperature range -31.0 to -32.9C.

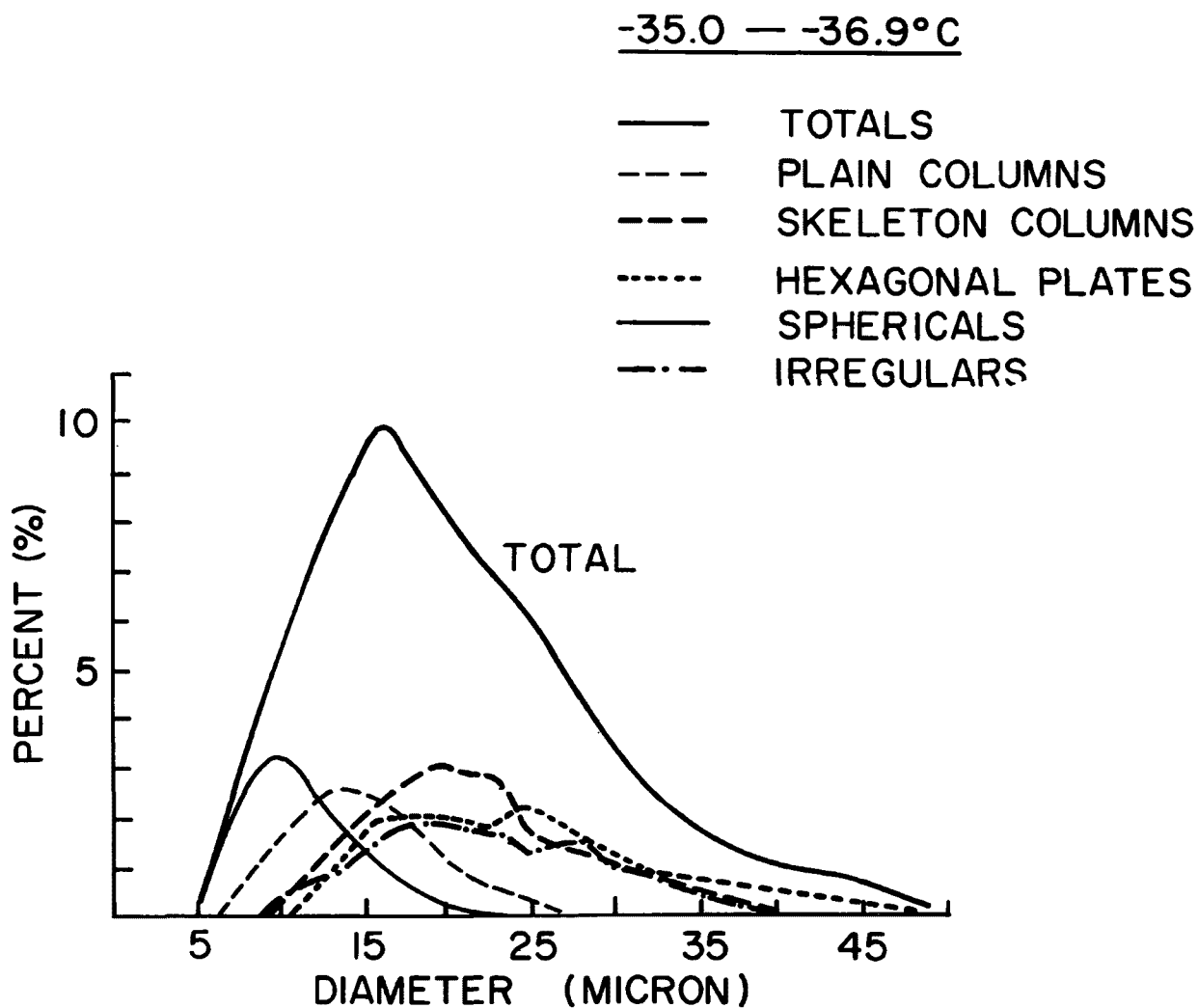


Fig. 41. Mean size distributions of ice-fog crystals for temperature range -35.0 to -36.9°C.

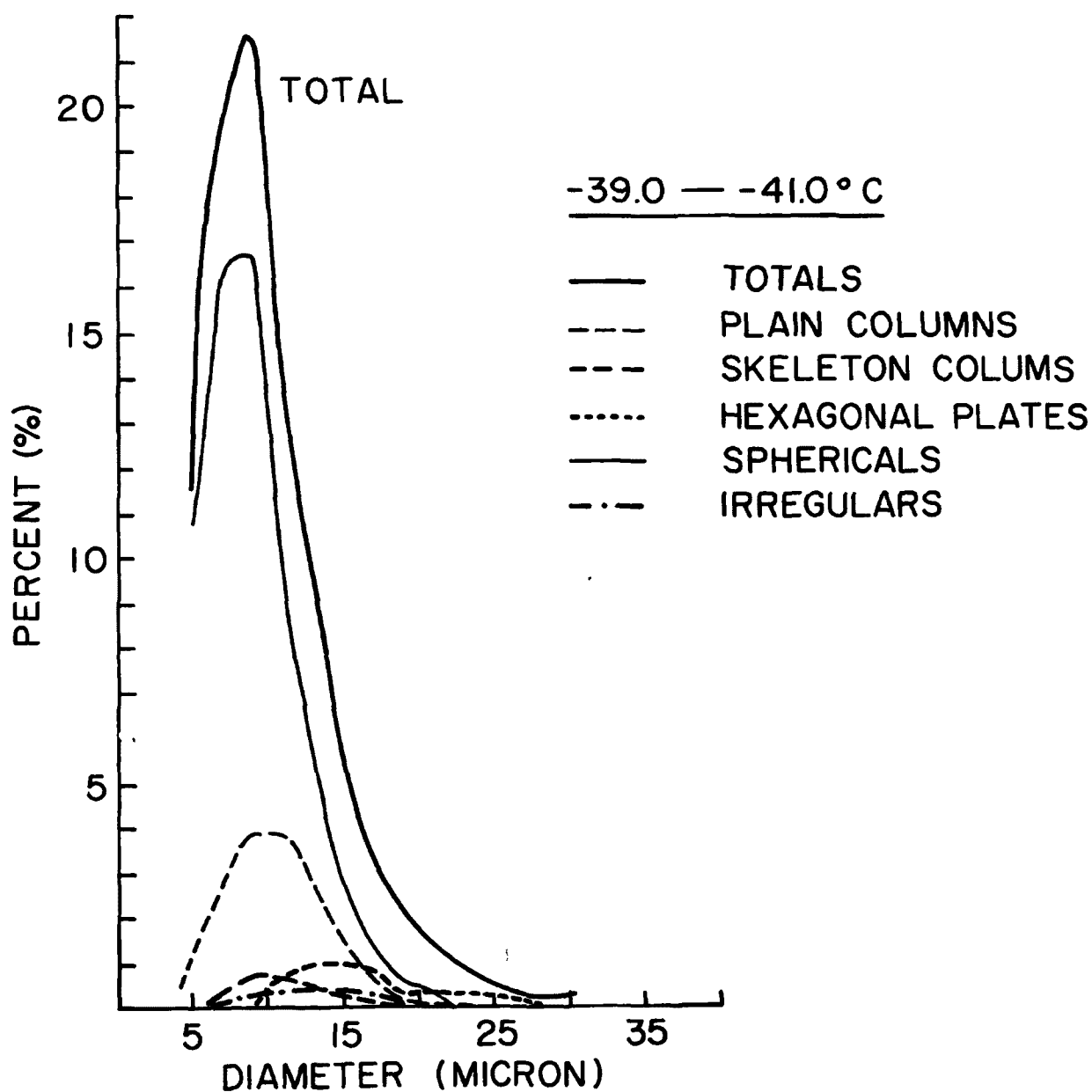


Fig. 42. Mean size distributions of ice-fog crystals in various shapes for temperature range of -39.0 to -41.0C.

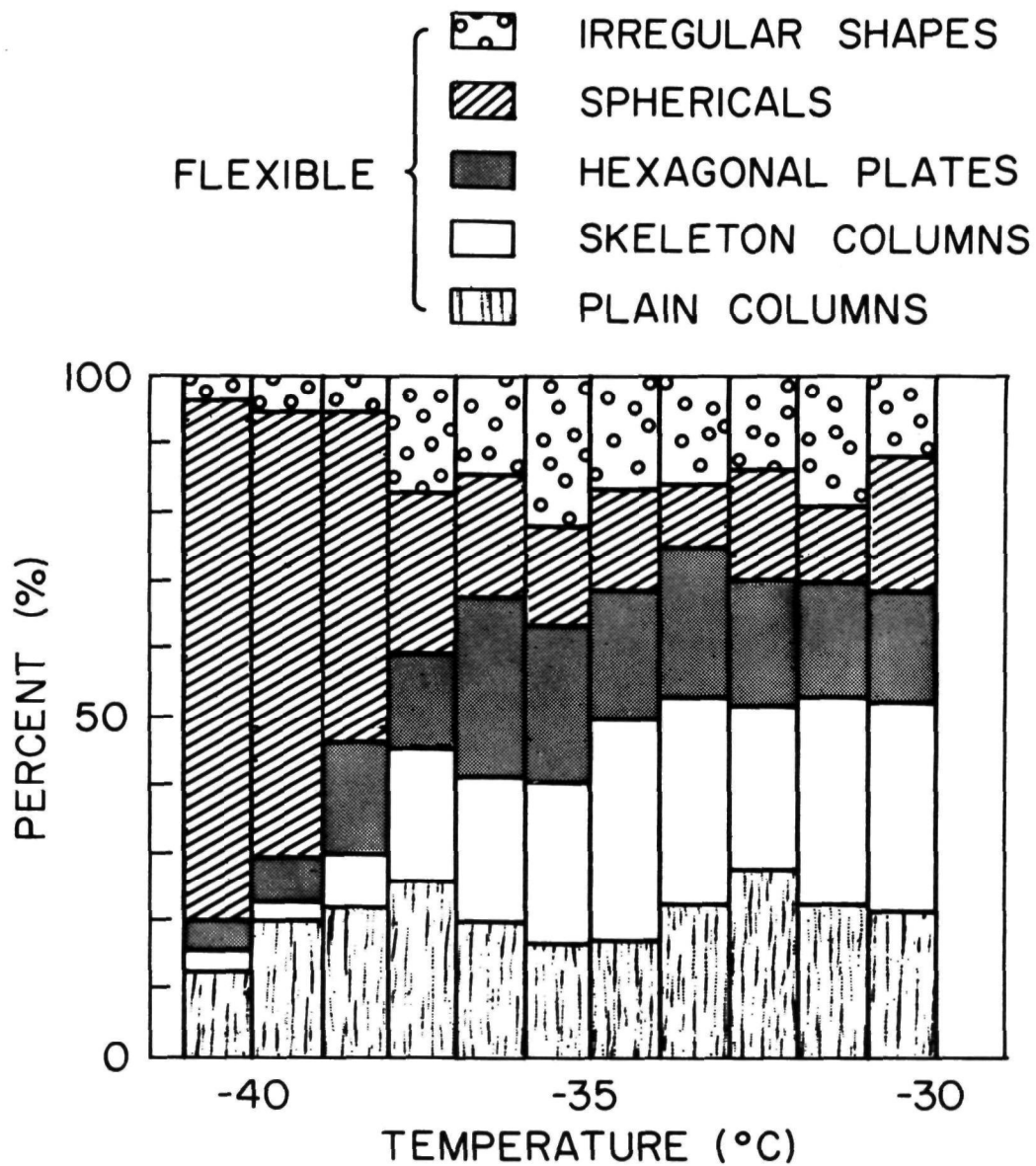


Fig. 43. Percentage distribution of the shapes of ice-fog crystals.

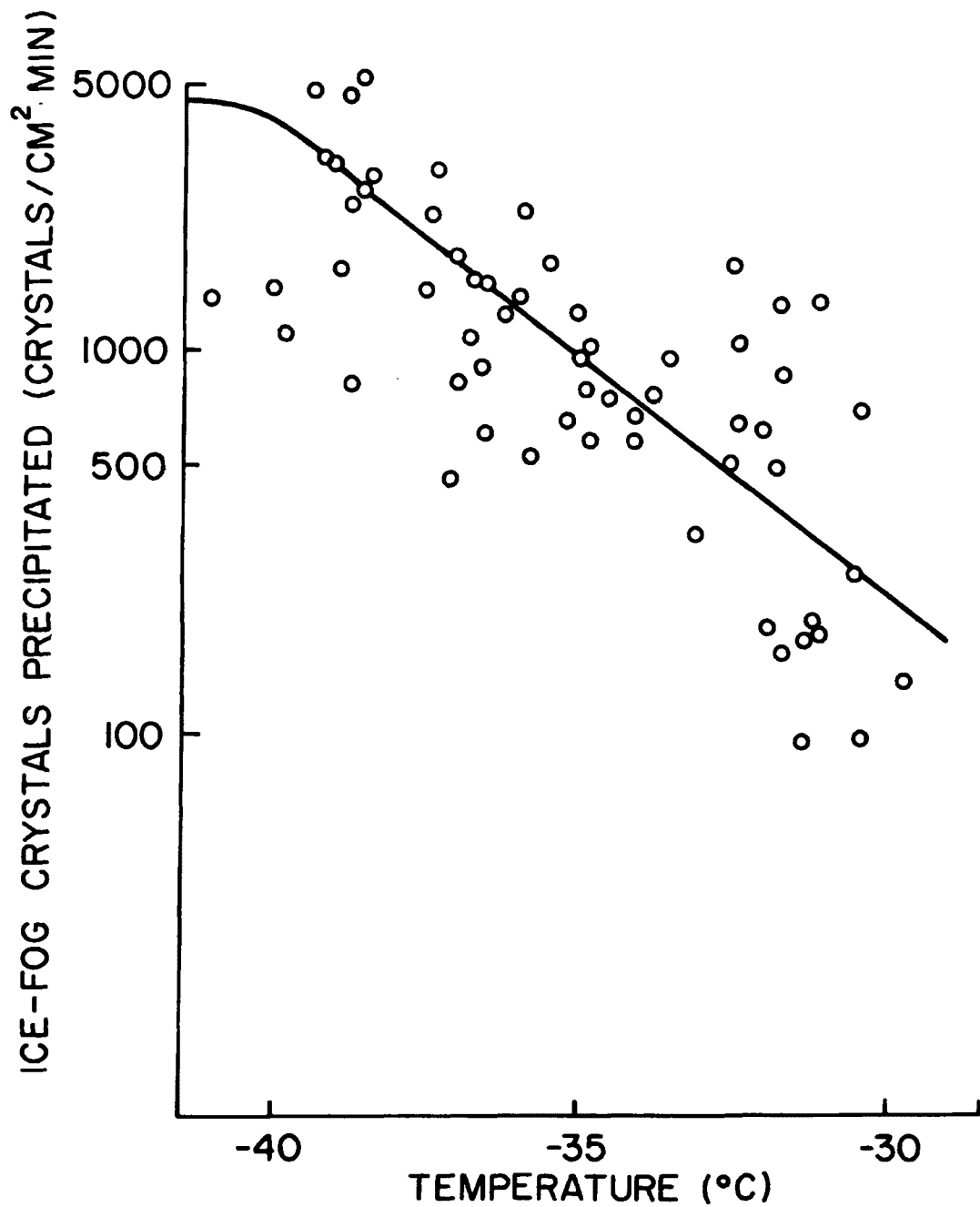


Fig. 44. Numbers of ice-fog crystals precipitated versus ambient air temperatures.

temperature. The change in N_H with temperature is given by the following equation derived empirically from Fig. 44.

$$N_H = 4.7 \times 10^{-2} \exp (-5.4 \times 10^{-2} T)$$

where T = temperature in degrees Celsius.

This increase in the number of precipitated crystals with decreasing temperature might be expected for two reasons: 1) the lower saturation vapor pressure at lower temperatures would lead to the production of more droplets for the same vapor input, and 2) the probability of activation of air pollutants as freezing nuclei, as well as the number of natural freezing nuclei, increases with decreasing temperature (Fletcher, 1962). According to prior work (Benson, 1965), data obtained by the precipitation method gave smaller values than are correct, due to upward winds. Therefore, in reality the gradient of the line may be steeper than that in Fig. 44, because there are more small particles at low temperature than at higher temperature. However, for temperatures lower than about -40°C the numbers of precipitated crystals tended to be constant in downtown Fairbanks. This might be due to a drop in the number of automobiles running. In addition, if spontaneous freezing takes place around -40°C reason (2) above is no longer valid below -40°C and a change in the form of dependence of N_H on T would be expected. The tendency for the curve in Fig. 44 to flatten for temperatures lower than -40°C might be due to spontaneous freezing.

d. Precipitation Rate and Solid Water Content of Ice-Fog Crystals:

Next, we calculate the precipitation rate and the solid water content of ice fog, assuming the lines drawn in Figs. 34 and 44 give the

average values of the mean diameter and precipitated number of ice-fog particles, respectively, as functions of temperature.

From Stokes' law, the terminal velocity v_τ of a spherical ice particle is given by

$$v_\tau = \frac{2}{9} \frac{\rho_i - \rho_a}{\eta} g r^2,$$

where

ρ_i = density of ice

ρ_a = density of air

η = viscosity of air

g = acceleration of gravity

r = radius of ice-fog particle

The precipitation rate $R(\text{g cm}^{-2} \text{ min}^{-1})$ of ice fog crystals is given by

$$R = \frac{4}{3} \pi \rho_i r^3 N_H,$$

when N_H is the number of ice crystals precipitated on a unit area during unit time. The solid water content (g cm^{-3}) of ice fog is given by

$$W = \frac{4}{3} \pi \rho_i r^3 N_H v_\tau^{-1}$$

Using these equations, the precipitation rate R and the solid water content W are obtained and listed in Table 7 and drawn in Fig. 45. The precipitation

TABLE 7

Mean Values of Precipitation Rates and Solid Water Content of Ice Fog (by precipitation method)

Temperature (°C)	Crystals Precipitated N_H ($\text{cm}^{-2} \text{min}^{-1}$)	Mean Diameter of Ice-Fog Crystals D (μ)	Terminal Velocity for Mean Size of Ice-Fog Crystals v_T (cm sec^{-1})	Precipitation Rate R ($\mu\text{g cm}^{-2} \text{min}^{-1}$)	Solid Water Content W (g m^{-3})
-30 (in city)	240	32.7	3.47	4.01	0.019
-32 (in city)	425	28.0	2.55	4.43	0.029
-34 (in city)	750	23.3	1.78	4.26	0.043
-36 (in city)	1350	18.5	1.12	4.08	0.061
-38 (in city)	2300	13.9	0.62	2.94	0.078
-40 (in city)	4200	9.1	0.27	1.51	0.094
(-47) (in city)	(3889)				(0.055)
Kumai -39 (in city)	2302	-	-	0.691	0.07
Kumai -41 (airport)	832	-	-	0.0287	0.02
Benson <-30 (in city)	no observation	-	+	2.18 (mean)	0.21
Benson <-35 (in city)	no observation	-	+	2.94 (mean)	
Benson (outlying area)	no observation	-	?	0.02	0.07

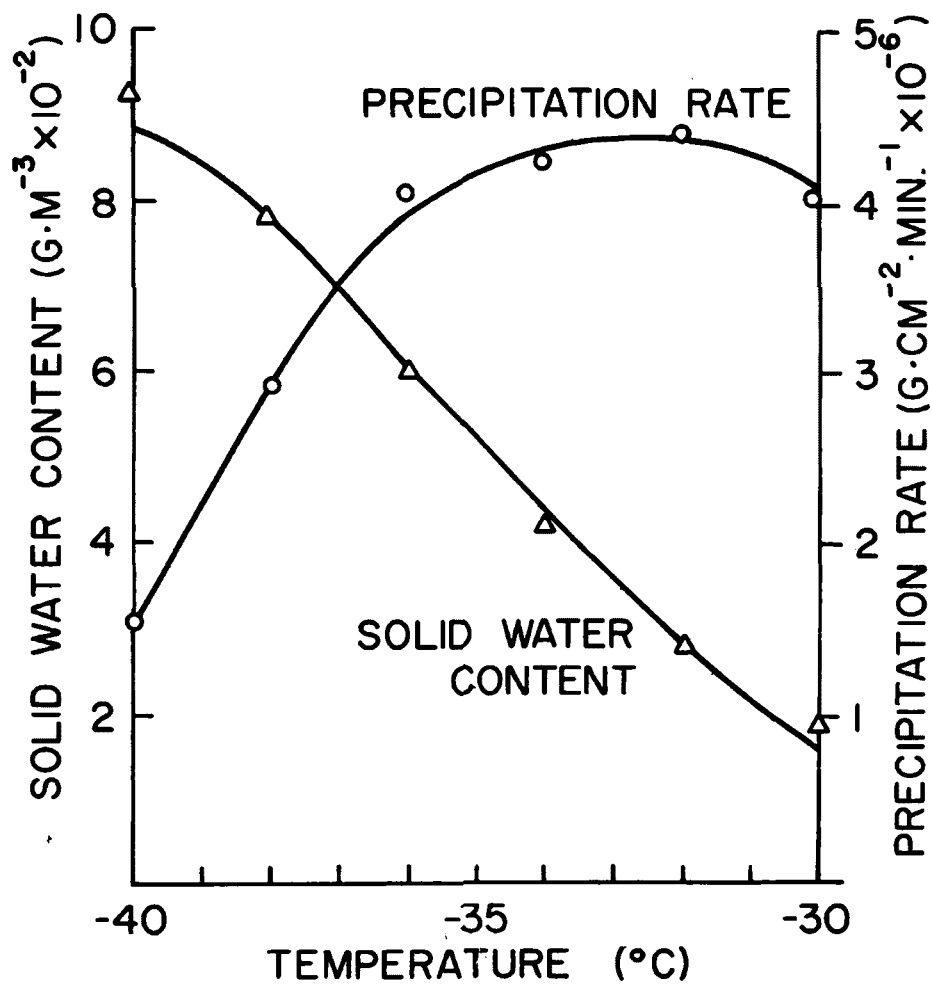


Fig. 45. Solid water contents and precipitation rates of ice fog.

rates were of the order of $1 \mu\text{g cm}^{-2}\text{min}^{-1}$. The solid water contents were of the order of 0.01 g m^{-3} and Kumai (1964) made similar calculations of the solid water content, using size distributions instead of the mean diameters used here. He reported that the solid water content is 0.07 g m^{-3} and 0.02 g m^{-3} at -39°C and -41°C , respectively. It must, however, be noted that Kumai's results were obtained by single sampling and do not represent average values of many data at these temperatures. Benson (1965) estimated 0.21 g m^{-3} for the core area of Fairbanks. Since this value was not derived from observation, it seems to be overestimated. The liquid water content in clouds has been extensively studied. Fletcher (1962) summarized the measurements made by many authors. According to his table, the liquid water content in clouds is of the order of 0.10 g m^{-3} , which is an order of magnitude larger than that of ice fog.

Precipitation rates were also studied by Kumai (1964) and Benson (1965). Kumai obtained $0.691 \mu\text{g cm}^{-2}\text{min}^{-1}$, and $0.0287 \mu\text{g cm}^{-2}\text{min}^{-1}$ at -39°C and -41°C , respectively. These values are one to two orders of magnitude smaller than the results obtained here. Benson directly measured precipitation rates, using a 1 m^2 plastic sheet as a collector. The precipitation rates he obtained are about 2 to $3 \mu\text{g cm}^{-2}\text{min}^{-1}$, which is the same order as obtained here. The reasons that Kumai's results are smaller than those of Benson and those obtained here may be due to the fact that the concentration of ice fog was small when he sampled, and also due to the upward winds in the ice-fog layer or variation in sample location, as described by Benson.

e. The Effect of Ambient Humidity on Ice-Fog Crystals:

So far, we have described the effect of temperature on ice-fog crystals. Now let us consider the effect of ambient humidity on ice fog crystals. As is well known, the theoretical equation for the growth rate of an ice crystal in water vapor is given as follows (Byers, 1965):

$$\frac{dM}{dt} = 4\pi CD (\rho - \rho_o)$$

where

M is the mass of the ice crystal

C is the capacity (dependent on crystal shape)

D is the diffusivity of water vapor in air

ρ is the vapor density of ambient air

ρ_o is the vapor density at the surface of the droplet

Therefore, there may be some relationship between the mean diameters of ice-fog crystals and ambient humidities.

In order to study this, Henmi (1969) plotted the mean diameters of different types of ice-fog crystals against supersaturation over ice for the temperature ranges -30.0 to -32.0C, -32.1 to -35.0C, -35.1 to -37.0C, -37.1 to -39.0C, and -39.1 to -41.0C. In these figures, he assumed the effect of temperature on ice-fog crystal growth to be the same in each temperature range. The precipitation rate of ice-fog crystals was also plotted against ambient supersaturation over ice and the resulting plot is given here as Fig. 46.

These figures seem to indicate that the mean diameters of ice-fog crystals were independent of ambient humidity, and that there was no

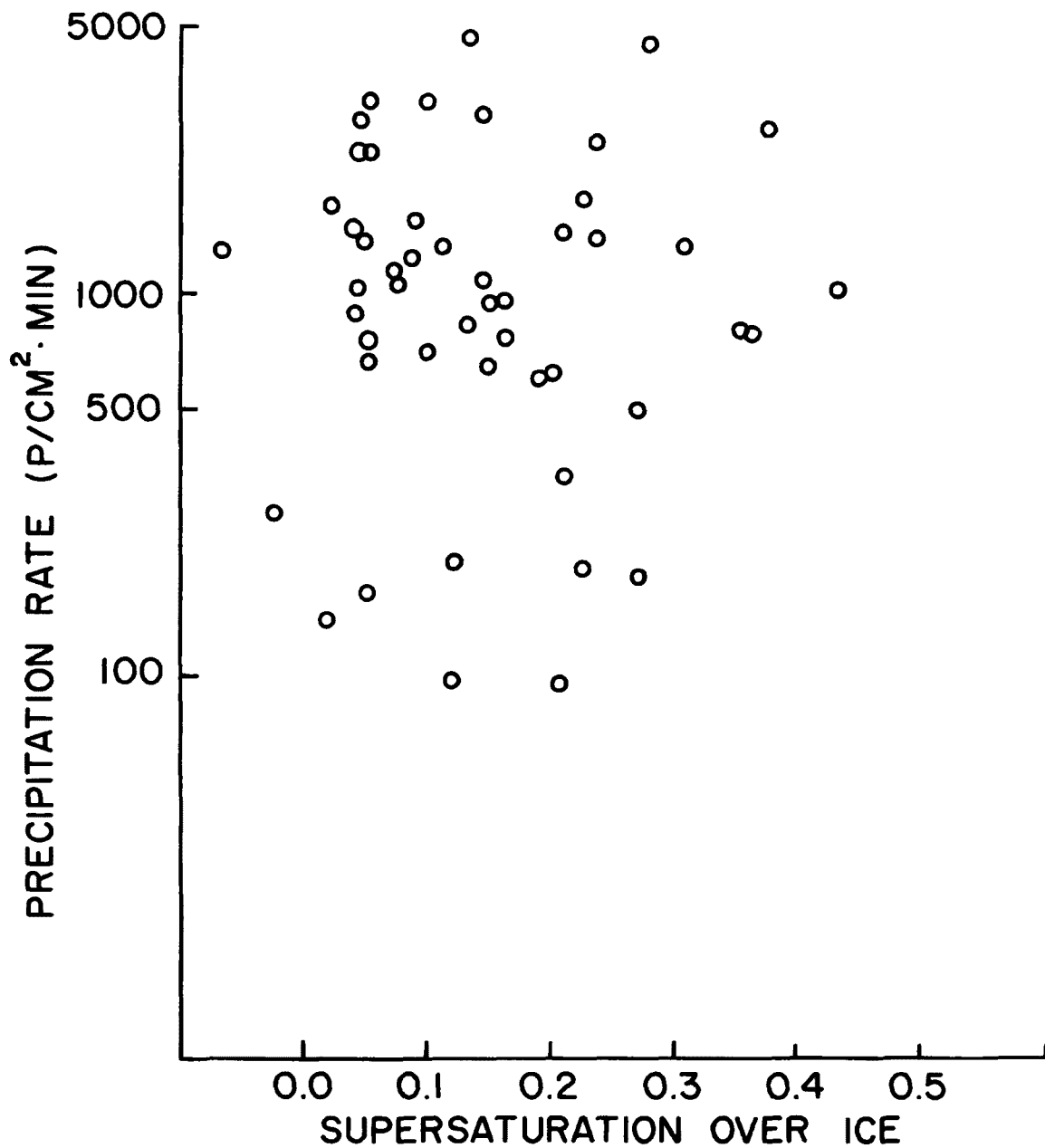


Fig. 46. Numbers of ice-fog crystals precipitated versus supersaturations over ice.

relationship between the precipitated crystals and ambient humidity. Therefore, it is probable that ice-fog crystals are almost completely developed around the sources, and that after dispersing away from the sources, they are only drifting without significant growth or evaporation. Had we observed the humidities and the mean diameters near water vapor sources, some relationships might have been found.

f. Ice-Fog Crystals from an Unpolluted Area with a Moisture Source:

We normally see dense ice fog only in inhabited areas such as the Fairbanks vicinity. This is the reason why ice fog is considered to be a form of "air pollution" and the importance of pollution in forming ice fog is emphasized. However, around the hot springs at Chena and Manley Hot Springs or along open water in a river (a rapidly running stretch or a small portion of open water made by overflow above thick ice), dense ice fog occurs even in very clean air with only 50 to 500 p cm^{-3} condensation nuclei. The size distribution of such ice fogs formed in clear air had a narrow peak at a diameter of about 10μ . All particles were spherical or nearly spherical (Figs. 30 and 47). The crystals with spicules did not seem to be aggregated from similar sized crystals or droplets but to be formed by expansion from mother crystals. A similar size distribution of crystals also occurs at the IAP (open water) site in Fairbanks. Normally at the MUS site in the city the size distribution has three peaks which correspond to ice-fog crystals originating from (1) automobile exhaust, (2) open water, and (3) heating and power plant exhausts.

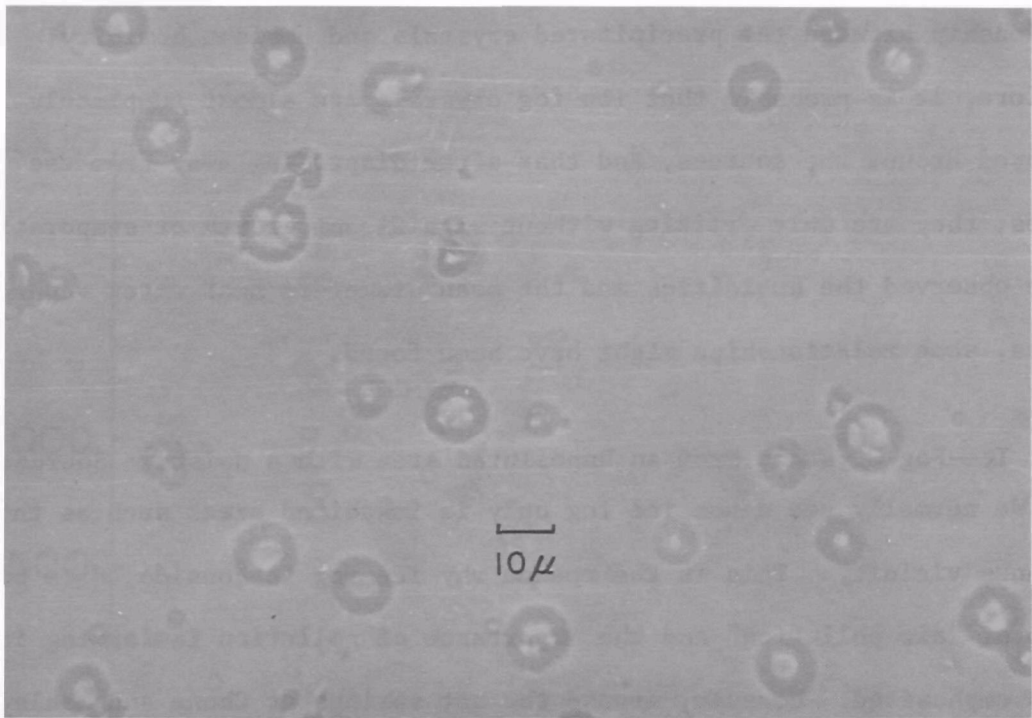


Fig. 47. Ice-fog crystals at Chena H. S. on December 31, 1968.

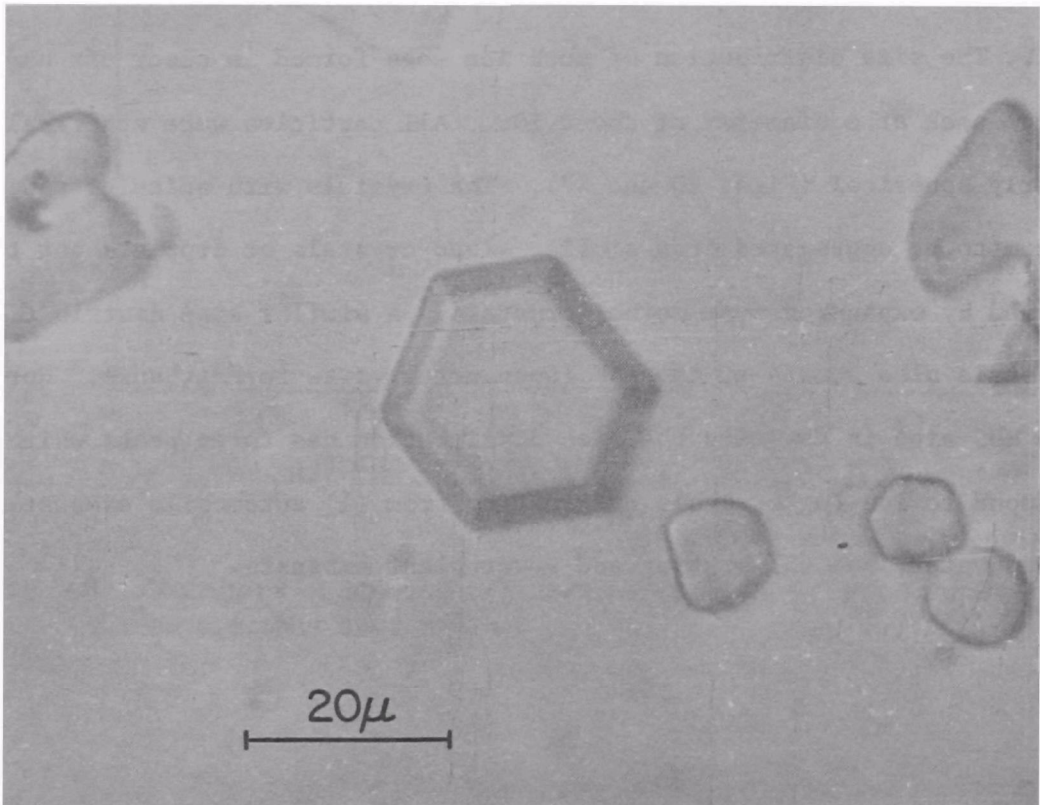


Fig. 49. A polyhedral crystal looking from the exact top. The crystal was collected under the same conditions as Fig. 48.

B. UNUSUAL CRYSTALS IN ICE FOG (POLYHEDRAL ICE CRYSTALS)

We have noticed many ice-fog crystals have abnormal shapes such as spherical and near-spherical irregular. Except for ice-fog crystals, we have never yet observed spherical ice crystals smaller than several hundred microns in the atmosphere. Since Thuman and Robinson (1954) first discovered the spherical ice crystals (which they called "droxtals") spherical ice crystals are well known in ice fogs. In the present research, we found some other shapes of ice-fog crystals different from the normal sphericals, columns, and plates etc. Figure 48 shows such a crystal with various focusing or observation angles. Since the crystal was suspended in silicone oil, the circle and two small dots apparently in the crystal may not be nuclei, but air bubbles in oil. Another picture (Fig. 49) or a crystal appears at first to be similar to a normal thin hexagonal plate, but if we look carefully at the edges of the crystal it is different from a regular hexagonal plate. This picture is probably a view from the top (along the c-axis) of the same type of crystal. Figure 50 shows the shapes of the crystals of Figs. 48 and 49 as drawings. Figure 51 shows a similar crystal but with a smaller hexagonal top. These crystals seem to be 14- or 20-faceted polyhedral crystals which have two hexagonal faces at the top and bottom, 2 sets of 6 trapezoidal faces (total 12) and 6 rectangular faces between the 2 sets of trapezoids (sometimes the rectangular faces are missing). Figure 52 is another similar crystal.

These 14- or 20-faceted polyhedral crystals were found in ice fog at the MUS site in Fairbanks at a temperature of -47°C . The finding of

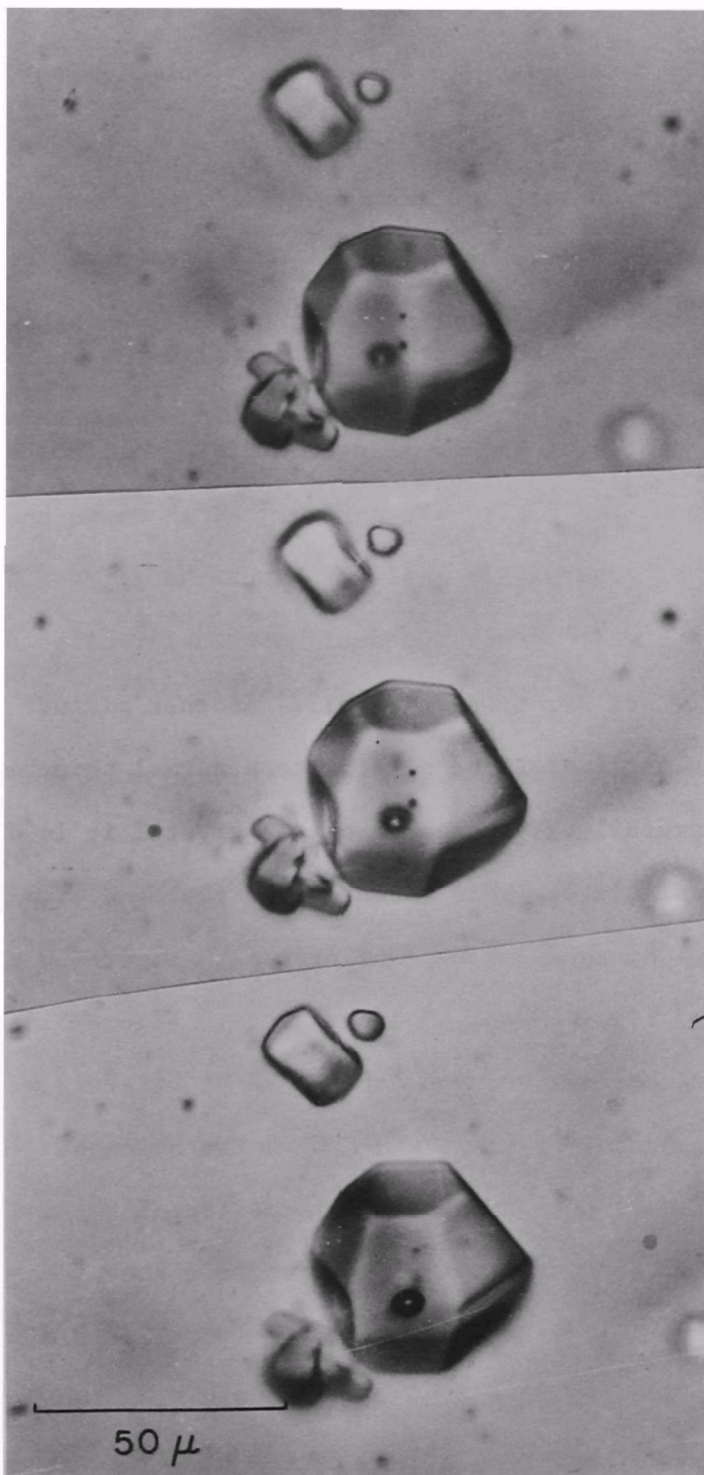


Fig. 48. A polyhedral ice crystal found in ice fog at the temperature of -47°C . The crystal was collected at the MUS site on Jan. 3, 1969. Three pictures show the crystal with different focussings. This crystal may be 14- or 20-faced polyhedral crystal. The crystal was suspended in silicone oil.

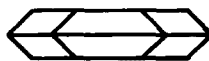
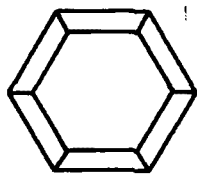
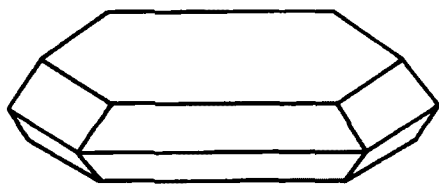
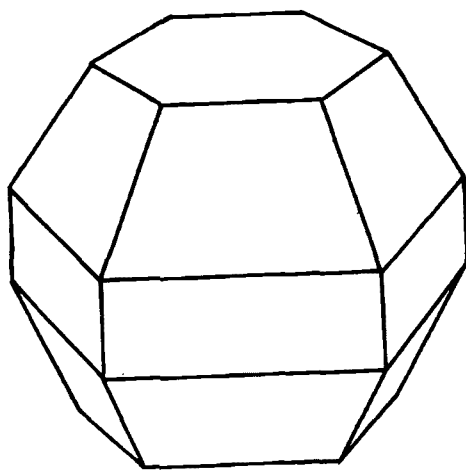


Fig. 50. Drawings of the crystals in Figs. 48 and 49.



Fig. 51. Another polyhedral ice crystal in ice fog under same conditions as Fig. 48.

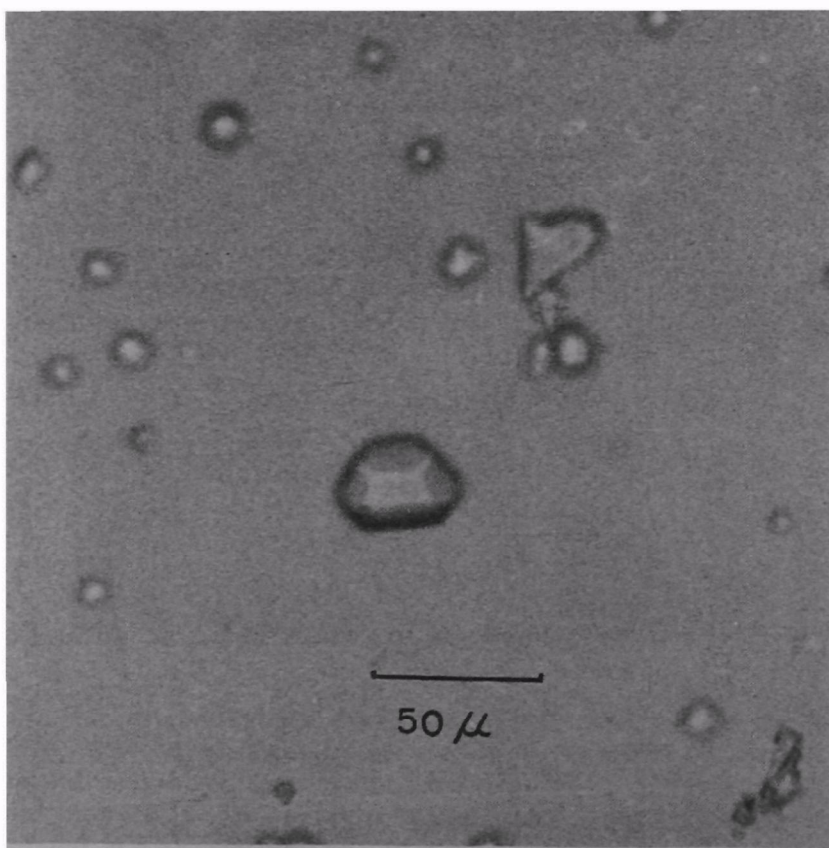


Fig. 52. An ice crystal similar to above polyhedral crystals under same conditions.

these crystals supports strongly Kobayashi's (1965) laboratory experiment, in which he found pyramid faces at an edge of a prism crystal at temperatures between -45 and -55°C . The crystal we found in ice fog appears to consist of 2 (0001) hexagonal faces, 2 sets of 6 $(10\bar{1}1)$ trapezoidal faces and 6 $(10\bar{1}0)$ prism faces. Sometimes the last 6 prism faces are missing. Therefore the crystals we found are 14-faced bi-pyramid crystals and/or 20-faceted bi-pyramids with short prism.

Although we do not have good evidence, it is possible that the formation of these crystals can be attributed to the fact that the super-cooled water droplets freeze so rapidly that the crystal does not have enough time to reach an equilibrium state for the development of normal hexagonal and rectangular faces. Shimizu (1963) found long prism crystals 100μ to 1 mm long with the ends probably (0001) faces in the precipitation in Antarctica. In our case we did not have long prism faces, but we discovered some other shapes of ice-fog crystals which do not have well-defined faces, such as the crystals indicated as B (for block ice) in Figs. 53 and 54. The crystals found by Shimizu in Antarctica may not have been formed by freezing of water droplets, because they were found in precipitation and were too long to be formed from freezing of water droplets. And in Kobayashi's experiment the crystal must be grown on a certain support in his cold chamber, under which conditions the crystal develops into a columnar prism with pyramid faces on an end of the prism.

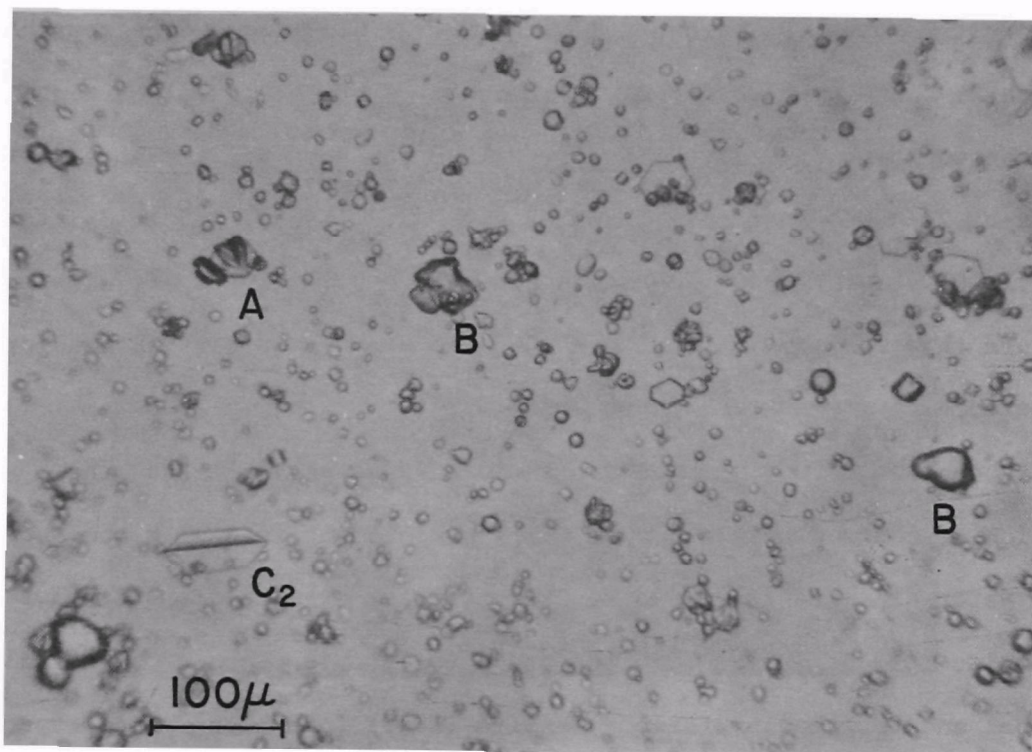


Fig. 53. Ice-fog crystals collected under same conditions as Fig. 48. Mark A shows a thin plate with two half hexagonal thin plates. Marks B illustrate "block ice crystal". C_2 is a plate crystal which has another plate angled 60° or 90° .

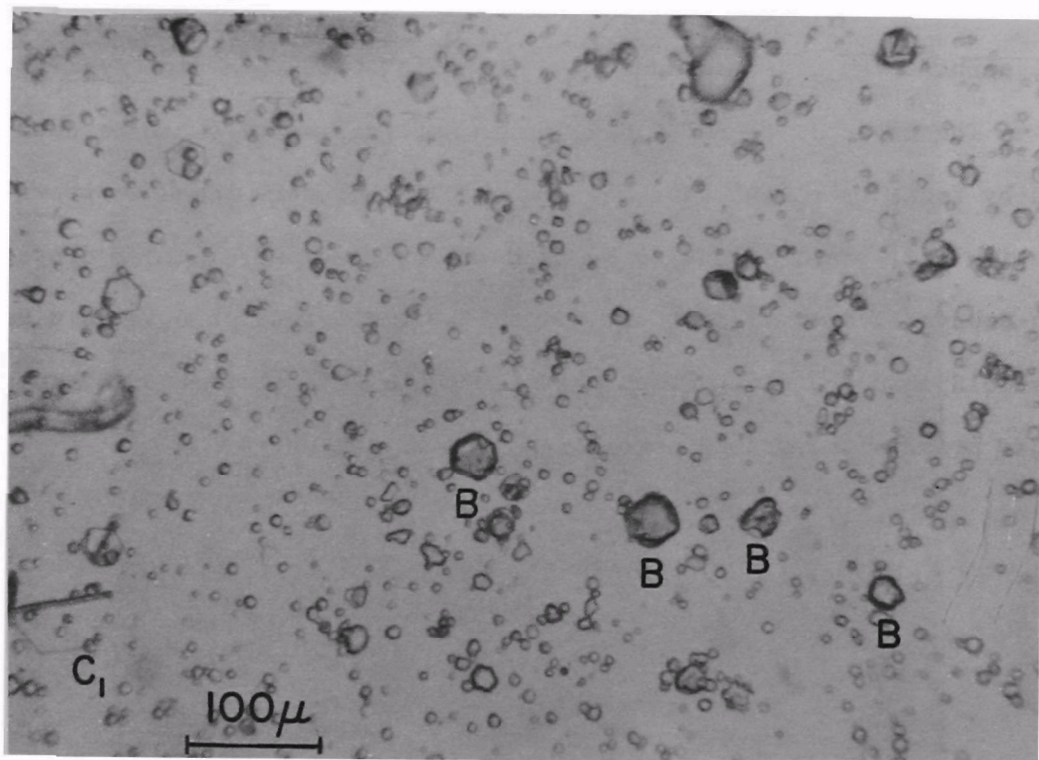


Fig. 54. Ice-fog crystals taken under same conditions as above. C_1 shows a half plate and a vertical plate attached with it. The weather conditions were the same as above.

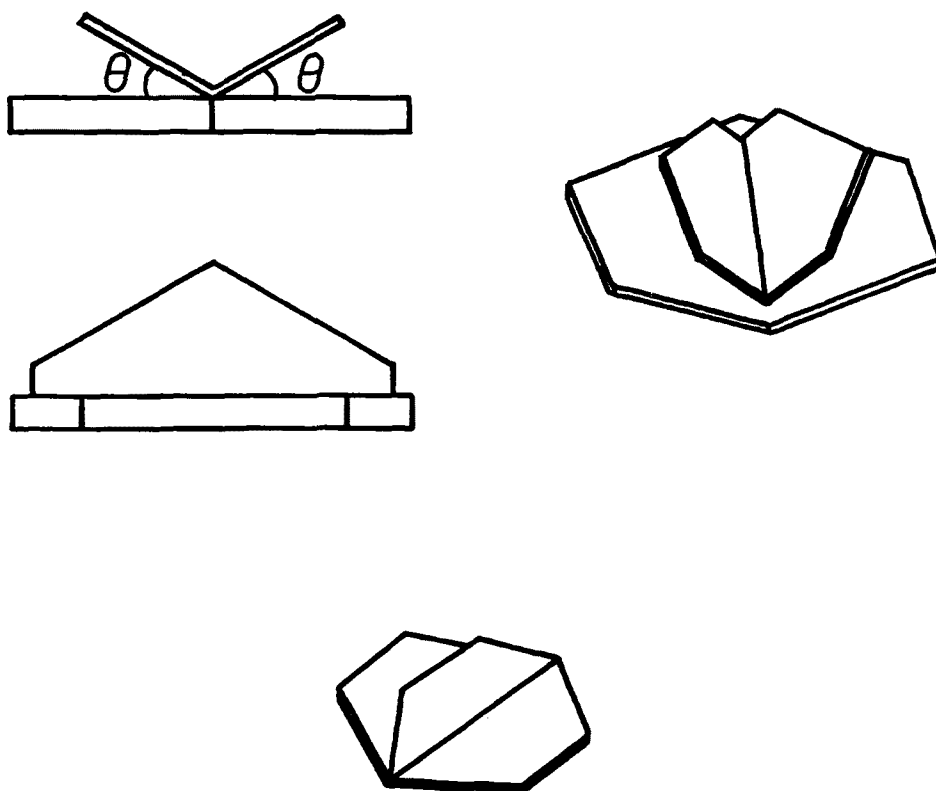
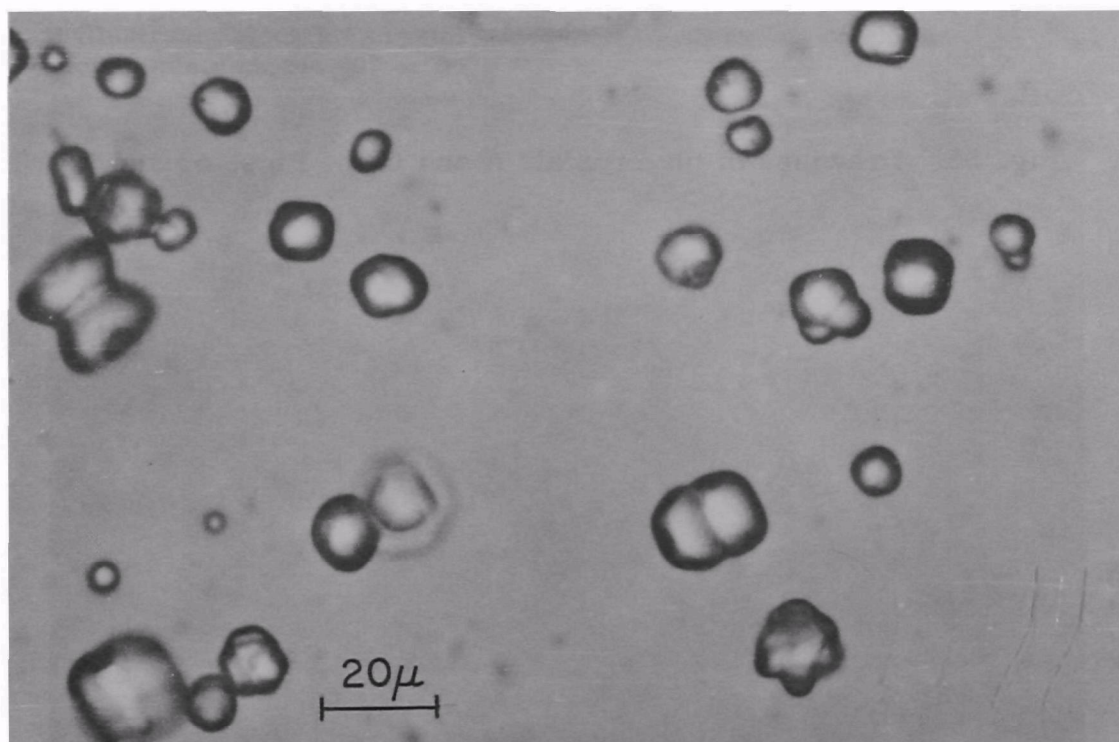
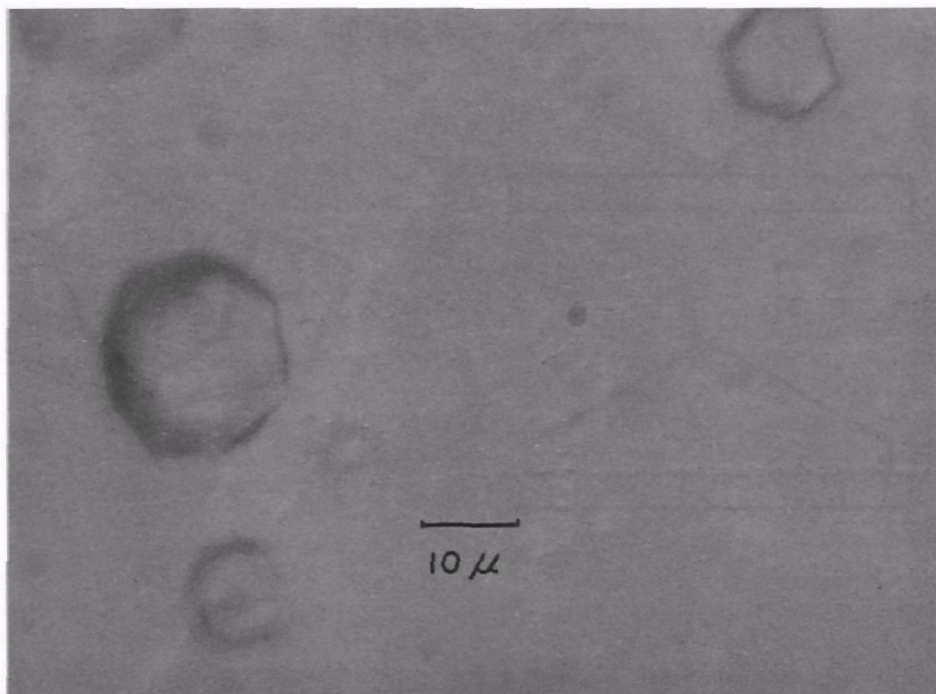


Fig. 55. Drawings of the crystals A and C_1 of Figs. 53 and 54.



Figs. 56 and 57. Block ice crystals. The crystal in Fig. 56 was collected under the same conditions as Fig. 48. The crystals of Fig. 57 were sampled on December 23, 1965 at the MUS site with temperature of -40°C . The crystals in Fig. 57 were suspended in formvar liquid.

The possible explanations for our polyhedral crystal are as follows:

1) Under low temperatures, a quasi-stable state can exist for growth of ice crystals toward the most stable state of ice because of a scarcity of thermal energy. A trapezoidal face is a quasi-stable surface which has higher free energy than the hexagonal and rectangular faces in the case of ice. Under rapid cooling, the growth of a quasi-stable surface of ice may become comparable to the completion of stable crystal faces which have lower energy. When the freezing of water droplets in a spherical shape is complete, the crystal is a little warmer than ambient air so that water molecules can move over the surface of the ice to form the quasi-stable surface from the spherical surface. However, the movement of molecules would be too slow to form the most stable crystal faces after the trapezoidal surfaces were completed because the temperature of the crystals has been lowered enough. 2) Due to absorption of air pollution (dusts inside or outside), the growth did not occur onto the normally most stable faces $[(0001) \text{ or } (10\bar{1}0)]$.

We could see such shapes of ice-fog crystals only in the largest crystals because of the poor resolving power of the optical microscope. However, these detailed shapes of ice crystals could exist in smaller ice fog crystals which have been considered as spherical.

In Fig. 53 many block shaped ice crystals can be seen. Among these a crystal (probably a hexagonal plate) marked as C_2 has an additional half a plate which seems to grow with an angle of 60° or 90° . Figure 54 has

also a thin half hexagonal plate marked as C_1 with an unknown edge, which might be at an angle of 90° with the basal plane. Figure 53 has another example of a crystal having a plate angled at 90° or 60° to the basal plane and the hexagonal plate ice crystal marked as (A) has somewhat smaller half plates aggregated or grown on the basal plane with angles of probably 60° each. See a sketch of this as a model in Fig. 54. In Figs. 55 and 56, many ice block crystals can be seen. The mechanism of formation of these block crystals can also be attributed to the rapid freezing of water droplets.

8. MECHANISM OF ICE FOG FORMATION

Normal fog or cloud droplets are formed when the relative humidity rises to more than 100% (but usually not more than 101%) in the atmosphere. Moisture in excess of that needed for saturation at the temperature involved condenses onto appropriate condensation nuclei. Thuman and Robinson (1954b) measured humidities but they did not observe or mention how the humidity changes during the development of ice fog. Benson (1965) thought that after the relative humidity reached 100% with respect to water, water droplets would form and then freeze. After the freezing of droplets the humidity should remain at ice saturation. However, there was no observational and theoretical evidence for such an explanation at that time. Thuman and Robinson (1954a) stated in their report that

"several boiler houses and various steam-line vents were probably the primary sources of moisture for ice-fog aerosols. It is postulated that, at temperatures below -30°C , droxtals and thus ice fog arise from the direct freezing of supercooled droplets that have been formed by condensation in moist gases discharged in the atmosphere. At these temperatures the moist gases can quickly saturate the air, so that the ice aerosol can persist."

Kumai and O'Brien (1965) reported observations by collection of particles in silicone oil of ice crystal nucleation process in exhaust gases coming out of a power plant stack, although the observation was made at -22°C . They also confirmed that water droplets were formed in exhausts from cars, heating and power plants, and it was suggested that the ice-fog crystals result from freezing of the supercooled water droplets. They did not give further conclusions. Benson (1965) stated, concerning the mechanism, that the rapid cooling condenses the water vapor into small droplets which become supercooled, and at temperatures below -30 to -35°C they freeze.

These three most comprehensive studies of Fairbanks ice fog have shown neither evidence nor detailed observation and theoretical consideration for the freezing of water droplets. (Kumai and O'Brien's experiment was carried out at higher temperatures than those at which ice-fog appears, and they used silicone oil which might freeze the supercooled droplets when they are collected in oil). From the observations we made in the present research some evidence on the freezing of water droplets has been given in the previous chapters in describing the positions of ice-fog nuclei and the appearance of spicules in ice-fog crystals. In this chapter more detailed observations and theoretical studies from various viewpoints will be discussed.

a. Measurements of Humidity under Low Temperature Conditions:

It is well known that it is difficult to measure the humidity of air in the temperature range below -30°C , although several methods have been developed. Even for temperatures between 0°C and -30°C data are scarce (Munn, 1966).

The traditional method of dry and wet bulb thermometers gives questionable accuracy at near and more than ice saturation environment. An attempt at humidity measurement of warmed samples of initially cold air by use of the dry and wet bulb thermometers has been proposed by Branton (1965). However, for air at temperatures of -40°C , the difference in readings of dry and wet bulb thermometers is several tens of degrees when the air has been warmed to above freezing temperatures. A dew point hygrometer is good for measurement of humidities lower than ice saturation for sub-freezing temperatures, but for ice fog studies we also need

accurate humidity measurement between ice and water saturation for temperatures as low as -55°C . A "dew cell" cannot be used for temperatures lower than about -30°C . A carbon coated sensor for the determination of humidity is also being used at the present time, especially in radio-sondes. However the electric resistance of the carbon humidity sensor is also changed by temperature variation, and at -40°C the resistance becomes unmeasurable according to Stine (1965) and the author's trial. Using infrared or electronic radiation we could probably measure both total water content and water vapor in the air with fair accuracy. However, at the present time the equipment for these methods is too expensive and requires too much time. Also there is no guarantee that the machine would operate well at the low temperatures involved. Traditional hair or membrane hygrometers also do not work below about -25°C , because the structure of the hair or membrane will be broken by freezing and a serious time lag develops. However, if the hair is treated with BaS to avoid the hysteresis effect, is rolled with a special technique, and is treated with H_2SO_4 , the accuracy of the hair hygrometer becomes better than $\pm 2\%$ in relative humidity (Kobayashi 1960), probably even for -40°C . It is possible that a recording hygrometer with the specially treated hair might work at lower temperatures.

1. Data from Hair Hygrometers:

As was previously mentioned a hair hygrometer would not work properly in low temperatures due to the low time lags. However, average values for a fairly long time interval by use of the specially treated hair may

be valid, even though it would not give very accurate values of instantaneous humidity. Fortunately, the weather of interior Alaska in the winter is so steady that sudden changes of humidity probably do not occur except during a very few cases of storms. Therefore, the data obtained from hair hygrometers may be useful for a comparison of humidity trends between different locations (with and without fog). Using these records, the humidities recorded at 0000 AST and 1200 AST from the middle of November 1967, through the middle of February 1968 were plotted against temperatures (see Fig. 58). The figure shows that humidities measured in the ice-fog area (the MUS site) are a little greater than those measured in the area free from ice fog, especially below -20°C . This implies that the humidities in the ice-fog area are always affected by the local sources of water vapor such as power and heating plants, automobiles and open water. It is important, however, to note that there is not an extreme difference between humidities in ice-fog areas and areas free from ice fog. Furthermore, it is also important to note that water vapor pressures near the ground lie on the average between ice - and water - saturation in the temperature range below -20°C in both the ice-fog areas and the areas free from ice fog.

The record of humidities at the Ester Dome site sometimes showed lower humidities than ice saturation and distinct variation even below -30°C (the minimum temperature recorded at Ester Dome in the winter of 1967 and 1968 was -34.4°C). On the contrary the records at the MUS site and at the Geophysical Institute site did not show such humidity variation below -30°C . These observations imply that above an ice-fog layer, humidities

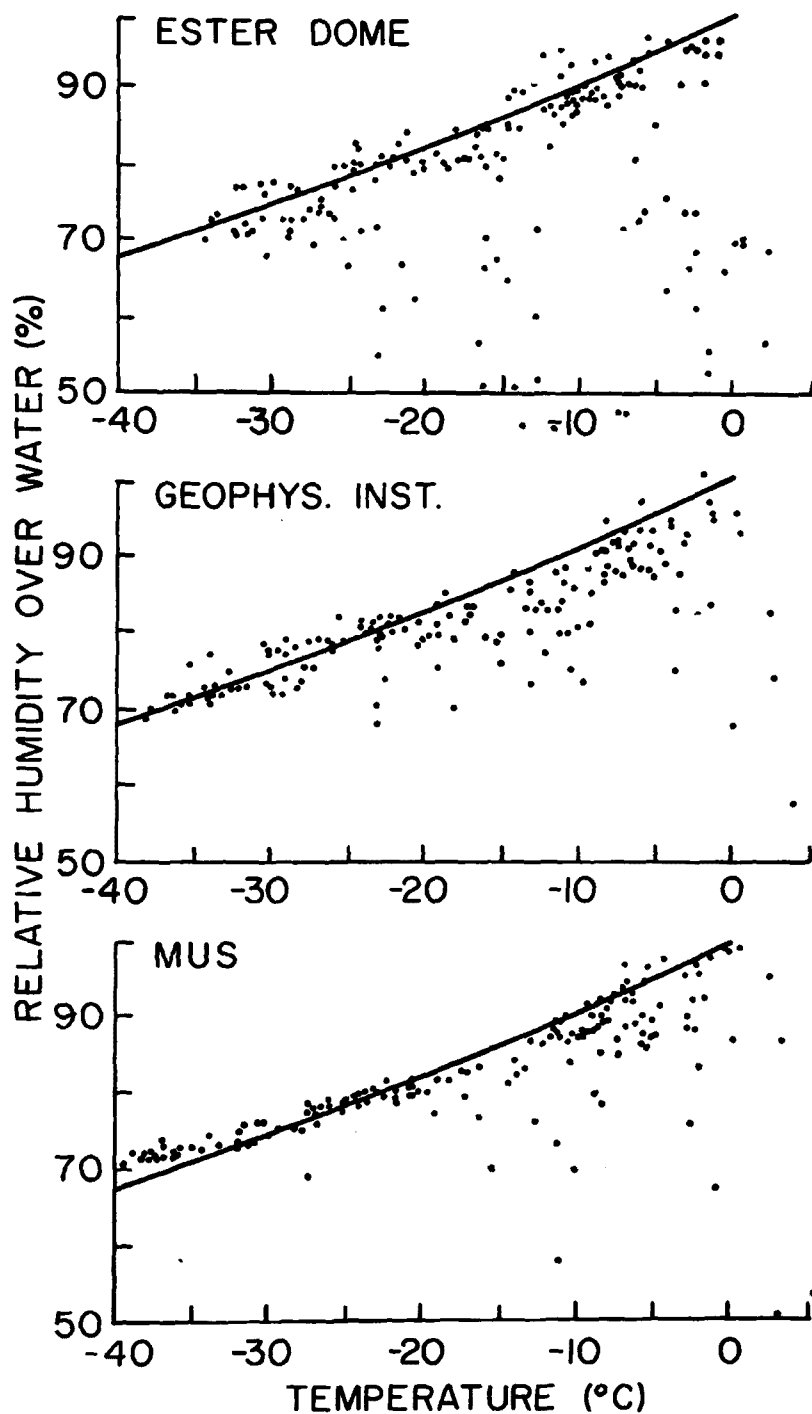


Fig. 58. Relationship between relative humidities provided by hair hygrometers and temperatures during the winter of 1967 to 1968 at various sites.

are affected by the air coming from distant areas, but in an ice-fog layer the air is stagnant. Also since the temperature and humidity records show almost simultaneous changes even below -30°C (at least down to -34.4°C) the hair of our hygrometers may have already been treated with BaS and H_2SO_4 and rolled and should probably work at temperatures below -40°C . The humidities recorded by our hygrothermograph (model H-311, Aerojet-General Corp.) at the MUS site were approximately equal, on the average, to those measured by the absolute method which is used to calibrate the hygrometer and which will be described in the next section.

ii) Absolute Method of Humidity Measurement:

Thuman and Robinson (1954b) measured humidities in the temperature range between -20 and -43°C in ice fog, using the Karl Fischer reagent method, which operates as follows: First a measured volume of air is drawn through absolute methanol which is used as a water extractant, and second, the amount of water dissolved in the methanol is determined by titration of the Karl Fischer reagent. However, this method requires considerable skill and also time for the determination. In addition to the above, there are some doubtful points at the measurement of amount of air drawn through the methanol and the ice-saturation reference. In order to measure the air volume, they used a test meter. However, in the low temperature below about -20°C , a test meter such as that used by Thuman and Robinson seems to be improper for measurements of flow rates, because the inside of such a meter does not respond accurately enough at the low temperature to changing flow rates. Nakaya (1954) used a method

similar to theirs, but he used a drying tube containing P_2O_5 (phosphoric pentoxide) which was the same material used by Tyndall (1922) and Hanajima (1944) as an absorbing agent of water vapor. Nakaya determined the amount of air through the tube by means of an evacuated 20 liter glass bottle, allowing the air to come slowly into the bottle until the pressure inside of the bottle reached barometric pressure. Even though the method works well at around $-20^{\circ}C$, for $-40^{\circ}C$ or below 20 liters of air does not contain enough water vapor to give a measurable weight difference in the P_2O_5 tube. In addition, operation of a vacuum pump at such low temperatures creates problems. Finally, we had mechanical problems with the barometer used to measure barometric pressures at the various sites in ice fog.

In the present research we used an air sampling method similar to the previous methods. We used magnesium perchlorate, $Mg(ClO_4)_2$ as an absorbing agent, as was suggested by Kumai and O'Brien (1964). Other than magnesium perchlorate or phosphorus pentoxide P_2O_5 , there are many kind of water absorbing agents such as sulfuric acid (H_2SO_4), calcium chloride ($CaCl_2$) etc. The magnesium perchlorate was chosen as the most effective and convenient absorbing agent. Also calculations of the expected temperature rise in its use for humidity measurement under ice-fog conditions give a negligibly small heat of reaction. To measure the volume of air, methods such as the use of a test meter or flowmeter cannot be applied because of inaccuracies caused by low temperatures. We had considerable difficulty in trying to use the flowmeter for the measurement

of air flow under ice-fog conditions with pressure and temperature corrections. Since the flowmeter was connected behind the drying tube, the pressure at the head of flowmeter was much different from 1 atmospheric pressure. Using a pressure gauge also gave us very inaccurate values. Mercury to measure pressure has also been frozen. Temperature correction for the original calibrated scale in use under ice-fog condition is not insignificant. Furthermore, we had to measure accurate barometric pressure and temperatures at the same locations simultaneously.

After wasting a lot of time, we finally used two 50 liter glass bottles filled with kerosene and connected by tubes through an electric pump (normally used for water transfer) to measure the amount of air. This seems to be the best technique developed so far for measuring the air volume at temperatures lower than -20°C . Kerosene neither freezes nor bubbles even below -50°C and the pump (with a brush-type motor) operates at ambient temperature below -40°C without any difficulties. Antifreeze liquids for automobiles also do not freeze but when they are transferred from a bottle to another bottle, bubbles develop in the bottle, so that the measurement of volume becomes inaccurate. As indicated in Fig. 59, two glass bottles are used to measure the volume of air. It is better to use a larger bottle, because the accuracy of the measurement increases with the weight of the drying tubes. But for the convenience of transportation for the device, 50 liter bottles were used.

In order to filter out solid water particles, a 0.45 micron pore size Millipore filter is used. This type of filter is a plastic, porous

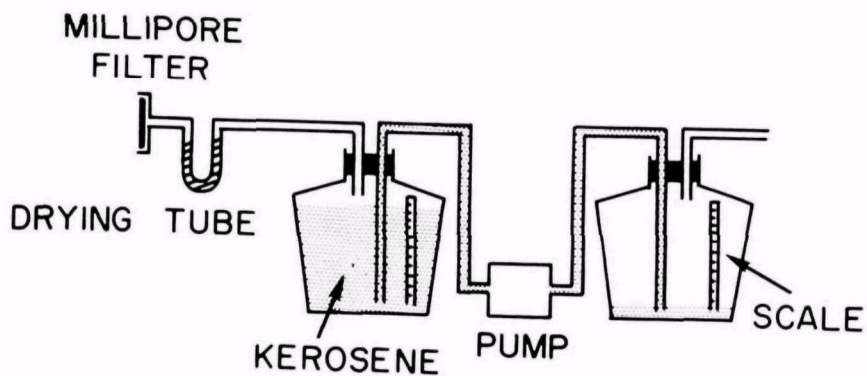


Fig. 59. Arrangement of apparatus for humidity measurement.

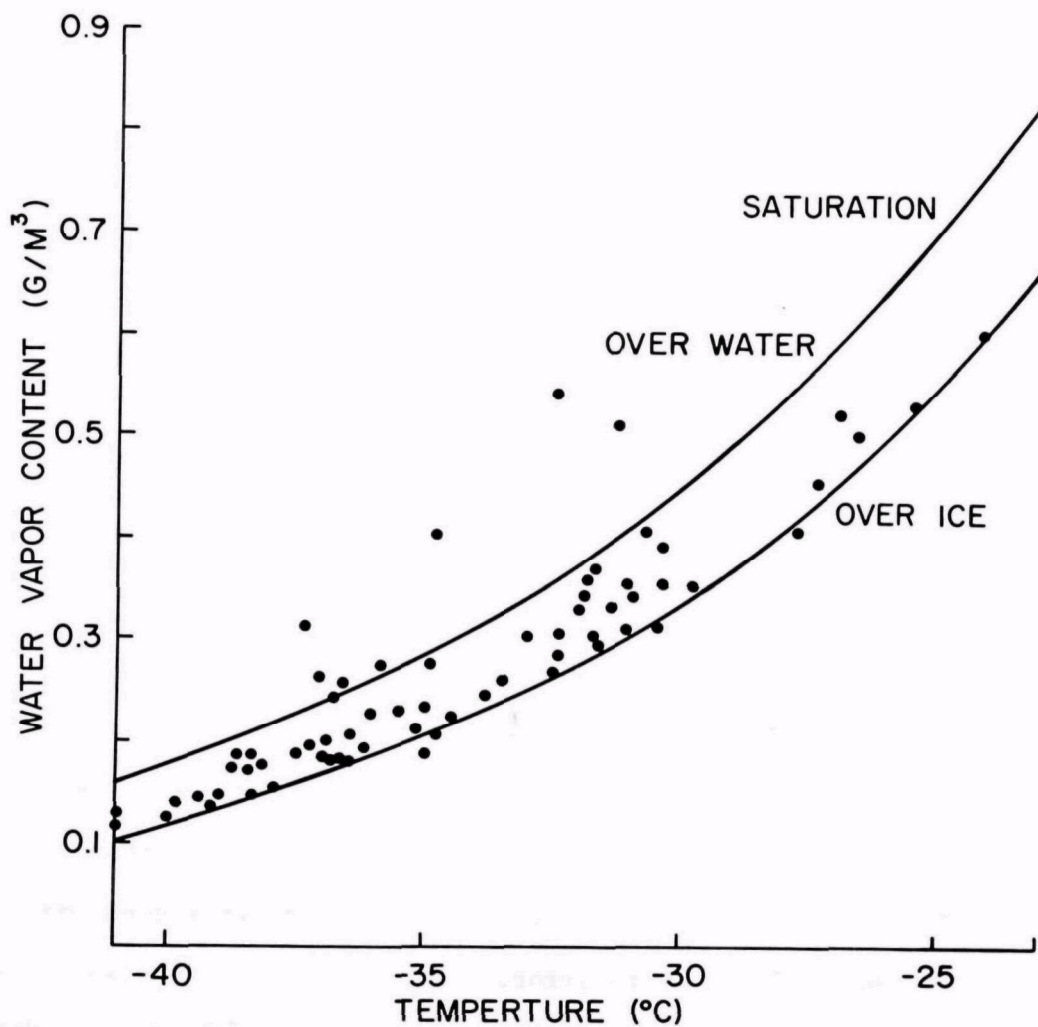


Fig. 60. Water vapor density versus temperatures under ice-fog conditions at the MUS site. The curves for water- and ice-saturation are according to Smithsonian Meteorological Table.

structure, and has a low resistance to the flow of air. It was confirmed that the filters do not absorb or release any appreciable amount of water vapor under the conditions of low water vapor pressure and that the visible deposits of ice-fog crystals on the surface of filter during suction of air through the filter give negligible error.

The procedure of measurement is as follows:

1. The dry weight of the drying tube containing magnesium perchlorate is measured with a chemical balance which has a precision of ± 0.01 mg.
2. The drying tubes, which are stored in a desiccator, are kept at ambient (outdoor) temperature until measurements are made.
3. The drying tube is connected to the rubber hoses, both glass stopcocks of the drying tube are opened, and the pump is switched on. To handle any part of the drying tube clean dry tissue paper should be used.
4. Air is taken into the bottle through a 0.45μ pore size filter and a drying tube. After 30 liters of kerosene are passed to the second bottle, the pumps are stopped. The volume of air which passes through the drying tube is measured by a scale on the kerosene-filled bottle.
5. The drying tubes are weighed on the chemical balance after the tubes are warmed up to room temperature. If the temperature of the tubes is lower than room temperature, water vapor condenses on the tubes, thus causing error.

6. The water vapor density A is given by

$$A = \frac{w}{V} \quad (\text{gm m}^{-3}),$$

where w is the difference of weight in mg before and after absorbing the water vapor and V is the volume in liters of air taken. Using the value A, water vapor pressure e in mb can be calculated by the equation

$$e = \frac{A T}{m_w/m_d} \frac{R}{\epsilon} \quad (\text{mb}),$$

where T is absolute temperature. R is the gas constant, ϵ is m_w/m_d ($= 0.622$), m_w and m_d are molecular weights of water and of dry air, respectively.

Relative humidities over water, U_w and over ice, U_i are easily calculated from e divided by the saturation vapor pressure over water E_w and ice E_i , respectively, from the Smithsonian Meteorological Tables. However, the values of E_w and E_i in these tables for temperatures below 0C were extrapolated from those at temperatures from 0C to 100C and are pending further research, according to the table.

A rough estimate of the error in vapor pressure is about 1 percent of value observed. However, care must be taken that the air is not passed through the drying tube too quickly because the water vapor cannot be fully absorbed by magnesium perchlorate at high flow rates. In order to check this two tubes were used in series. However, the second tube showed

no sensible increase in weight. Hence, throughout the observations, only one tube was used for each measurement. Measurements were made at a flow rate of 10 liter per minute.

In order to check the reliability of the data obtained, we measured simultaneously the humidities with an Assman type hygrometer in the temperature range 0C to -10C and then compared the values. The two values agreed to within 1 to 2 percent in units of relative humidity. (See Table 8). An Assmann type hygrometer, in general, shows accurate values to several degrees below the freezing temperature.

TABLE 8

Comparison of the Data on Humidities between
The Method Used here and Assman Type Hygrometer

Temperature	Absorbing Method	Assmann Hygrometer
-1.8	65.0 percent	65.2 percent
-5.4	75.0	74.0
-6.9	49.4	48.0
-7.2	77.3	76.0
-8.0	49.4	50.0

The water vapor content was observed at the MUS site during the ice-fog events of the winter of 1967-1968. The results appear in Fig. 60, which shows the relationship between temperatures and water vapor densities. In the figure two curves illustrate water saturation and ice saturation according to the Smithsonian Meteorological Tables. From the figure, it

is obvious that generally the water vapor density under ice-fog conditions lies between ice - and water-saturation, assuming the values for E_w and E_i are accurate. Assuming accurate values of E_w and E_i on the figure, we can express the water vapor content in terms of relative humidity. Thuman and Robinson (1954b) reported that the average value of relative humidity with respect to ice was 91 percent under ice-fog conditions. The average humidity obtained in the present study is 23 percent higher than this. The reason for this difference cannot be found at the present stage. However, since ice-fog crystals stay stable or grow very slowly under conditions of persistent ice fog in the central area of the city, the water vapor density must lie between ice - and water - saturation, as we obtained experimentally.

b. Visual Observations of Ice-Fog Sources:

On the basis of careful observations of ice fog from the ground and the air, we can say that the densest ice fog originates from open water such as cooling water dump areas from power and heating plants, while relatively thin but widely spread ice fog comes from automobile exhausts. Exhausts from power plants and commercial and residential heating plants also make ice fog. Figure 61 is a photograph* of the Fairbanks area taken by Mr. Mobley of the National Geographic Society from the air on a morning in November 1968. Although the exact time and ground temperature are not

*The original color picture is available in "Alaska", published by National Geographic Society, Washington, D. C., 1969.

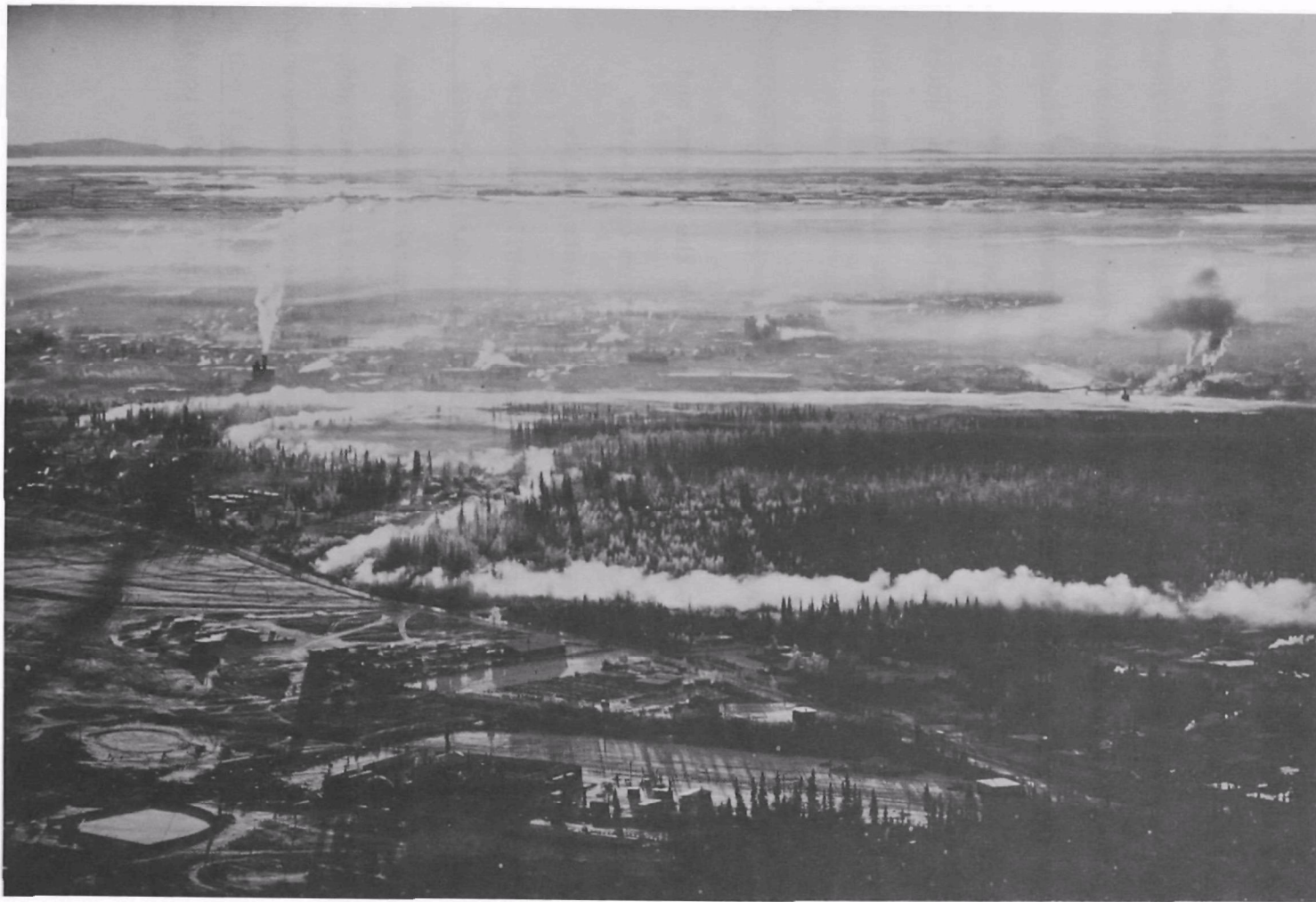


Fig. 61. An aerial photograph of Fairbanks taken just before ice fog forms. (Photo by Mobley, National Geographic Society).

known, the picture appears to have been taken around 10 a.m. and at a temperature of about -25C (which is a little warmer than the temperature at which ice fog appears). The picture splendidly displays some of the major sources of moisture which produce dense ice fog. The thick steam shows up clearly along the slough which is kept open by cooling water dumped by the Golden Valley Electric Assn., but the steam from the right foreground of the picture to the foreground bend of the slough seems to be evaporating before freezing, probably due to a shortage of moisture and freezing nuclei in this area. However, just beyond the second bend of the slough there is a thin layer of ice fog spreading out from near the actual dump point below the large plume of the Golden Valley generating plant, and there is a long layer of ice fog above the ground. It is obvious that the exhaust from the stack of the MUS power plant (on the far right side, of the picture) goes up and down in the city, dissolving and changing into thin ice fog. Many small stacks of home or store heating are also making ice fog. Beyond the Golden Valley Electric Association plant, the Fort Wainwright power plant and its cooling pond are also making heavy ice fog. Along the road which can be seen from the lower right hand corner to the middle left of the picture, several cars are running, but their contribution to formation of ice fog does not seem to be significant in this picture. Even though the picture does not show true ice fog, the moisture sources for ice fog are identical.

Along highways we normally can see dense ice fog and it seems to form from automobile exhaust. However the contribution of car exhaust may be

over-emphasized by many people. In fact, during the severe cold spell from the end of 1968 through the middle of January, 1969, dense ice fog around the International Airport of Fairbanks originated from the main airport building and several attached cargo, post office, oil service, and local air-line offices rather than from automobile exhaust in the parking lot of the airport. Under the -50°C condition on 2 January 1969, the visibility leeward of the building was about 100 m but between the building and leeward of the parking lot was 120 m, and windward of the parking lot the visibility was also 120 m. The poor visibility windward of the parking lot was due to the small amount of open water west of the Bureau of Land Management office (BLM) and the University power plant (see Fig. 2) and/or coming from the residential area located just northwest of the airport. At any rate, from our visual observations, car exhausts were not the most important source of water vapor for ice fog. However, concerning air pollution in general, we agree with Benson's (1965) conclusion that car exhausts are very serious sources of such components of air pollution as hydrocarbon materials and lead compounds, although we did not have definite evidence for these materials.

Exhausts from power plants also make ice fog under low temperature conditions*. The smoke from a stack initially rises higher than the top of the ice-fog layer because of its warmer temperature, but the plume then cools and sinks back down into the fog layer. Leeward of the stack we could see wide spread diamond dust (= ice crystal display) when ambient

* This description is revised from the former progress report entitled "Alaskan Ice Fog" (Ohtake, 1967).

temperatures were lower than -21°C . The particles of the smoke were confirmed to be a major source of ice-forming nuclei effective at temperatures below -13°C with a high degree of supersaturation (Ohtake and Henmi, to be published).

Observations of the development of ice fog in the Fairbanks area from its beginnings also showed that at first the fog develops from open water and spreads out into the area downwind from the open water, as can be seen in Fig. 61; then at temperatures below -21°C ice-crystal displays appear downwind from power plants as well as open water. Under these conditions visibility is reduced to about 1 km. As temperatures continue to drop to about -30°C , slight ice fog appears in the vicinity of houses and along the roads. At temperatures lower than -35°C the ice fog completely covers the city. Although ice fog from open water is dense, it does not seem to spread out over very wide areas (the exact area varies with the direction of the wind), while ice fog originating from automobile exhausts was thin but widespread.

The onset temperature of ice fog has been gradually increasing. In 1911 there was virtually no ice fog even at -50°C , even in Fairbanks city as shown in the photograph reproduced by Benson (1965) as Fig. 20. Benson (1965) gave -35°C as the upper temperature limit for ice-fog formation, while our own more recent observations suggest that the current upper temperature limit for ice fog is nearer -30°C . With the current 'oil boom', the population, number of houses and cars, and airport traffic are all increasing

rapidly. Figures 62 and 63 show the relationships between temperatures and visibilities at the Fairbanks International Airport for the winters (December through February of the next year) of 1964 to 1965 and of 1968 to 1969, respectively. The plots were taken from 3-hourly data which appear in the Local Climatological Data of Fairbanks published by the US Weather Bureau. From the figures it can be seen that the visibility in recent years has become worse than that of several years ago at the same temperatures. Also the onset temperature for ice-fog formation has risen. So the onset temperature of ice fog is becoming steadily higher, and this tendency will continue in the future unless a deliberate effort to reduce ice fog is made. Air pollution other than ice fog (or rather the pollutants other than water vapor) will also be more serious and the visibility will continue to deteriorate due to higher concentrations of ice-fog crystals.

The airplanes at the airport are also producing ice fog, especially during take-off. But as far as we are able to observe at the Fairbanks International Airport, such ice fog normally drifts with the wind at about 2 m sec^{-1} toward the south to southwest, away from the airport. However the buildings incidental to the airport are making more serious ice fog on the runway than are the airplanes themselves. Again, the oil activity on the North Slope has resulted in a tremendous increase of buildings adjacent to the runway.

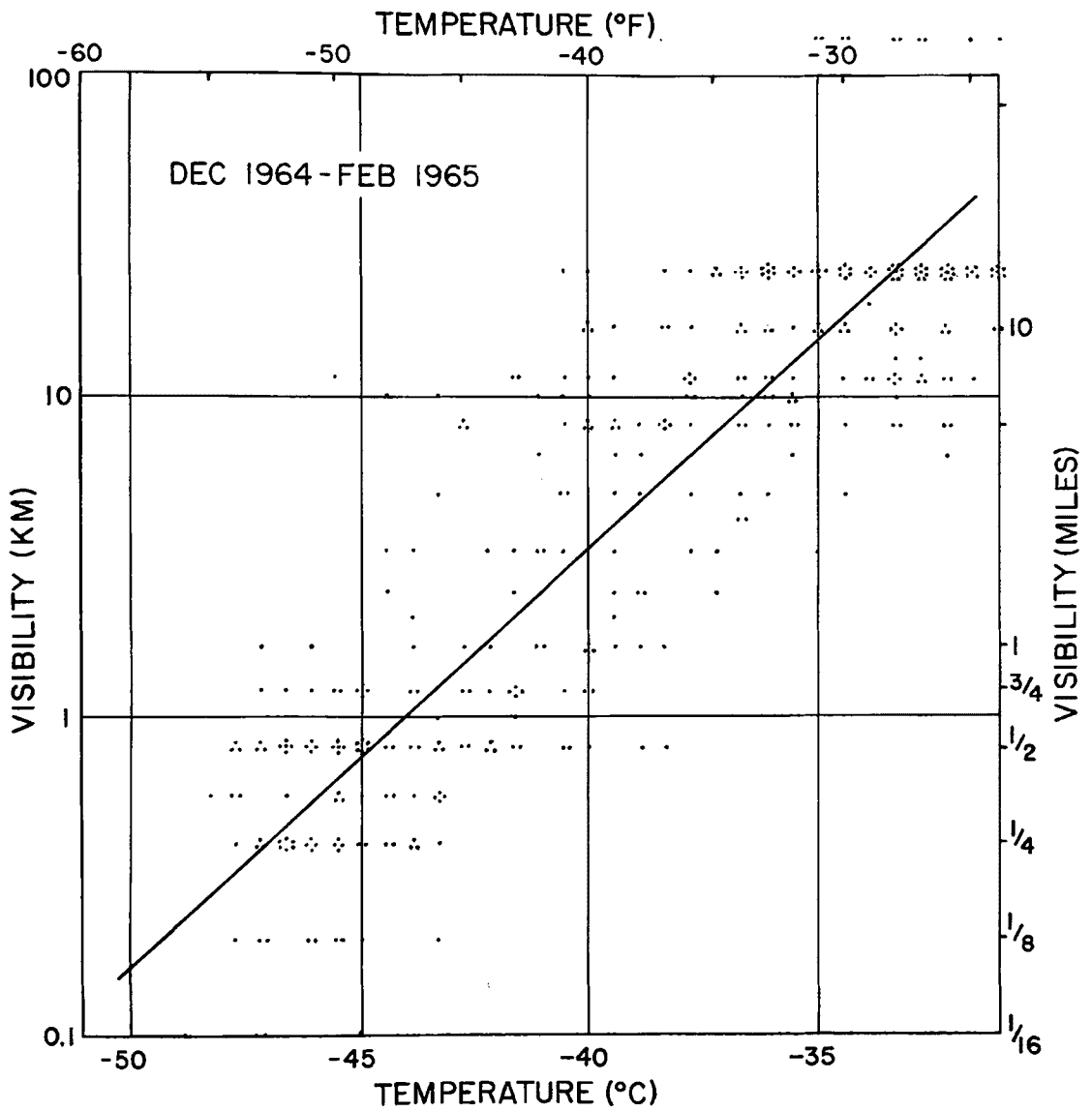


Fig. 62. Relationship between temperatures and visibilities at the Fairbanks International Airport during December 1964 through February 1965.

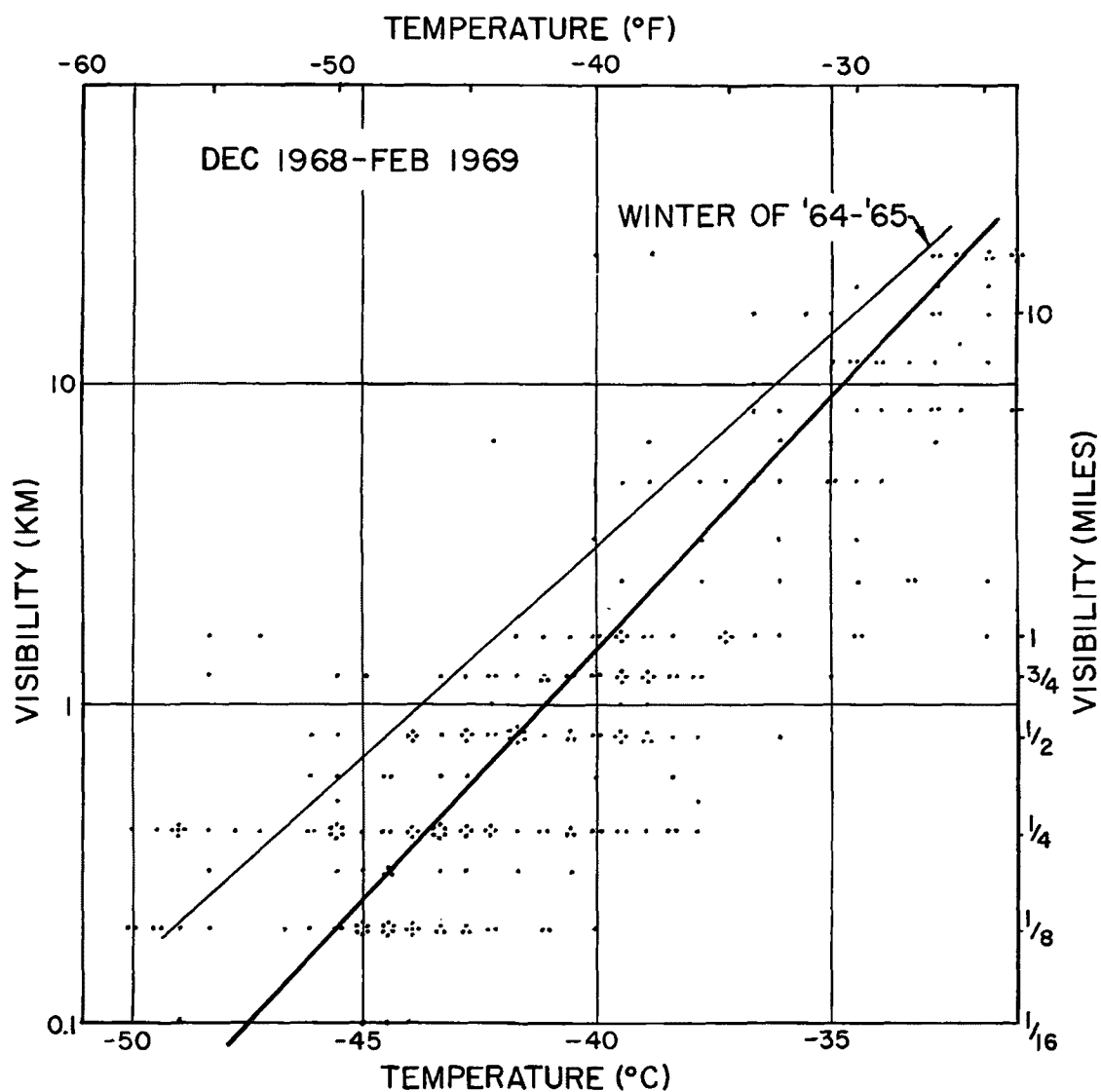


Fig. 63. Relationship between temperatures and visibilities at the Fairbanks International Airport during December 1968 through February 1969. Compare with the situation as of four years ago.

c. Measurement of Evaporation of Water from the River or a Pan and the Formation of Water Droplets from the Vapor:

Benson (1965) estimated the amount of water vapor evaporated from the open water area of about $1.5 \times 10^8 \text{ cm}^2$ maintained by dumping hot water from the MUS power plant into the Chena River at rate of $482 \times 10^6 \text{ g day}^{-1}$ during clear weather and $522 \times 10^6 \text{ g day}^{-1}$ for ice fog weather. (The increase may be due to increased power demand in colder weather.) These estimates give evaporation rates per unit area of the surface of the river at 0C of $32,100 \text{ g m}^{-2} \text{ day}^{-1}$ and $34,800 \text{ g m}^{-2} \text{ day}^{-1}$, respectively. Since he estimated these values by means of the heat budget of dumped water, and his values of evaporation under low temperature conditions were rather high (of the order of 30 mm day^{-1}), we tried to observe these values directly. Benson reported that the largest source of water vapor for ice fog comes from open water along the river, sloughs or ponds. In the present research we concentrated our attention on the open water as a main source of ice fog. On the other hand we could not find any observations of evaporation rates under such low temperatures.

An attempt has been made to observe the evaporation rate by using shallow pans and a heat lamp under ice-fog conditions. Two shallow pans (13.4 cm and 30.5 cm diameters with depth of 1.7 cm; lids of 35 mm film cans) were filled with about 1 cm of water, put on a wooden box and exposed to the atmosphere. The water was kept free from freezing by use of an industrial infrared lamp (infrared and visible light). The resultant temperatures of the water were

kept around 4 to 10C, with an occasional maximum of 15C. The temperatures were measured by dipping small thermometers into the water and we tried to keep them around 4 to 6C by controlling the distance between the lamp and pan. As can be seen in Table 9, the amount of water evaporated in ice fog was roughly $5,000 \text{ g m}^{-2}\text{day}^{-1}$ (or 5 mm day^{-1}) which is much smaller than the value Benson estimated. This value indicates that the production rate of water droplets is about 10^4 droplets sec^{-1} from 1 cm^2 of water surface assuming droplet diameters of 10μ . This value implies that 100 droplets are continuously supplied into the atmosphere from 0C water surface when the strength of wind is assumed to be 1 m sec^{-1} . In comparison with evaporation rates in a room at 23C (water and air temperature) much more water evaporated from a pan in the colder outside than in the room. This result is of course, due to larger air movement on the water surface and larger temperature differences between air and water in the outdoor conditions. Thompson (1967, unpublished) also estimated an evaporation rate of about $2780 \text{ g m}^{-2}\text{day}^{-1}$ using Thornthwaite and Holzman's equation (see Munn, 1966) with a steady-state assumption (no large-scale transport of fresh air coming into the river area and an adiabatic lapse rate).

For constant water temperature, lower air temperatures should give higher rates of evaporation, but we could not verify this because of difficulties in keeping the water temperature constant. However an evaporation rate of about $5000 \text{ g m}^{-2}\text{day}^{-1}$ for air temperatures of around -40C should be valid under normal ice-fog conditions.

TABLE 9.

Observation of Evaporation Rate of Water from Pans in Low Temperature

November 17, 1967

Room Temperature 23 C

Time ASTTotal Weight

0930	300.0 ^{gm}	start
1036	299.0	
1212	297.7	
1342	296.6	
1702	294.3	end

During 447 min. (0930 1702), 5.7 gm of water evaporated.

This value gives $1300 \text{ gm}^{-2} \text{ day}^{-1}$.

<u>Time</u>	<u>Date</u>	Mean Air Temp. (°C)	Water Temp. (°C)	Small Pan $\text{gm}^{-2} \text{ day}^{-1}$	Water Temp. (°C)	Large Pan $\text{gm}^{-2} \text{ day}^{-1}$
0930-17 Nov.	1702-17 Nov. 1967	23	23	1300	-	
1445-26 Nov.	0906-27 Nov.	-23	(2) w/ice	2890		
0910-27 Nov.	2007-27 Nov.	-18	(-) wo/ice	3190		
1700- 5 Dec.	0900- 6 Dec.		4	3200		4440
0900- 6 Dec.	0900- 7 Dec.	-30	7	5700	4	5320
1130- 7 Dec.	0830- 8 Dec.	-25	6	5460	6	6860
0900-13 Jan.	0900-14 Jan. 1968	-39	5 ~ 10	5580	7	6110
0900-14 Jan.	- 0900-15 Jan.	-41,	10	5170		5460
0900-15 Jan.	- 0900-16 Jan.	-42	15	8530	11	7370
0900-16 Jan.	- 0900-17 Jan.	-44	15	7160	10	7560
0900-17 Jan.	- 0900-18 Jan.	-43	4	3110	6	4280
0900-18 Jan.	0900-19 Jan.	-43	5	4530	5	4350

d. Temperature Measurement above Water Surface:

The main sources of moisture in the formation of ice fog are open water and exhausts from automobile, heating and power plants. The temperatures of car exhausts were measured by Benson (1965), and he gave an empirical formula

$$\frac{dT}{dx} = -k (T - T_a)^2,$$

where T is the temperature of the exhaust gas ($^{\circ}\text{C}$), T_a is the ambient air temperature, x is the distance (cm) from the exhaust tube outlet, measured in the center of the exhaust plume, and k is a constant. We obtained similar data (Ohtake, 1966) and the equation seemed to fit well.

Open water is maintained where power plants dump into the river a lot of cooling water, which keeps some of the river from freezing up. Since the temperature of this open water on the Chena River is close to 0°C , even in ice-fog condition evaporation is high and the resulting steam fog drifts into the city of Fairbanks. Measured temperature profiles above the water surface using a thermistor probe at the end of a long pole are shown in Fig. 64. These temperature profiles seemed also to fit Benson's equation for car exhaust. With this steep temperature gradient and slight air drainage winds (about 1 to 2 m sec^{-1}) blowing down from both sides of the banks, the steam rises and is cooled very rapidly. Kumai and O'Brien (1965) measured the temperature downwind of a power plant stack at the height of the stack top. Their results seem to be reasonable.

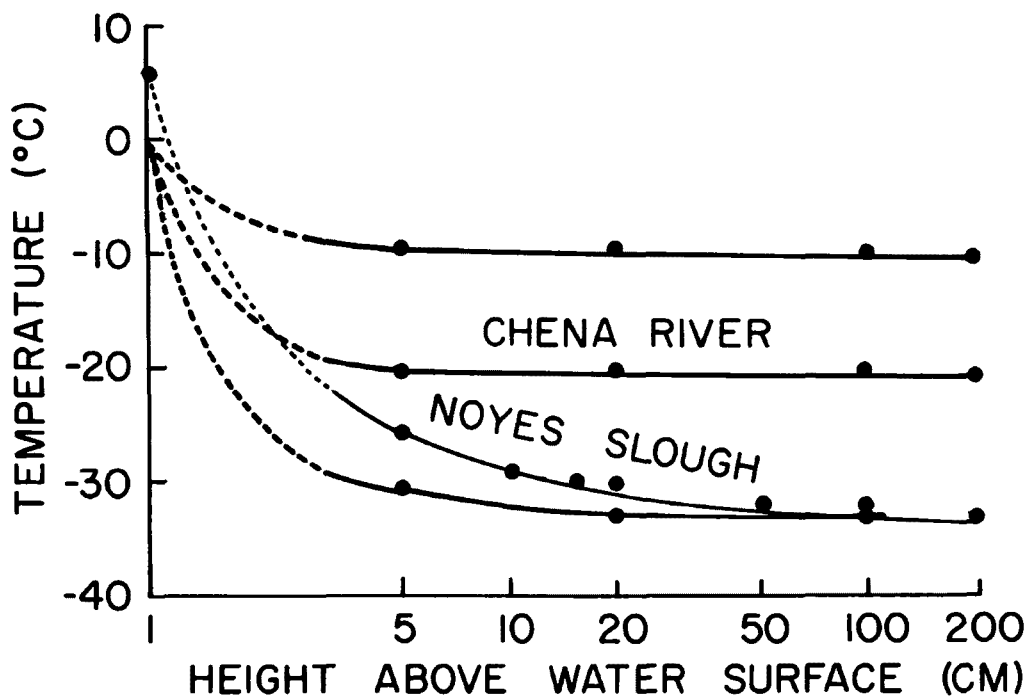


Fig. 64. Temperature profiles above open water under the conditions of several ambient air temperatures.

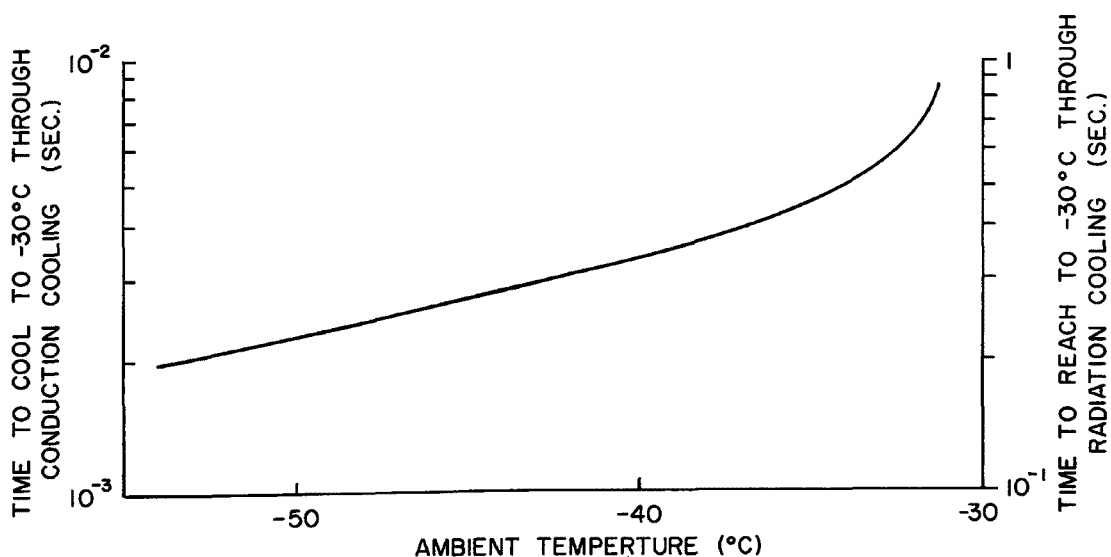


Fig. 65. Result of calculation of time for water droplet to cool from 0°C to -30°C through conduction cooling or radiation cooling.

e. Derived Supersaturation Degrees, Compared with Supersaturation Required to Activate Condensation Nuclei:

From the previous section, we know that the temperatures above the open water are almost the same as the ambient air temperature more than a few centimeters above the water surface. Exhausts from automobiles and power plants also cool very rapidly. Air over the open water is easily moved by slight winds and small scale convection to a few centimeter above the water surface, where it encounters extremely cold air. If the air is saturated at the water surface, the vapor pressure is 6.11 mb (or saturation vapor density is 4.85 g m^{-3}), while saturation vapor pressure over water may be 0.19 mb (or 0.18 g m^{-3} vapor density) for -40°C . Even at -30°C the corresponding values are 0.51 mb or 0.45 g m^{-3} . If the saturated air at 0°C cools to -40°C in 5 cm, we will have a factor of 30 times saturation (relative humidity 3000%). Even if the ambient air is considerably warmer the supersaturation will be very large. At these high supersaturations, water vapor from open water or combustion exhausts can very easily condense into water droplets. If water temperatures are higher as at hot springs, the supersaturation will be even higher. As was stated in the previous chapter, at Chena Hot Springs and Manley Hot Springs concentrations of condensation nuclei effective at about 400% of saturation were normally 200 to 400 cm^{-3} . Even at such low concentrations of nuclei, the supersaturation was high enough that condensation of water vapor into water droplets can easily occur. In the Fairbanks area where we can find more than 10^5 cm^{-3} condensation nuclei, condensation will be even faster. This is quite a different situation from that in natural clouds, where such

supersaturations would never occur. Only in a contrail are conditions similar. At low temperatures, automobiles and heating and power plants produce water droplets in the air in the same manner as does open water. Even though available dusts must be effective as condensation nuclei in areas where nuclei are scarce, it is very possible that fog droplets form without any nucleus.

f. Time Required for Droplets to Freeze:

Some water droplets may evaporate and the water vapor added to the atmosphere may provide moisture for growth of ice-fog crystals, but this evaporation of droplets does not seem to occur to any great extent in the vicinity of the water surface. If much evaporation occurs, the latent heat of evaporation has to be taken from the droplets themselves, so that freezing proceeds in the droplets. Thus the water droplets are cooled down and frozen into ice crystals. Once the droplets freeze, the crystals cannot evaporate so quickly. They then drift into the ice fog. Exhaust from cars and heating plants react similarly except that these exhausts may produce nuclei as well as water vapor.

In order to explain the transition from a water droplet to a spherical ice-fog crystal, it is necessary to know the time required for water droplets to freeze. Two mechanisms for cooling of droplets, conduction and radiation, are considered in this report.

1. Conductive Cooling:

Since a water droplet is small, the temperature in it is assumed homogeneous, assuming that temperature $T(r)$ in the air satisfies Poisson's equation, $\nabla^2 T(r) = 0$,

$$-4\pi r_a k (T - T_o) = m C \frac{dT}{dt}$$

where

- r : distance from the center of droplet
- r_a : radius of droplet
- k : coefficient of thermal conduction in air
- T : temperature of droplet
- T_o : ambient temperature
- m : mass of droplet
- C : specific heat of water

The time required for water droplets of 12μ diameter initially at $0C$ to cool down to $-30C$ is shown in Fig. 65. The time is proportional to the reciprocal of the square of the diameter of the droplet.

2. Radiation Cooling:

The fundamental equation is

$$-\sigma \frac{S}{2} (2T^4 - T_u^4 - T_\ell^4) = m C \frac{dT}{dt}$$

where

- S : surface area of water droplet
- T_u : radiative temperature of upper hemisphere
- T_ℓ : radiative temperature of lower hemisphere
- σ : Stefan-Boltzmann's constant

The measurements of radiative temperature for several objects were made by use of a Linke-Feussner radiometer in the ice-fog condition, as

shown in Table 10 including data of Stoll and Hardy (1955). On the basis of the observations, the following cases may be considered:

- i) Droplets above the water surface and without fog; $T_u = 213^\circ\text{K}$ and $T_\ell = 273^\circ\text{K}$.
- ii) Above the water surface and with fog; $T_u = \text{ambient temperature}$ and $T_\ell = 273^\circ\text{K}$.
- iii) Above the snow surface and without fog; $T_u = 213^\circ\text{K}$ and $T_\ell = \text{ambient temperature}$.
- iv) With fog and above snow surface; $T_u = T_\ell = \text{ambient temperature}$.

We now calculate the time for the droplet to cool down to -30°C . In cases i) and ii), the droplets never get colder than -25°C regardless of their size. Case iii) gives results similar to those for case iv). Therefore we will show only the result for case iv). The form of the curve of time versus ambient temperature is approximately the same as that for conduction cooling, though the time is now proportional to the reciprocal of the diameter. Therefore, we need only change the scale in Fig. 65 to show the result.

TABLE 10		
Radiative Temperature of Various Objects		
	Air Temperature $^\circ\text{C}$	Radiative Temperature $^\circ\text{C}$
Sky without fog (after Stoll and Hardy, 1955)	-40.0	-65
Sky with thin cloud	-35.2	-41
Sky with ice fog	-40.1	-40
Snow Surface	-40.0	-36
Water (0°C) through 20m thick of ice fog	-40.4	-20

In the above calculation, the 0C means the steam has formed just above a water surface of temperature 0C and the -30C means the ice fog begins to appear about -30C according to our observation. The initial temperature for droplets originating from exhaust of cars and heating units may be approximated as 50C to 100C. Even for an initial temperature of 100C, the time to reach -30C is of same order as that for the initial temperature 0C.

As an experimental verification of the above calculation the frequency of appearance of water droplets near water sources has been examined by two methods: the collodion or formvar film method and water-blue film method. Droplets and crystals in the air are captured by very weak suction on a collodion or formvar film supported by an electron microscope grid, the temperature of which can be controlled by varying the voltage to the illumination lamp or by warming the microscope stage. When the air containing water droplets and ice crystals is sucked through a small impactor (Fig. 66) by mouth, both kinds of particles hit the film. Ice crystals do not evaporate during a very long time on the grid, while water droplets hitting the film do evaporate in about a second. This is due to the difference of saturation vapor pressure for ice and water, and also the thinnest formvar or collodion film provide a very small heat capacity which prevent the deeply supercooled water droplets from being frozen by hitting a cold support. Unfortunately, we did not succeed in obtaining good demonstration pictures by use of a microscope and a 16 mm camera. By this method we confirmed that some water droplets were still in the liquid phase 5 m downwind from 0C open water at an ambient air temperature of -42C with a wind speed of

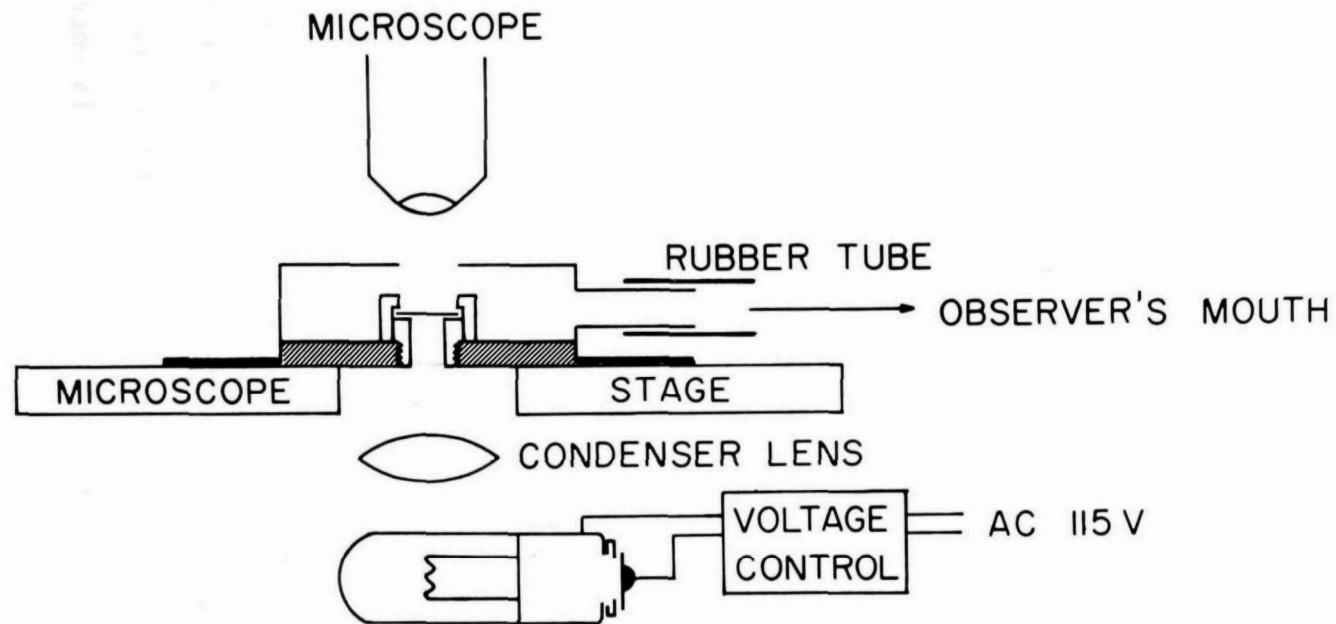


Fig. 66. A small impactor to check whether the water droplets have been frozen or not.

1.5 m sec^{-1} . 10 m from the open water few droplets can be found. These values indicate that the time required for water droplets of about 10μ diameter to freeze is about 3 to 7 seconds at an ambient temperature of -42C .

Another method is based upon Okita's (1958) water-blue film method to determine the drop size of water fogs. He used a cellulose nitrate film coated by a 2.5% aqueous solution of water-blue (same as aniline blue) dye. If any water droplets contact the film, they produce clear spots on the blue film base. These clear spots are undoubtedly made by re-solution of the water-blue coat, but under very low temperature conditions it is not certain that such water droplets will have time to dissolve the dye before freezing on the film. However under -42C temperatures and at nearly the same time as the formvar film method was being done, we found many droplet spots on the water-blue film which was tested at the bank (0 m) and 20 cm above the open water. The films were attached to slide glasses 3 mm wide, which were waved 30 times (about 1 m of traverse) by hand as fast as possible to improve collection efficiency. At 1 m from the open water many faint spots and several clear spots were found. We presume that the faint spots were made when a water droplet hit the water-blue film, froze and evaporated, while the clear spots were made by water droplets which evaporated from the film without freezing. On the other hand, the water droplets (= ice crystals) which are frozen before impact will not make any spots on the water-blue film. There were small clear spots and faint spots at 2 m, some faint spots and no clear spots at all at 5 m and no spots at all in any shape 10 m from the open water.

These results are almost the same as those made by the formvar film method. At the MUS site in downtown Fairbanks and 20 m or more from the hot springs at Chena Hot Springs, we have never found any spots in several trials. These observations verify that all particles in ice fogs are completely frozen (except near water-droplet sources) under conditions of about -35°C or below. This result is not in agreement with Borovikov's (1968) who observed some supercooled water droplets in a natural cloud at a temperature of -40.6°C , but we could not obtain detailed information about the method he used.

g. Theoretical Study of the Size Distribution of Ice-Fog Crystals:

Considerable theoretical attention has been given to the nucleation and growth of ice crystals in clouds (Mason, 1957; Fletcher, 1962; Byers, 1965). The present study deals with the theoretical treatment of the nucleation and subsequent growth of ice-fog crystals, based upon the observations we have made such as the measurements of temperature profile above water and behind automobile exhausts, high supersaturation near the sources, absolute humidities, and possible homogeneous condensation and freezing of water droplets. Since a full paper has been submitted to "Tellus", by Huffman and Ohtake, and is attached to this report as an appendix, only the abstract of the paper is given here.

A mechanism is proposed for the formation of ice-fog crystals in the city and environs of Fairbanks, Alaska. Equations are developed for calculating the size distribution resulting from growth by sublimation of water vapor. These equations are solved numerically, with the use of a computer, for three major types of ice-fog sources: A) automobile exhaust, B) exhaust from heating plants and C) open water. For

source type A, the computed size is much smaller than that observed; but for source types B and C, the computed size distributions are found to be in good agreement with experimentally obtained values.

The discrepancy between the computed and observed sizes for source type A is possibly due to the large degree of supercooling exhibited by small water droplets. Only very few of the small water droplets, initially formed by condensation, freeze. These frozen particles may then grow to the observed size at the expense of the more numerous evaporating liquid droplets. On the other hand, the larger droplets produced by source types B and C probably nearly all freeze very shortly after their formation, leaving no appreciable supply of liquid droplets to provide for their further growth.

h. Effects of Lower Air Temperature:

It is important to realize that the lower temperatures are not only responsible for the early freezing of water droplets but also affect many aspects related to the ice-fog crystals. The rate of evaporation from the water surface depends upon the differences between water vapor densities of ambient air and air at the water surface. Since the water vapor density at the water surface is constant because the water temperature is constant at 0°C, the lower temperature gives the higher evaporation rate because colder air has lower water vapor density. Also, colder air can maintain smaller amounts of water vapor. Thus the lower air temperatures give the higher rates of water-droplet formation even in same wind profile above water surface, and quicker freezing.

Under the lower air temperature conditions such frozen water droplets (= ice crystals) can grow only at a minor rate because values of vapor density differences ($\rho - \rho_0$) is smaller in the cold air assuming ambient vapor density is at middle value between water - and ice - saturation

(refer to the equation on the page 83 and observation of humidity in ice fog). This results in many small rudimentary faceted ice crystals which have very slow fall speeds and are persistently suspended in the air near the ground for long time periods; thus ice fog is continued. This mechanism explains that at lower temperature the mean size of crystals becomes smaller and the concentration of ice crystals becomes higher. Also, the solid water content should be temperature-dependent, providing that the moisture source remains constant and water droplets are released from the same area.

With the lowering of temperature, the air loses its capability to maintain the same amount of moisture as vapor, and steam or ice crystals which come from open water evaporate only with great difficulty. Such unevaporated ice crystals make ice fog.

This descriptive explanation was made based upon our observations for the case of open water, but it analogizes the cases of exhausts from heating plants and cars in which the temperatures are higher than 0C in these cases.

These low-temperature effects may be more important than the role of freezing nuclei for ice-fog formation in the inhabited area. From figures 62 and 63 we could not find any threshold for appearance of ice fogs at temperatures between -37C to -40C which have been considered to be the most important temperature for ice-fog formation. If the critical temperature for formation of ice fogs in relatively uninhabited areas such as Manley Hot Springs or Chena Hot Springs would be -40C, the explanation of low temperature effects may be more valid than that through the spontaneous nucleation of purer water droplets.

1. Conclusions on the Mechanism of Ice-Fog Formation:

Although many former studies (Thuman and Robinson, 1954; Kumai, 1964; and Benson, 1965) have suggested that the mechanism of ice-fog formation is the freezing of water droplets resulting from moisture of car exhaust or open water, they did not show either verifications or considerations based upon observations for the purpose. In the present research we have shown that: 1) Large amounts of steam (small droplets), formed initially from water evaporated from open water, are formed in the layer very close to the water surface and disperse into the atmosphere. The evaporation rate of water vapor from the surface and production rate of water droplets were also estimated, based upon the observations. 2) Aerial photographs showed steam or water clouds, which are important sources of ice-fog moisture, coming from the open water of the river, slough and cooling ponds, power plants and private heating systems. 3) Such water droplets will freeze in several seconds within a distance of 3 to 5 m from open water under low temperature conditions. This was confirmed by the observations of the time required for droplets to freeze, and temperature profiles above water surfaces. Also, it was supported by calculation of conductive cooling and radiative cooling, which were also directly measured by means of a radiometer for various objects in ice fog. Auto exhausts supplement water droplets and they will be changed to ice-fog crystals in the same way. So running cars are sprinkling ice crystals rather than adding moisture as vapor into the atmosphere. 4) The humidity in ice fog lies between water- and ice-saturation, allowing the ice-fog crystals

to grow, but very slowly because of the small differences of saturation vapor pressure between them. This results in ice-fog crystals having the smallest size of ice crystals and being suspended in the air for a long time. The modal size of the ice crystals changes with the changes in the moisture content of the environmental air. In an area which has less moisture than ice saturation, the crystal sizes will be smaller and smaller until the crystals disappear. A typical size distribution of ice fog is shown in Fig. 6. These observations are also supported by a theoretical consideration of size distribution of ice-fog crystals.

5) The most important factor in the formation of steam or water droplets is not the concentration of condensation nuclei in the case of formation of steam from open water, heating plants and car exhausts under ice-fog conditions but rather the temperature differences between water (not ice) and ambient air temperature. However, condensation nuclei or other particles contained in the water droplets accelerate the freezing of water droplets at a higher temperature than the spontaneous freezing. We believe that the onset temperature of ice-fog formation is higher in inhabited areas than in unpolluted areas due to the greater numbers of condensation nuclei and effective freezing nuclei in the city, as well as the difference of moisture supply between in-city and out-of-city sites. However, at temperatures lower than about -37°C , the homogeneous nucleation of condensation and successive spontaneous freezing of water droplets are quite possible even in contaminated areas.

6) The lowering of air temperature increases the

rate of evaporation, i.e. rate of water-droplet formation, speed of the droplet freezing, suppression of the frozen ice-crystal growth, and formation of more numbers of smaller crystals. Thus, denser ice fog can be seen at lower temperatures. So the low temperatures are essential for dense ice fog, providing constant moisture sources are available.

9. SYNOPTIC METEOROLOGICAL STUDIES OF ICE FOG

Local radiative cooling as described by Wexler (1936), or as modified by Gotaas and Benson (1965), has generally been used to explain the low temperatures and unusually strong inversions observed in interior Alaska. The association of anticyclones with extreme cold is well known in general, but little effort has been made to distinguish between the effects of high pressures produced locally by radiative cooling and those associated with advection from regions outside Alaska. An attempt has been made in the present project to show the effects of advective and dynamic processes in producing, or inhibiting the production of, the low temperatures and to some extent the steep inversions which lead to the formation of ice fog. Since the report has already been published (Bowling, Ohtake and Benson, 1968), only the abstract is included here in the section a).

a. Winter Pressure System and Ice Fog in Fairbanks, Alaska:

The production of the low temperatures which are responsible for ice fog in inhabited areas of interior Alaska would appear to be a classic example of clear sky radiative cooling under nearly polar night conditions. However, examination of the meteorological conditions associated with 15 periods of dense ice fog at Fairbanks indicates that local radiative cooling is important only in producing the observed steep ground inversion. The most rapid decreases in temperatures at heights > 1 km occurred with cloud cover and cold air advection preceding the cold weather at the ground.

The most common synoptic pattern (observed for the 12 shortest events) consisted of the migration of a small high from Siberia across Alaska. Rapid growth of the high was common, and the resulting subsidence was strong enough to counter-balance not only radiative cooling, but further cold air advection as well. This resulted in an observed warming aloft during all but the first 12-24 hr of the clear, cold weather observed at the ground. Three of the 15 events did not follow this pattern. Two long and very cold events were associated with warm highs in northeastern Siberia, continuous belts of moderately high pressure extending from Siberia across the Bering Strait into Alaska, and advection from Siberia and the Arctic Ocean. The remaining long but relatively mild event was associated with a warm high north of Alaska and advection from Canada and the Arctic Ocean.

b. Analysis of Air Mass Trajectories:

As mentioned previously, water vapor measurements in the vicinity of Fairbanks show near-ice-saturation in the winter. Since, in general, water vapor is transported with air mass, it is interesting to study the origin of dry or wet air masses which arrive at Fairbanks. Using 500 mb synoptic maps for the winter of 1967 to 1968, an air trajectory analysis was made. In the analysis, the trajectories were followed for 5 to 7 days before their arrival in the Fairbanks area, and also at the 500 mb level geostrophic winds were assumed as predominant. With omission of full trajectory maps which can be seen in Henmi's (1969) master's thesis, the following results may be noted: 1) Warm and wet air masses are associated with the

trajectories over the Pacific Ocean. 2) Cold and dry air came with air from the Arctic Ocean, in which air ice fogs occurred in the winter of 1968. 3) The cooling of the air in the Fairbanks area was partly caused by the advection of the cold air mass from the Arctic Ocean. 4) The cessation of the ice-fog events occurred when air was advected from the Pacific Ocean.

c. Practical Ice Fog Prediction:

Appleman (1953) reported an interesting method of forecasting ice fogs, which is based upon a combination of temperature and relative humidity. Although he considered only the effects of burning hydrocarbons under conditions of high relative humidity, the proposed diagram for the conditions necessary for formation of ice fog seems to be correct. However, to predict ice fog using his diagram we have to predict relative humidity as well as temperature. As previously mentioned, the measurement even of the present value of humidity is very difficult. Even at the U.S. Weather Bureau, current relative humidities at temperatures below -35F are reported by assuming ice saturation and converting to relative humidity over water.

From a) and b) in this chapter we propose the following simple method for forecasting ice fog. From the middle of November through February every year, the proposed method may be applicable. If the predicted 500 mb flow has a component from the north over most of central Alaska, ice fog will occur in the inhabited areas. In practice this type of flow will occur with a ridge located between the west coast of Alaska and a position well into Eastern Siberia. The surface expression of the ridge will

normally be in central Alaska. (The surface high pressure in itself is not an adequate predictor, as a warm core anticyclone from the Pacific may result in high pressure at the ground with warm weather). If a 500 mb ridge is located farther east, so that the upper air at Fairbanks has a source to the south, relatively warm temperatures aloft will prevent excessive radiative cooling at the ground. Southwesterly flow is almost always accompanied by cloud cover, while southerly or southeasterly flow over the Alaska Range will show a foehn effect, giving clear skies and near normal temperatures.

As was mentioned before, in interior Alaska during the winter the humidities are almost ice saturation at the surface even outside the city, due to the extensive snow cover. This means that we have to watch only temperature for making ice-fog forecasts, even though Appleman proposed the method of forecasting considering both temperature and humidity. However, the present method is sensitive to errors in the prognostic 500 mb charts being made by the U.S. Weather Bureau, especially if a ridge is located near the Alaskan west coast. During late November, February and March, it is difficult to predict definite ice fog. In these months ice fog generally appears only at night. To improve the accuracy of the prediction even for other areas than Alaska the prediction of the planetary wave around the poles is essential.

10. VISUAL RANGE IN ICE FOG

For water fogs and clouds which consist of water droplets, a relationship between the meteorological visual range (= visibility), the liquid water content and mean diameter of the droplets was originally developed by Trabert. However, distinctive size distribution and shape of ice-fog crystals might give a different relation between them.

An article published previously presented the results of an experimental investigation into the relationship between the visual range and the size distribution of ice-fog crystals at the MUS site, the Eielson Air Force Base, and the International Airport, Fairbanks. An empirical function is developed for the constant appearing in the Trabert formula. Use of this function gives visual ranges that agree with measured values for size distributions of different width. For a full description, see the published work (Ohtake and Huffman, 1969).

11. ELECTRIC PROPERTIES OF ICE-FOG CRYSTALS

One of the purposes of ice fog research is to find methods of eliminating ice fog. In order to provide basic information for feasibility studies, the electric properties of ice fog crystals have been investigated. From the viewpoint of general atmospheric electricity, research on the electric properties of micron-sized ice crystals may lead to new information about the mechanisms of charge generation which occur in natural clouds.

A relatively small number of workers has investigated the electric properties of fog, cloud droplets and snow and ice crystals. Gunn (1955) reported that warm clouds (20C) carried charges of about 1.3×10^{-9} coulomb m^{-3} for particles larger than 10μ diameter. Assuming 100 droplets cm^{-3} of air, which is obtained from Weickmann and Kampe's (1953) average concentration of droplets in fair-weather cumulus clouds, from the above value of the charge of the cloud the individual net charge of droplets is 1.3×10^{-17} coulomb (81 elementary charges). Twomey (1956) measured the net charges on individual cloud droplets and reported that the charges in water clouds were always positive, while negative charges were detected when ice crystals were present. The negative charges observed on particles with diameters of 10μ were about 1.6×10^{-16} coulomb (1000 elementary charges). Scott and Hobbs (1968) measured individual charges acquired by an ice sphere exposed to snow or cloud particles. These workers found that individual particles produced charges of both signs ranging from -10^{-2} to $+10^{-2}$ esu (from -2×10^7 to $+2 \times 10^7$ elementary charges). In

the present paper, preliminary results are described for some rather simple experiments performed on ice fog.

a. Experiments with Ice Fog Crystals in Electric Fields:

1. Non-Uniform Electric Field:

During the first experiments, ice fog crystals were observed in the non-uniform field of two parallel copper wires (2.08 mm diameter) mounted vertically at a distance of 1.5 cm on a bakelite board. Both wires were coated with enamel and potential differences up to 12 kV could be maintained between the wires.

The wire electrodes were placed in natural ice fog in downtown Fairbanks at temperatures of about -35°C . The average concentration of ice fog crystals was 500 cm^{-3} . After applying a voltage of 3 kV between the wires for a period of about 18 hours, we could observe an appreciably thicker deposit of ice fog crystals on the positive wire than on the negative one. The deposits occurred in radially oriented dendritic shapes.

For these first observations, the high voltage power supply could produce only positive voltages with respect to ground. In order to check why the predominant deposit on the positive wire was affected by the polarity of the applied voltage, the observations were repeated using another power supply which was able to produce negative high voltages with respect to the ground. One minute after applying 12 kV, we again observed a larger deposit on the positive wire, which was at the same potential as the ground, than on the negative one. An additional experiment

using 3 kV showed the same thing, but the amount of the deposit was less than that for 12 kV. Unfortunately, since the temperature was as high as -28°C , some particles could have been in the liquid phase (Borovikov, 1968).

Experiments were also performed with artificial ice fog in a cold chamber which is open at the top only (76 cm x 40 cm x 46 cm high) and in an environmental cold room (450 cm x 290 cm x 208 cm high). The walls of both cold chamber and room are made of stainless steel which can easily frost on the surfaces. To avoid the possibility of some parts of the wall frost flying to the electrodes, the walls of the cold chamber were painted with enamel and coated with ethylene glycol. On the other hand the walls of the cold room did not have any coating nor painting.

Also to wipe the deposited ice away from the electrodes, a paper towel which was soaked with a small amount of glycol was used between successive experiments. This procedure was applied to eliminate undesirable charge generation on the wires and ice in the chambers resulting from rubbing between ice depositions.

Observations were made every 60 seconds after applying a high voltage. During the experiment the observer tried to be as far away from the electrodes as long as possible, excepting the times of observation of deposit on the electrodes. If the observer is standing close to the wires when the high voltage is applied, he will act as another electrode.

The experiments in the cold chamber were carried out by applying the high voltages with different polarities; a) 3 kV positive potential and zero electric potential with respect to the ground, b) 3 kV negative

potential and zero potential with respect to the ground, and c) 3 kV positive and 3 kV negative potential with respect to the ground (potential between both electrodes, accordingly, was 6 kV). In the case of a) both wires received a deposit of ice fog crystals but the amount of deposit on the positive wire was much more than on the negative wire for the first 60 seconds. 120 seconds after applying the high voltage, the positive wire had a very much heavier deposit in radially oriented dendritic shapes. Case b) showed that both wires had approximately equal amounts of deposits after the first 60 seconds, but the positive wire seemed to have just a little more deposit than the other wire. After 120 seconds the appearance was the same as after 60 seconds, but the deposit on the positive wire developed radially oriented needle shapes, which are an earlier stage of the dendritic shape. 180 seconds after the voltage was applied, deposit on both wires developed and the positive wire collected ice crystals in the shape of radially oriented needles appreciably more than the negative wire. In c), also both wires received a deposit, but the positive wire obviously had more deposit after the first 60 seconds. 120 and 180 seconds after 6 kV was applied with a neutral ground, much more deposit could be found on the positive wire than on the negative wire.

In summarizing the experiments using non-uniform fields, the positive wire always received more deposit than the negative wire. Throughout the above experiments the temperature in the cold chamber was maintained between -40°C and -45°C , and ice fog was produced by evaporation of water vapor from distilled water (about 5°C) in a dish for 30 seconds, a half minute before applying the high voltage in the chamber. The concentration

of ice fog crystals was approximately 2000 cm^{-3} . Each time, the deposition of ice crystals on the wires occurred earlier in the chamber than in natural ice fog outside. This was at least partly an effect of higher concentration of ice fog crystals. The observer who was standing perpendicular to the plane of the two wires could see the development of the deposition in time, observing that the initial deposition occurred on the positive wire and that some small parts of the deposition in the shape of radially oriented needles or dendrites broke off and flew to the other wire on paths approximately along field lines.

Similar experiments in the environmental cold room showed also the same results, but they were not very clear compared with those obtained in the cold chamber. This could be explained by the effects that first some frost from the walls deposited on the negative wires and second that the observer tried not to disturb the air and watched both wires from a distant position. The temperature was kept between -40.0°C and -42.5°C . Ice fog was made by mixing the air inside with outside air when the observer entered in the room. Higher voltages and thicker ice fog caused the ice crystals to deposit rapidly on the wires.

ii) Uniform Electric Field:

In order to gather further information about the nature of the forces acting on ice fog crystals in electric fields, ice crystals were observed in the uniform field between two parallel plates. The plates were 25 cm square made of uncoated copper mounted on a wooden board. Separation was

1 cm. The edges were rolled with a radius of 4 mm and the corner were rounded to avoid excessive non-uniform field; (see Fig. 67). The electrodes were placed in natural ice fog parallel to slight winds so that ice crystals could more easily pass through the field. A voltage of 3 kV positive and 0 kV with respect to the ground was applied to the plates and observations were made at temperatures of around -35°C .

Even in dense ice fog, no ice particles were deposited on the plane surface of either electrode during an observation time of approximately 20 hours. Some deposition radially oriented in the directions of electric field lines was found on the edges of the positive plate where the electric field is non-uniform.

Artificial ice fog was also observed in a uniform field in both cold chamber and environmental cold room at temperatures ranging from -47°C to -35°C . The uniform field was produced with the same set of electrodes to which voltages of plus and minus 3 kV with respect to the ground were applied. No visible deposition of ice-fog particles was observed on the electrodes in the uniform part of the field during 5 min in much thicker artificial ice fog than real ice fog. As in the case of natural ice fog, a dendritic oriented deposit was found on the edges of the positive plate. Even though high voltages the same as a) and b) for non-uniform fields were applied to the plates, we found no deposit on the inside surface of the plates in the uniform part of the field, although many ice-fog crystals were observed in the region between the plates. The experiment was repeated with electrodes coated with an insulating layer of varnish. Voltages up to 16 kV with

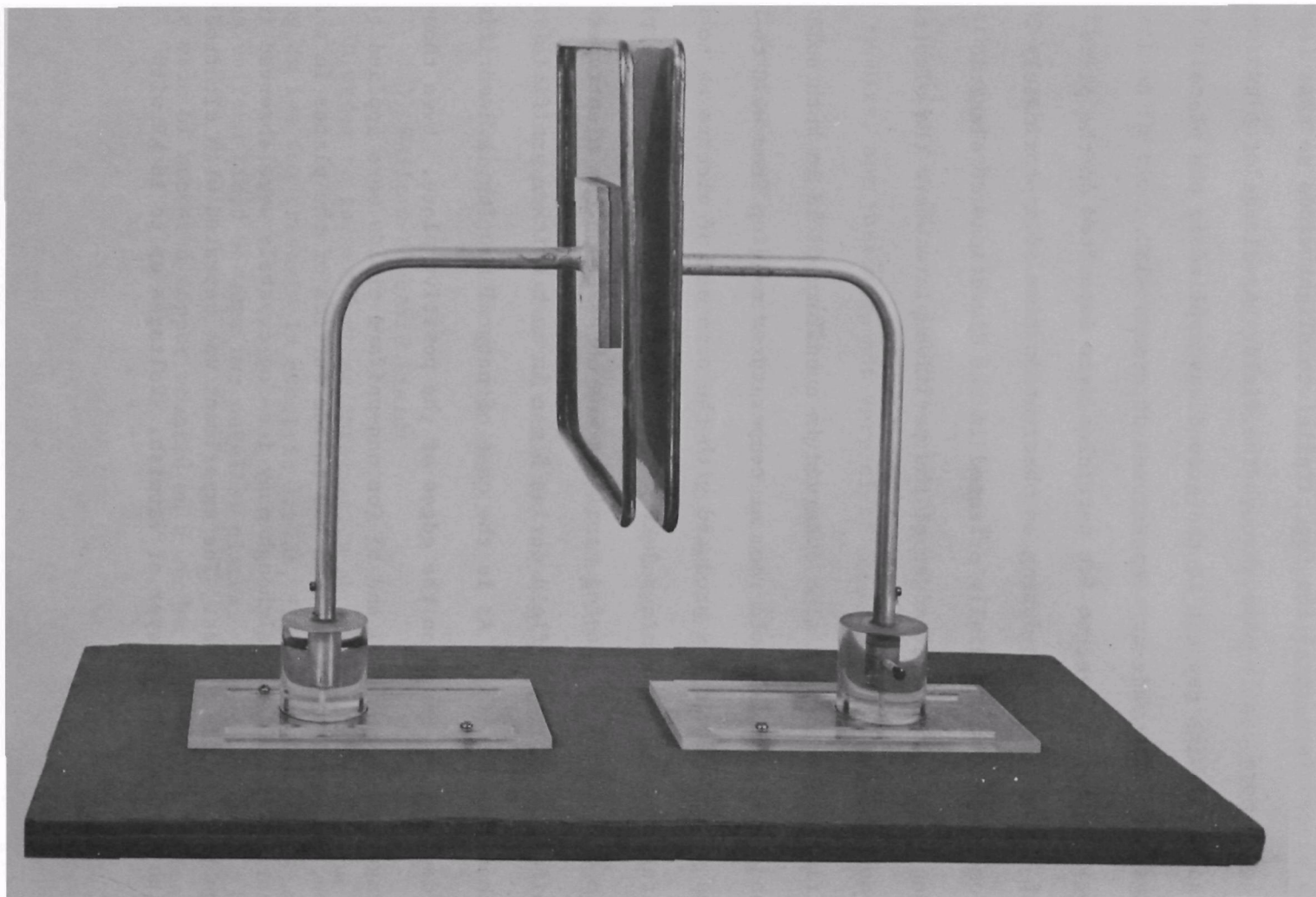


Fig. 67. The parallel plates to produce a uniform electric field.

respect to the wall were applied to the plates, but no deposit of ice fog crystals was observed on the electrodes in the uniform part of the field. At the highest electric potential of 16 kV per cm, the uniform field was appreciably higher than the maximum of the field of two parallel wires (with a potential difference of 3 kV and a distance of 1.5 cm) which gave rise to a clearly visible deposit of ice fog crystals on the positive wire and the negative wire.

b. Discussion:

From the failure of ice-fog crystals to deposit on the electrodes in a uniform electric field, one might conclude that attractive forces are sufficiently strong only in non-uniform electric fields to produce drift motion of the crystals. The equation for the motion of the center of mass of a particle in an electric field is

$$M \ddot{\mathbf{R}} + \kappa \dot{\mathbf{R}} = \sum_i q_i \cdot \mathbf{E}(\mathbf{r}_i), \quad (1)$$

where M is the mass of the particle, \mathbf{R} is the radius vector to the center of mass, q_i is the i -th elementary charge on the particle, $\mathbf{E}(\mathbf{r}_i)$ is the electric field at the location of the i -th charge, and $\kappa \dot{\mathbf{R}}$ is the friction force due to the surrounding medium.

If the electric field is uniform, eq. (1) can be rewritten in the following form

$$M \ddot{\mathbf{R}} + \kappa \dot{\mathbf{R}} = E_0 \sum_i q_i \quad (2)$$

E_0 denotes the uniform field. If the net charge $Q = \sum_i q_i$ is zero, it is apparent from eq. (2) that the total force acting on the particle vanishes. In this case the motion of the center of mass is unaffected by the uniform field, i.e., no drift motion of the ice crystal occurs.

For the motion of a particle in a non-uniform field we must consider the more general eq. (1). The term $\sum_i q_i \cdot E(r_i) = F$ can represent a non-vanishing force even if Q is zero. This is demonstrated by the example of a dipole. The sum of the forces exerted on the two opposite and equal charges is given by the expression

$$F_d = (P \cdot \nabla) E, \quad (3)$$

where P is the dipole moment. In general, F_d is a non-zero force, in a non-uniform field. In the case of a uniform field E , however, the differential operator on the right hand side of eq. (3) vanishes and F_d is zero in agreement with eq. (2).

Since no evidence for drift motion of ice-fog crystals in uniform electric fields has been observed, we can assume that any net charge Q of the particles must be insignificantly small. A drift velocity of 0.1 cm sec^{-1} would produce within 3 minutes a visible deposit on the attracting electrode under the ice-fog condition of the cold chamber. As neither a depletion of ice fog between the parallel plates bounding the uniform field nor a deposit has been observed, we can assume that any drift

velocity \dot{R} has been smaller than 0.1 cm sec^{-1} , and an upper bound for the net charge Q on ice-fog crystals can be derived. From Stokes' law we get the relation

$$Q \leq \frac{6 \pi \eta r |\dot{R}|}{|E|} \quad (4)$$

where $|E|$, r and η are the electric field, the particle radius and the coefficient of viscosity, respectively. For $r = 5\mu$, $|E| = 16 \text{ kV cm}^{-1}$ and $\eta = 1.510 \times 10^{-4} \text{ g cm}^{-1} \text{ sec}^{-1}$ at a temperature of -40°C (Mason, 1957), we find $Q \leq 6$ elementary charges.

The observation of an insignificantly small net charge of ice-fog crystals is supported by the result of our optical and electron microscope studies, which do not indicate any effects of generally proposed mechanisms for charge separation such as freezing in the presence of thermal gradients, chemical impurities in small droplets, droplet shattering during freezing or splintering from larger crystals.

Forces acting on ice-fog crystals only in non-uniform electric fields can be explained by polarization of the crystals. The force F_d exerted on a dipole moment P is given by eq. (3) and vanishes in a uniform field. P could be a permanent as well as an induced dipole moment. In either case P is oriented in the direction of the electric field and F_d has the direction of the field gradient, which points toward the nearest electrode if one considers only the field in the vicinity of each of the two wires. The assumption of a dipole moment therefore leads to attractive forces

toward both wires, and deposits on both wires have in fact been observed (see Fig.68a).

An induced dipole moment P_i of ice-fog crystals must always be present, and an approximate value of P_i can be obtained from the equation (Jefimenko, 1966).

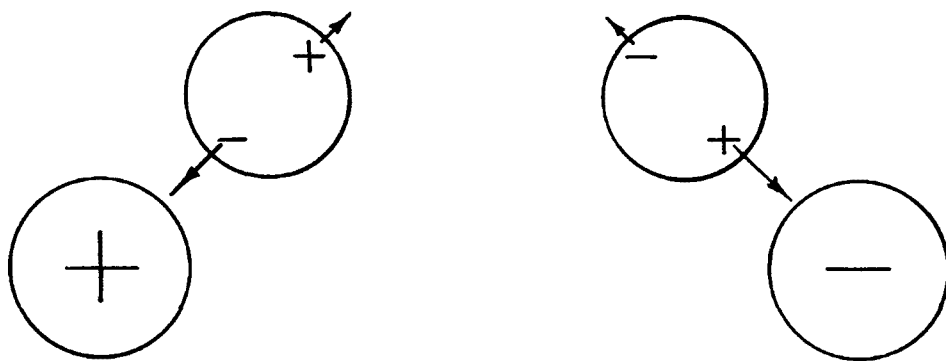
$$P_i = \frac{4 \pi r^3 \epsilon_0 (\epsilon - 1)}{\epsilon + 2} E \quad (5)$$

where ϵ is the dielectric constant (for ice, it is a tensor quantity) of the spherically shaped particles of radius r . At a temperature of 0C the components of ϵ along the c-axis and perpendicular to the c-axis are 106 and 92, respectively (Gränicher, 1963). Approximate values of P_i can be calculated using the scalar dielectric constant in eq. (5) as the value $\epsilon = 99$ and the field strength E of the non-uniform field. The potential ψ of two parallel cylinders of the same radius ρ , whose center lines are oriented along the z-axis and intersect the x-axis at $+d$ and $-d$, is given by the following equation:

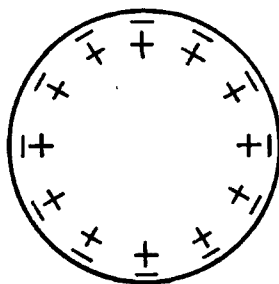
$$\psi = \frac{\phi}{2 \log \left(\frac{\rho}{d+a} \right)} \log \left\{ \frac{[(x-a)^2 + y^2]^{\frac{1}{2}}}{[(x+a)^2 + y^2]^{\frac{1}{2}}} \right\} \quad (6)$$

where ϕ is the potential difference of the cylinders, and a has the value of

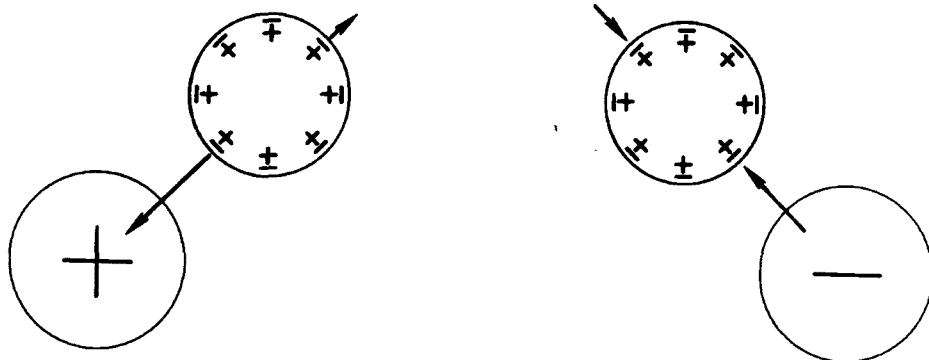
$$a = (d^2 - \rho^2)^{\frac{1}{2}} \quad (7)$$



a.



b.



c.

Fig. 68. Drawings for the possible explanations of ice-fog crystal depositions on the parallel wires. The upper drawing (a) shows ice crystals which have induced dipole moments; (b) shows crystal which has dipole layer on the surface; and (c) shows forces exerted to the ice crystals near positive and negative electrodes.

Using $\phi = 6$ kV, $\rho = 1.04$ mm and $d = 8.5$ mm, which correspond to the experimental conditions, one can compute the electric field E at the inside wire surface ($x = 7.46$ mm, $y = 0$ mm) from eq. (6), and from eq. (5) one gets for the magnitude of the induced dipole moment P_i the value 1.58×10^{-21} amp sec m. This value is based on a particle radius $r = 5\mu$. The field gradient at the same location is 1.14×10^9 V m $^{-2}$, and the resulting force $|F_d|$ on an ice-fog crystal is 1.8×10^{-7} dyne. For a viscosity $\eta = 1.510 \times 10^{-4}$ g cm $^{-1}$ sec $^{-1}$, this force corresponds to a drift velocity $|\dot{R}| = 0.13$ cm sec $^{-1}$. Although the force F_d due to an induced dipole moment in non-uniform field is sufficiently large to produce significant drift motion of ice-fog crystals, the existence of a permanent dipole moment cannot be ruled out on the basis of the experiments reported in this paper.

The observation that ice crystals are preferentially deposited on the positive wire cannot be explained by a dipole moment of the particles. A possible explanation can be seen in Weyl's (1951) model of ice crystals. Weyl postulated that, due to the crystal structure at the surface, ice crystals are covered by a dipole layer such that the extreme outer layer is negative (Fig. 68b). A schematic drawing of Weyl's model is shown in Fig. 2. The dipole moment p per unit area is directed toward the interior of the particle. The force exerted on a crystal is

$$F_1 = \int_{S_c} (p \cdot \nabla) E \, ds \quad (8)$$

S_c is the crystal surface and ds denotes the surface element. Considering that the dominating contribution to the integral comes from surface elements closest to a wire, we can see that the resulting force attracts particles toward the positive electrode and repels them from the negative wire thus leading to a predominant deposit on the positive electrode (Fig. 68c). From the discussion of equations (1) and (2) it follows that F_1 vanished in a uniform field. Further investigation of p could be of interest to the physics of ice crystal surfaces and related phenomena.

REFERENCES

- Appleman, H., 1953: The cause and forecasting of ice fogs, Bull. Amer. Met. Soc., 34, 397-400.
- Benson, C. S., 1965: Ice fog: Low temperature air pollution defined with Fairbanks, Alaska as type locality. Geophysical Institute Rept., UAG R-173.
- Blanchard, D. C., 1951: A verification of the Bally-Dorsey theory of spicule formation on sleet pellets, Journ. Meteor., 8, 268-269.
- Borovikov, A. M., 1968: Supercooling of water in the atmosphere and the phase of various type of clouds. Proc. Intern'l. Conf. on Cloud Physics, Aug. 1968, Toronto, Canada, 290-294.
- Bowling, S., T. Ohtake and C. S. Benson, 1968: Winter pressure systems and ice fog in Fairbanks, Alaska. J. Appl. Met., 7, 961-968.
- Branton, C. I., 1965: A proposed technique for measuring relative humidity at below freezing temperature, Humidity and Moisture, New York, Reinhold Pub. Corp., 95-100.
- Byers, H. R., 1965: Elements of cloud physics, Chicago, Univ. of Chicago Press. pp. 191.
- Dorsey, N. E., 1948: The freezing of super cooled water, Transactions Ame. Phil. Soc., 38, 247-328.
- Fletcher, N. H., 1966: The physics of rainclouds, Cambridge, Cambridge University Press, pp. 390.
- Fournier d'Albe, E. M., 1949: Some experiments on the condensation of water vapor at temperature below 0°C, Quart. Jour. Roy. Met. Soc., 75, 1-14.
- Gotaas, Y., and C. S. Benson, 1965: The effect of suspended ice crystals on radiative cooling, J. Appl. Met., 4, 446-453.
- Gränicher, H., 1963: Properties and lattice imperfections of ice crystals and the behavior of H₂O-HF solid solution, J. Physik kondensierter Materie, Vol 1, 1-12.
- Gunn, R., 1955: Droplet-electrification processes and coagulation in stable and unstable clouds, J. Meteor., 12, 511-518.

- Hanajima, M., 1944: Supplement of artificial snow-crystal growth, J. Met. Soc. Japan, Ser. II, 22, 121-127.
- Henmi, T., 1969: Some physical phenomena associated with ice fog, Master's thesis at the Univ. of Alaska, pp. 90.
- Hobbs, P. V., 1965: The aggregation of ice particles in clouds and fogs at low temperatures, J. Atmos. Sci., 22, 296-300.
- Houghton, H. G., 1951: On the physics of clouds and precipitation, Compendium of Meteorology, Boston, Amer. Met. Soc., 165-181.
- Huffman, P. J., 1968: Size distribution of ice fog particles, Master's thesis at the Univ. of Alaska, pp. 93.
- Huffman, P. J., and T. Ohtake, 1970: Formation and growth of ice fog particles at Fairbanks, Alaska, submitted to J. Geophys. Res.
- Isono, K., 1969: On the term "Hyoshokaku (ice nucleus)", Tenki, 16, 83-84.
- Jefimenko, O. D., 1966: Electricity and Magnetism, Applets-Century-Crofts, New York, Division of Meredith Publishing Co., 591.
- Junge, C., 1953: Die Rolle der Aerosole und der gasförmigen Beimengungen der Luft im Spurenstoffhaushalt der Troposphäre, Tellus, 5, 1-26.
- Kline, D. B. and G. W. Brier, 1961: Some experiments on the measurement of natural ice nuclei, Monthly Weather Review, 89, 263-272.
- Kobayashi, J., 1960: Investigation on Hygrometry, Papers in Meteorology and Geophys., 11, 213-338.
- Kobayashi, T., 1956: Experimental researches on the snow crystal habit and growth by means of a diffusion cloud chamber (preliminary report), Low Temperature Sci., 15, 1-12.
- Kobayashi, T., 1965: Vapor growth of ice crystal between -40 and -90°C, J. Met. Soc. Japan, Ser. II, 43, 359-367.
- Kocmond, W. C., 1965: Investigation of warm fog properties and fog modification concepts, 2nd Annual Report, CAL Report No. RM-1788-P-19.
- Köhler, H. 1925: Untersuchungen über die Elemente der Nebels und der Wolken, Meddel. Met.--Hydr. Aust. Stockholm, 2, No. 5.

- Kozima, K., T. Ono and K. Yamaji, 1953: The size distribution of fog particles, Studies on Fogs, 303-310, Sapporo, Tanne Publishing Co.
- Kumai, M. 1964: A study of ice fog and ice-fog nuclei at Fairbanks, Alaska, Part I, CRREL Res. Rep. 150, pp. 27.
- Kumai, M. 1951: Electron-Microscope study of snow crystal nuclei J. Met., 8, 151-156.
- Kumai, M. and H. W. O'Brien, 1964: Method of measuring of total water content by absorbing agent, CRREL Technical report (informal).
- Kumai, M. and H. W. O'Brien, 1965: A study of ice fog and ice-fog nuclei at Fairbanks, Alaska, Part II, CRREL Res. Rep. 150, 14 pp.
- Kumai, M. and K. E. Francis, 1962: Nuclei in snow and ice crystals on Greenland ice cap under natural and artificially stimulated conditions, J. Atmos. Sci. 19, 474-481.
- Kuroiwa, D., 1951: Electron microscope study of fog nuclei, J. Met., 8, 157-160.
- Landsberg, H., 1938: Atmospheric condensation nuclei, Ergebn. Kosm. Phys., 3, 155, [or see Fletcher, 1966].
- Langer, G., J. Rosinski and C. P. Edwards, 1967: A continuous ice nuclei counter and its application to tracking in the troposphere, J. Appl. Met., 6, 114-125.
- Mason, B. J., 1957: The physics of clouds, Oxford, The Clarendon Press, 481 pp.
- Munn, R. E., 1966: Descriptive micrometeorology, New York and London, Academic Press, 245 pp.
- Nakaya U., 1954: Snow crystals, Cambridge, Harvard University Press, 510 pp.
- Ogiwara, S. and T. Okita, 1952: Electron microscope study of cloud and fog nuclei, Tellus, 4, 233-240.
- Ohtake, T., 1964: An airborne cloud-droplets sampler, Sci. Rep. Tohoku Univ., Ser. 5, Geophys. 15, 59-65.
- Ohtake, T., 1967: Alaskan ice fog. Phys. of Snow and Ice, Part I, Hokkaido Univ., Sapporo, 105-118.
- Ohtake, T. and P. J. Huffman 1969: Visual Range in Ice Fog, J. Appl. Met. 8, 499-501.

- Ohtake, T. and H. Isaka, 1964: Determination of effectiveness of artificial stimulation snow in Tohoku District, Japan, Sci. Rep. Tohoku Univ., Ser. 5, Geophys., 15, 97-110.
- Okita, T., 1958: Water blue film method for measurement of cloud and fog droplets, J. Met. Soc. Japan, 36, 164-165.
- Oliver, V. J. and M. B. Oliver, 1949: Ice fog in the interior of Alaska, Bull. Amer. Met. Soc., 30, 23-26.
- Radke, L. F. and P. V. Hobbs, 1969: An automatic cloud condensation nuclei counter, J. Appl. Met., 8, 105-109.
- Robinson, E., G. B. Bell, W. C. Thuman, G. A. John and E. J. Wiggins, 1954: An investigation of the ice fog phenomena in the Alaskan area, Final Report, Contract No. AF19(122)-634, Stanford Res. Inst.
- Schaefer, V. J., 1962: The vapor method for making replicas of liquid and solid aerosols, J. Appl. Met., 1, 413-418.
- Scott, W. D. and P. V. Hobbs, 1968: The spectra of changing events due to the collision of natural ice particles with an ice surface, Quart. J. Roy. Met. Soc., 94, 510-522.
- Shimizu, H., 1963: "Long prism" crystals observed in precipitation in Antarctica, J. Met. Soc. Japan Ser. II, 41, 305-307.
- Stine, S. L., 1965: Carbon humidity elements--Manufacture, performance and theory, Humidity and Moisture, New York, Reinhold Pub. Corp., 316-330.
- Stoll, A. M. and J. D. Hardy, 1955: Thermal radiation measurements in summer and winter Alaskan climates, Trans. Ame. Geophys. Union, 36, 213-226.
- Tanaka, T. and K. Isono, 1966: A technique for identification of substances of ice nuclei, (in Japanese). Preprint of Japan. Met. Soc. Meeting May, 1966.
- Thuman, W. C. and E. Robinson, 1954a: Studies of Alaskan ice-fog particles, J. Met. 11, 151-156.
- Thuman, W. C. and E. Robinson, 1954b: A technique for the determination of water in air at temperatures below freezing, J. Met., 11, 214-219.
- Twomey, S., 1956: The electrification of individual cloud droplets, Tellus, 8, 445-452.

- Tyndall, A. M., 1922: Proceedings of Physical Society, (London), 34, 72.
- Warner, J., 1957: An instrument for the measurement of freezing nucleus concentration, Bull. Obs. Puy de Dome, No. 2, 33-46.
- Weickmann, H., 1948: Die Eisphase in der Atmosphäre, Ber. deutsch. Wetterd. U. S. Zone, No. 6, 54 pp.
- Weickman, H. K. and H. J. aufm Kampe, 1953: Physical properties of cumulus clouds, J. Meteor., 10, 204-211.
- Weller, G., 1969: Ice fog studies in Alaska, Geophysical Institute Report, University of Alaska, UAG R-207, 49 pp.
- Wexler, H., 1936: Cooling in the lower atmosphere and the structure of polar continental air, Mon. Weather Rev., 64, 122-136.
- Weyle, W. L., 1951: Surface structure of water and some of its physical and chemical manifestations, J. Coll. Sci., 6, 389-405.
- Yamamoto, G. and T. Ohtake, 1953: Electron microscope study of cloud and fog nuclei, Sci. Rep. Tohoku Univ. Ser. 5, Geophys. 5, 141-159.
- Yamamoto, G. and T. Ohtake, 1955: Electron microscope study of cloud and fog nuclei II, Sci. Rep. Tohoku Univ. Ser. 5, Geophys. 7, 10-16.

APPENDIX

THEORETICAL STUDY OF ICE-FOG SIZE DISTRIBUTION

by

P. J. Huffman

AFCRL, Bedford, Massachusetts

and

T. Ohtake

Geophysical Institute, University of Alaska, College, Alaska

ABSTRACT

A mechanism is proposed for the formation of ice fog particles in the city and environs of Fairbanks, Alaska. Equations are developed for calculating the size distribution resulting from growth by sublimation of water vapor. These equations are solved numerically, with the use of a computer, for three major types of ice fog sources: A) automobile exhaust; B) exhaust from heating plants and C) open water. For source type A, the computed size is much smaller than that observed; but for source types B and C, the computed size distributions are found to be in good agreement with experimentally obtained values.

The discrepancy between the computed and observed sizes for source type A is possibly due to the large degree of supercooling exhibited by small water droplets. Only very few of the small water droplets, initially formed by condensation, freeze. These frozen particles may then grow to the observed size at the expense of the more numerous evaporating liquid droplets. On the other hand, the larger droplets produced by source types B and C probably nearly all freeze very shortly after their formation, leaving no appreciable supply of liquid droplets to provide for their further growth.

1. INTRODUCTION

In an area as sparsely populated as interior Alaska, air pollution at first sight would not appear to be a problem. During periods of clear sky, the long winter nights of the arctic permit extreme radiative cooling of the earth's surface. In protected valley sites, this radiative cooling is often responsible for strong temperature inversions of extended duration (Benson, 1965). One such location is the city and environs of Fairbanks.

At temperatures below -30°C , a large concentration of microscopic ice fog particles* is normally present in the inversion layer. The most prominent feature of the ice fog is a severe restriction in visibility through the lowest part of the atmosphere. At present, ice fog is most pronounced in and around Fairbanks city, but it is a major problem which must be considered in the development of interior Alaska or the arctic regions in general.

The first detailed study of ice fog particles was made by Thuman and Robinson (1954). They found that the mean statistical diameter decreased with decreasing temperature. At -40°C , the mean diameter of the irregular shaped particles, referred to as droxtals, was 13μ . Kumai (1964) found

*The term "ice fog particle" is used throughout to describe the elemental solid objects, regardless of shape, that compose the ice fog phenomenon. The purpose of this nomenclature is to distinguish ice fog particles from "ice crystals", the latter term being reserved to refer to the products of sublimation and freezing occurring in the higher atmosphere. Ice fog particles may be symmetrical, but are more often irregular in shape. The term "ice fog particle" does not imply a lack of crystal structure but refers rather to the mechanism of production.

that most ice-fog particles were between 2μ and 15μ in size with a sharp peak in the distribution near 7μ . More recent measurements (Huffman, 1968) show that the size distribution varies with location and often has more than one mode. Electron microscope analysis (Ohtake, 1967) reveals that the nuclei of most ice-fog particles are located well away from the geometric center and many ice-fog particles have no apparent nucleus at all. Recent measurements by Henmi (1969) using the method of Ohtake (1968), show that during ice fog conditions the ambient atmospheric water vapor content lies between saturation values with respect to water and ice.

Considerable theoretical attention has been given to the nucleation and growth of ice crystals in clouds (Mason, 1957; Fletcher, 1962; Byers, 1965). This paper deals with the theoretical treatment of the nucleation and subsequent growth of ice-fog particles. In the upper atmosphere, water droplets and ice crystals form when the air cools gradually. Throughout the growth period, the air mass is not far removed from the saturation level. On the other hand, it will be shown that ice-fog particles are produced by the injection of saturated warm water vapor directly into a cold environment. The condensation and subsequent freezing takes place at a higher degree of supersaturation and at much greater cooling rates than in the former case. As the ice-fog particles diffuse away from their source of production, any remaining water droplets soon evaporate, providing for the further growth of existing ice-fog particles by sublimation and maintaining the environment near ice saturation.

2. THEORETICAL CONSIDERATIONS

Consider an exhaust gas containing water vapor at initial temperature T_1 injected into an environment at temperature T_0 , $T_1 \gg T_0$. The saturation ratio first increases as the gas begins to cool and then decreases as condensation proceeds. At any time, the saturation ratio S is given by

$$S = \frac{e}{e_s}, \quad (1)$$

where e is the water vapor partial pressure and e_s is the saturation vapor pressure at the same temperature. The time rate of change of the saturation ratio is thus

$$\frac{dS}{dt} = \frac{1}{e_s} \frac{de}{dt} - \frac{S}{e_s} \frac{de_s}{dt}. \quad (2)$$

Using the ideal gas law for water vapor, the first term of (2) can be rewritten as

$$\frac{1}{e_s} \frac{de}{dt} = \frac{RT}{e_s M} \frac{d\rho_v}{dt} + \frac{S}{T} \frac{dT}{dt}, \quad (3)$$

where R is the gas constant, T is the absolute temperature, M is the molecular weight of water and ρ_v is the water vapor density. The time rate of change of water vapor density is

$$\frac{d\rho_v}{dt} = -\sum_j \frac{dm_j}{dt}, \quad (4)$$

where m is the particle mass, the summation being over all particles per unit volume. Substituting (4), (3) can be expressed as

$$\frac{1}{e_s} \frac{de}{dt} = \frac{S}{T} \frac{dT}{dt} - \frac{RT}{e_s M} \sum_j \frac{dm_j}{dt} . \quad (5)$$

The rate of change of saturation vapor pressure with time can be expressed as

$$\frac{de_s}{dt} = \frac{de_s}{dT} \frac{dT}{dt} = \frac{LMe_s}{RT^2} \frac{dT}{dt} \quad (6)$$

where the Clausius - Clapeyron equation for an ideal gas has been used.

In (6), L is the latent heat of the phase change.

Inserting (5) and (6) into (2) gives

$$\frac{dS}{dt} = \frac{S}{T} \left(1 - \frac{LM}{RT}\right) \frac{dT}{dt} - \frac{RT}{e_s M} \sum_j \frac{dm_j}{dt} \quad (7)$$

For the temperatures with which we are concerned ($233K \leq T \leq 333K$), LM/RT is always considerably greater than unity and (7) may be simplified to

$$\frac{dS}{dt} = - \frac{LMS}{RT^2} \frac{dT}{dt} - \frac{RT}{e_s M} \sum_j \frac{dm_j}{dt} \quad (8)$$

The appropriate values for e_s and L in (8) are the average values for the system of particles. Condensation first occurs to form water droplets which then freeze and continue to grow by sublimation. In general, the system consists of both water droplets and ice particles. It is assumed that the probability of freezing P for a droplet of radius r, supercooled to a temperature T after t seconds is given by* (Bigg, 1953)

* The validity of (9) for ice fog is doubtful since the referenced literature deals with much lower cooling rates than those encountered here. The absolute temperature, T, is that measured in the environment surrounding the particles. This is essentially the same as the particle temperature only for sufficiently small cooling rates. However, since the values of e_s and L for ice do not differ greatly from the corresponding values for water, use of (9) for computing these parameters does not introduce appreciable error.

$$\ln (1-P) = -Ar^3t (\exp T_s - 1), \quad (9)$$

$$T_s = \begin{cases} 0 & ; T > T_m \\ T_m - T & ; T < T_m \end{cases}$$

where $A = 6.5 \times 10^{-4} \text{ cm}^{-3} \text{ sec}^{-1}$ and $T_m = 273^\circ\text{K}$ is the melting temperature.

Thus e_s and L have the form

$$e_s = e_w + \{1 - \exp [-Ar^3t (e^{T_s} - 1)]\} (e_i - e_w) \quad (10a)$$

$$L = L_v + \{1 - \exp [-Ar^3t (e^{T_s} - 1)]\} (L_s - L_v) \quad (10b)$$

where e_i and e_w are respectively the saturation vapor pressures over ice and water; and L_v and L_s are respectively the heats of vaporization and sublimation.

Three major types of ice fog sources can be classified: A) automobile exhaust; B) exhaust from heating plants (commercial and residential) and C) open water. Benson (1965) has shown that the rate of cooling of automobile exhaust along the centerline of the exhaust plume is given by the empirical relationship.

$$\frac{dT}{dx} = -a (T - T_o)^2; T > T_o \quad (11)$$

where x is the distance from the source and a is a constant. Air temperature measurements (Ohtake, 1968) indicate that the temperature gradient above open water can also be expressed by (11); the temperature drops from a value near

OC at the water surface to the ambient value at a height of about 2 meters. Thus, the theoretical aspects of ice fog formation from exhaust sources and from sources of open water can be traced in the same mathematical manner, subject of course to different boundary conditions.

Integration of (11) gives the temperature as a function of distance from the source by

$$T = \frac{T_i - T_o}{(T_i - T_o) ax + 1} + T_o \quad (12)$$

Near the source, a reasonable expression for the velocity of the exhaust gas as a function of distance is

$$v = v_o e^{-x/b} \quad (13)$$

where v_o is the initial velocity and b is a constant, the value of which depends on the geometry of the source. Integrating (13) and substituting into (12) gives the temperature of an elemental volume of exhaust gas as a function of time by

$$T = \frac{T_i - T_o}{ab(T_i - T_o) \ln(ct + 1) + 1} + T_o \quad (14)$$

where $c = v_o/b$. Figure 1 shows the temperature as a function of time given by (14) for typical values of a , b , T_i and T_o .

Neglecting curvature and chemical effects, the diffusion growth rate of water droplets and ice crystals is usually given by the classical expression

$$\frac{dm}{dt} = \frac{4\pi C}{u+v} (S-1) \quad (15)$$

$$u = \frac{L^2 M}{KRT^2} \quad , \quad v = \frac{RT}{e_s^{DM}}$$

where C is the capacitance of the particle in air, K is the thermal conductivity of air and D is the diffusivity of water vapor in air. Equation (15) is not strictly correct when the growth rate is appreciable. If it is assumed, for mathematical simplicity, that the particle is approximately spherical throughout the growth period, the growth rate can be expressed more correctly by (Rooth, 1957)

$$\frac{dm}{dt} = \frac{4\pi}{u+v} (S-1) \frac{r^2}{f+r}, \quad (16)$$

where f is a correction term that takes into account the kinetics of vapor molecules and the accommodation coefficient of the particle surface. The exact value of f as a function of temperature is not known for water or ice because information regarding the variation of the accommodation coefficient is incomplete. We chose the value $f = 5 \mu$ based on the measured value of the condensation coefficient at 10C and 100 mb (Alty and Mackay, 1935). Using (16), the summation in (8) can be expressed as

$$\sum_j \frac{dm_j}{dt} \rightarrow \frac{4\pi}{u+v} (S-1) \int_0^t I(t_n) \frac{r^2(t_n, t)}{f+r(t_n, t)} dt_n \quad (17)$$

where $I(t_n)$ is the rate of formation of embryo droplets per unit volume at time t_n . Thus $r(t_n, t)$ is the radius at time t of particles formed at time t_n .

The cooling rates encountered (Fig. 1) are sufficiently great to produce the degree of supersaturation required for homogeneous nucleation. Electron microscopy also reveals that ice-fog particles are possibly nucleated homogeneously since some of the particles did not

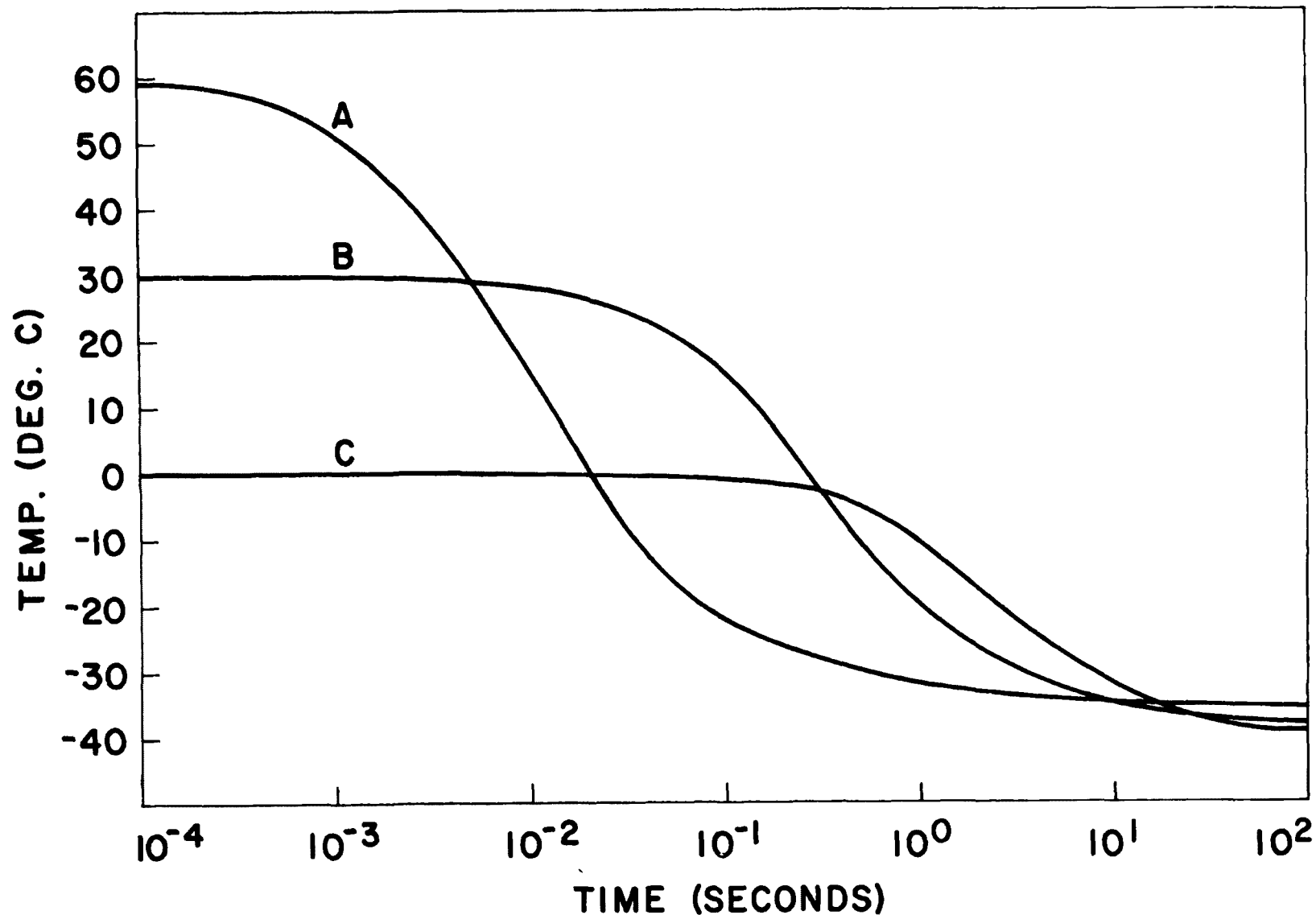


Fig. 1. Typical examples of temperature of exhaust gases computed from equation (14). Curve A: automobile exhaust, $a = 5 \times 10^{-4} \text{ cm}^{-1} \text{ deg}^{-1}$, $b = 66.7 \text{ cm}^{-1}$, $v_o = 2000 \text{ cm sec}^{-1}$. Curve B: exhaust from heating plant, $a = 2 \times 10^{-4} \text{ cm}^{-1} \text{ deg}^{-1}$, $b = 667 \text{ cm}^{-1}$, $v_o = 200 \text{ cm sec}^{-1}$. Curve C: above open water, $a = 5 \times 10^{-4} \text{ cm}^{-1} \text{ deg}^{-1}$, $b = 6670 \text{ cm}^{-1}$, $v_o = 20 \text{ cm sec}^{-1}$.

contain larger nuclei in their replicas (Ohtake, 1967). In the use of the replica method, it is normally difficult to produce very clean supporting films. Even though we have tried hard to make cleaner films for this purpose, so far most ice fog particle replicas contained very small nuclei or contaminations. However, many ice fog particles taken at Chena Hot Springs, where there is a much smaller amount of air pollution, did not have any nuclei or contamination in the replicas. Also, it is possible that the aerosol could have been captured by an existing drop-let previously nucleated homogeneously. In this paper it is assumed that ice fog particles are nucleated homogeneously and the presence of any foreign matter has no effect on the nucleation process. The homogeneous rate of embryo formation is given by (Farley, 1952).

$$I = \frac{e_s^2 S^2}{R^2 T^2} \left(\frac{2\eta^3 M \sigma}{\pi} \right)^{1/2} \exp \left\{ - \frac{16\pi\eta M^2 \sigma^3}{3R^3 T^3 \ln S} \right\}, \quad (18)$$

where σ is the surface tension of water and η is Avagrado's number.

The set of Eqs. (8), (14), (17) and (18), with e_s and L determined by Eqs. (10a) and (10b), can be solved numerically to give the resulting size distribution as a function of the source parameters and the ambient temperature.

3. COMPARISON WITH EXPERIMENT

A computer was programmed to calculate the saturation ratio as a function of time. The results of this calculation are shown in Fig. 2 for the three cooling rates of Fig. 1. From the time dependence of S , the size distribution was evaluated by calculating $I(t_n)$ versus $r(t_n, t)$

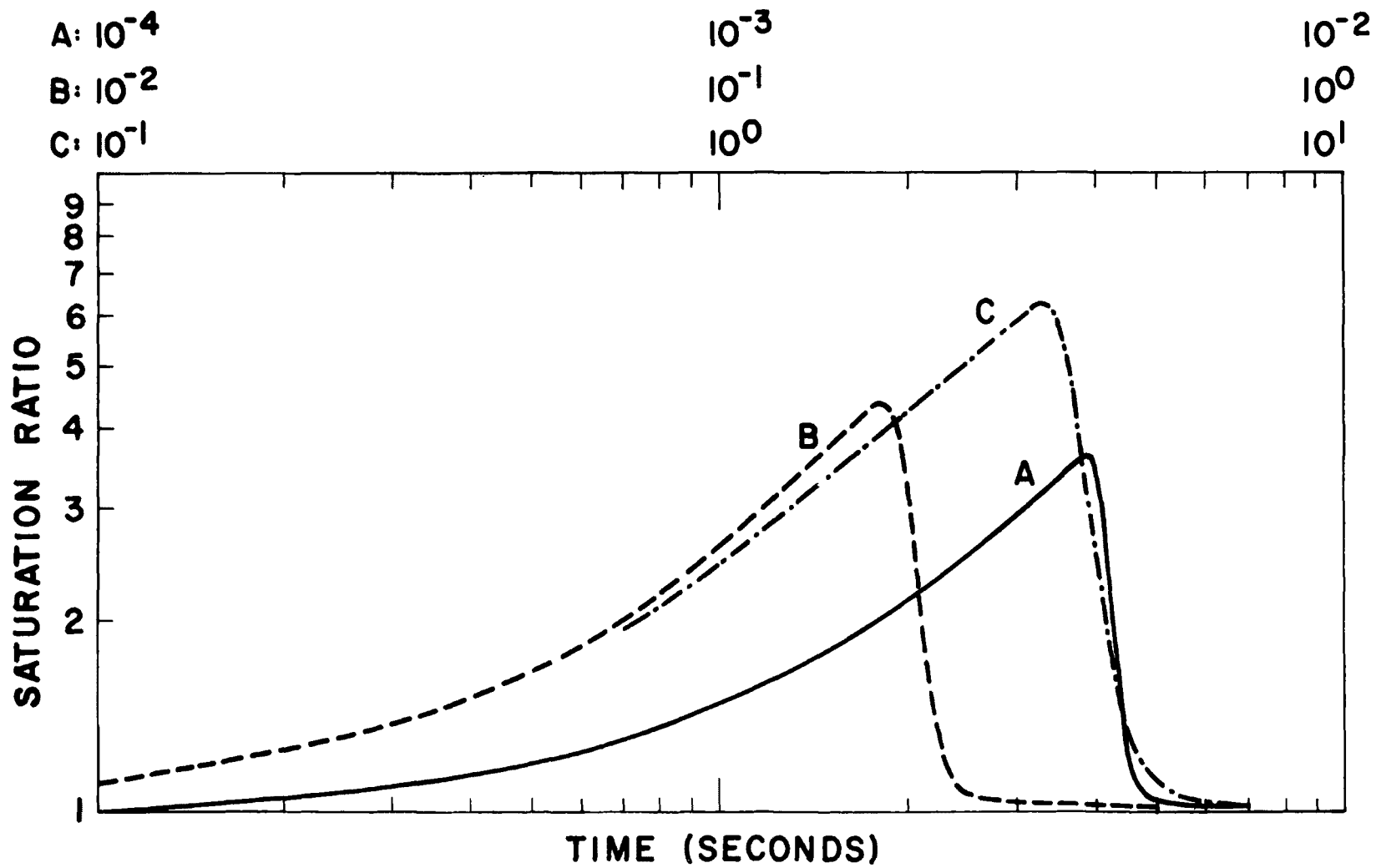


Fig. 2. Saturation ratio versus time for the cooling rates of Fig. 1.

in the limit as t becomes large without bound. Figure 3 shows the size distribution obtained in this manner.

It would be impossible for ice-fog particles represented by curve A of Fig. 3 to exist very long after the saturation ratio begins to diminish; such small particles would evaporate almost immediately after diffusing from the source. It must be remembered, however, that only growth by diffusion has been considered. The 0.05μ peak could be shifted toward a larger diameter by coalescence. Calculations show that the maximum rate of droplet production is of the order of $10^{11} \text{ cm}^{-3} \text{ sec}^{-1}$. Even with such a high concentration of embryo droplets and assuming a coalescence efficiency of one hundred percent (a factor difficult to justify), the collision frequency between droplets due to Brownian motion would not be sufficient for appreciable growth by coalescence during the short time period available.

Because of the small size of the particles represented by curve A of Fig. 3, probably only a few of them freeze; these may then grow to a diameter of several micrometers at the expense of the more numerous, evaporating liquid droplets. This important effect has not been taken into account by the computational procedure which only permits calculation of the average growth rate for the system consisting of both liquid droplets and frozen particles. The frozen particles grow faster than the liquid droplets because the saturation vapor pressure is lower for ice than for water. In fact, there comes a time in the growth period when the saturation ratio falls below unity for

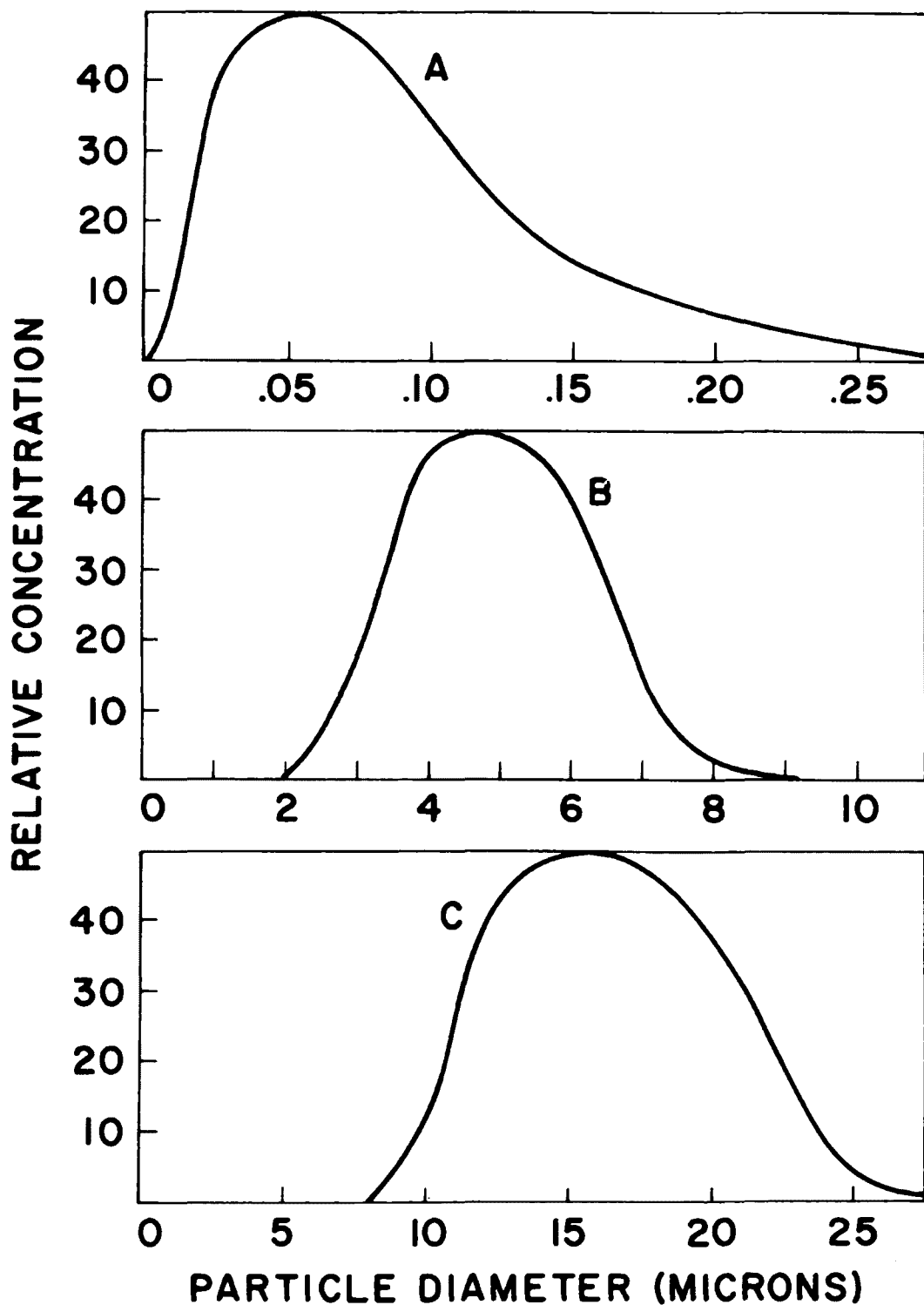


Fig. 3. Computed size distributions for ice fog particles produced by the cooling rates shown in Fig. 1.

the small liquid droplets and they evaporate, liberating additional water vapor for further growth of the frozen particles. If the system consists predominantly of liquid droplets, the few existing ice fog particles can grow appreciably by this process. On the other hand, the larger particles represented by curves B and C of Fig. 3 probably nearly all freeze very soon after their formation and thus, in contrast to the previous case, there is not a large amount of excess water vapor available from liquid droplets to provide for rapid growth by sublimation.

Figure 4^{*1} presents typical experimental ice-fog particle size distributions obtained by impaction at several locations (see Fig. 5)^{*2} in the vicinity of Fairbanks, Alaska at temperatures between -32C and -40C (Huffman, 1968). Location 1 (MUS) is in the downtown area. The Chena River adjacent to location 2 (IAP) is always free of an ice cover due to the operation of an electric power plant slightly upstream. Locations 3 (AIRPORT) and 4 (EIELSON AFB) are near airport facilities. The shape of the distribution at each location is usually (but not always) as shown in Fig. 4,^{*1} although the position of the peaks may be shifted by one or two microns.

The experimental results compare favorably with the computed size distributions if we assume curve A of Fig. 3 to be shifted several microns as previously discussed. The usual occurrence of a

*
1. Fig. 4 is omitted from this appendix, same as Fig. 3 of the text.
2. Fig. 5 is omitted from this appendix, same as Fig. 2 of the text.

trimodal distribution at location 1 (MUS) in the downtown area with peaks near 3.5, 6 and 12 μ diameter is believed due to the prevalence of the three types of ice-fog sources: automobile exhaust, exhaust from heating plants, and open water respectively. At location 2 (IAP) the distribution is dominated by a single broad peak near 10 μ diameter. We expect this peak to be that of ice-fog particles produced by open water of the Chena River. The occurrence of a single narrow peak of 3.5 μ diameter at locations 3 and 4 is attributed to automobile and aircraft exhaust.

4. CONCLUSION

The size of ice-fog particles can be derived on the basis of diffusion growth with the assumption of homogeneous nucleation if the source temperature is not too high (i.e. open water and exhaust from heating plants for which $T_i \leq 30C$). Because of the nature of the interdependence between the instantaneous size distribution, saturation ratio and growth rate, the method of computation must be numerical rather than analytical.

For higher temperature exhaust sources (i.e. automobile exhaust for which $T_i \geq 60C$), the computational method results in ice-fog particle sizes about 60 times smaller than those observed. Because of the small size of the droplets initially produced by such sources, only very few of them probably freeze and grow to sizes of several micrometers by sublimation at the expense of the more numerous evaporating water droplets. This important effect, which is not taken into consideration by the computational procedure, may explain the reason for the

discrepancy between the derived and observed size distributions for higher temperature exhaust sources. Such sublimation growth for lower temperature sources is probably negligible since the larger sized particles produced by such sources should nearly all freeze very shortly after formation, leaving no appreciable concentration of water droplets from which to grow further.

The most likely cause of the discrepancy between the observed and computed size distributions other than that discussed above is an incorrect assumption for the source velocity, Eq. (13) or somewhat incorrect choices for one or more of the values for the parameters a , b , v_0 , T_i . Since the values for these parameters vary considerably among sources of the same type, and since at present the experimental data available is limited, the values chosen may not be typical.

Perhaps further comment on the nucleation of ice fog particles is in order. It was assumed that nucleation occurs homogeneously from the vapor to the liquid phase. Certainly much particulate matter is ejected by exhaust sources along with the water vapor; and much of this particulate matter is capable of serving as condensation nuclei. A thorough study of the nucleation process must include detailed information of the active heterogeneous nuclei concentration near the source as a function of temperature and saturation ratio. However, if no heterogeneous nuclei were present, the cooling rates encountered are sufficient to cause the degree of supersaturation required for homogeneous nucleation and therefore, it is water vapor

that is of primary importance in the formation of ice fog. In fact, the cooling rates are so rapid that even the presence of large concentrations of heterogeneous nuclei should not be expected to quench the rapidly rising supersaturation before the critical value for homogeneous nucleation is reached. In general then, both homogeneous and heterogeneous nucleation should be effective.

ACKNOWLEDGEMENTS

The programming required for the numerical computations was performed by Mr. T. Spuria of Analysis and Computer Systems, Inc., Burlington, Massachusetts. This research was supported in part by National Center for Air Pollution Control, Department of Health, Education and Welfare, Public Health Service, under grant AP-00449.

REFERENCES

- Alty, T. and C. A. Mackay, 1935: The accommodation coefficient and the evaporation coefficient of water. Proc. Roy. Soc., A, 199, 104-116.
- Benson, C. S., 1965: Ice fog: low temperature air pollution. Geophysical Institute Report UAG R-173, 43, (DDC No. 631553).
- Bigg, E. K., 1953: The supercooling of water. Proc. Phys. Soc., B, 66, 688-694.
- Byers, H. R., 1965: Elements of Cloud Physics. Chicago, University of Chicago Press, 191 pp.
- Farley, F. J. M., 1952: The theory of the condensation of super-saturated ion-free vapor. Proc. Roy. Soc., A, 212, 530-542.
- Fletcher, N. H., 1962: The Physics of Rain Clouds. Cambridge, Cambridge University Press, 386 pp.
- Henmi, T., 1969: Some physical phenomena associated with ice fog. Unpublished M. S. Thesis presented to the Faculty of the University of Alaska, 90 pp.
- Huffman, P. J., 1968: Size distribution of ice fog particles. Unpublished M. S. Thesis presented to the Faculty of the University of Alaska, 93.
- Kumai, M., 1964: A study of ice fog and ice fog nuclei at Fairbanks, Alaska. CRREL Res. Rept. 150, part I (DDC AD451667).
- Mason, B. J., 1957: The Physics of Clouds. Oxford, Clarendon Press, 481.
- Ohtake, T., 1967: Alaskan ice fog. Phys. of Snow and Ice, Part 1, Sapporo, Hokkaido University, 105-118.
- Ohtake, T., 1968: Freezing of water droplets and ice fog phenomena. Proc. Int. Conf. Cloud Phys., Toronto, 285-289.
- Rooth, C., 1957: On a special aspect of the condensation process and its importance in the treatment of cloud particle growth. Tellus, 9, 372-377.
- Thuman, W. C. and E. Robinson, 1954: Studies of Alaskan ice-fog particles. J. Meteor., 11, 151-156.

UNCLASSIFIED

Security Classification

DOCUMENT CONTROL DATA - R & D

(Security classification of title, body of abstract and indexing annotation must be entered when the overall report is classified)

1. ORIGINATING ACTIVITY (Corporate author)

Geophysical Institute
University of Alaska, College, Alaska 99701

2a. REPORT SECURITY CLASSIFICATION

UNCLASSIFIED

2b. GROUP

3. REPORT TITLE

Studies on Ice Fog

4. DESCRIPTIVE NOTES (Type of report and inclusive dates)

Final Report - June 1970

5. AUTHOR(S) (First name, middle initial, last name)

Takeshi Ohtake

6. REPORT DATE

June 1970

7a. TOTAL NO. OF PAGES

177

7b. NO. OF REFS

67

8a. CONTRACT OR GRANT NO.

AP-00449

9a. ORIGINATOR'S REPORT NUMBER(S)

UAG R-211

9b. OTHER REPORT NO(S) (Any other numbers that may be assigned this report)

10. DISTRIBUTION STATEMENT

Distribution Unlimited

11. SUPPLEMENTARY NOTES

-

12. SPONSORING MILITARY ACTIVITY

National Center for Air Pollution Control
Department of Health, Education & Welfare

13. ABSTRACT

In order to clarify the mechanism of ice-fog formation, various atmospheric factors in ice fogs such as size and concentration of ice fog crystals, condensation nuclei and ice nuclei, amount of water vapor, temperature profile near the sources of ice fog, etc. were measured.

Nuclei of the ice-fog crystals were studied by use of an electron microscope and electron-diffraction. The examination showed that most nuclei of ice fog crystals were combustion by-products and many individual crystals collected near open water did not have a nucleus, especially at temperatures below -40C. Dust particles or particles from air pollution are not essential for formation of ice fog; they merely stimulate freezing of water droplets at higher temperatures than the spontaneous freezing temperature. The essential factor is to first form many water droplets in the atmosphere through condensation of water vapor.

Based on these measurements and calculations of time required for water droplets to freeze, a physical mechanism of ice fog formation is proposed as follows: 1) Water vapor coming from open water which is exposed to a low temperature atmosphere, plus water vapor from various exhausts of combustion processes is released into the almost ice-saturated atmosphere and condenses into water droplets, 2) The droplets freeze very shortly after their formation and before entirely evaporating, 3) Such ice particles do not evaporate or grow much and stay in the atmosphere with insignificant fall out, and 4) These processes operate more efficiently in colder environments, which make ice fog more serious at lower temperatures.

DD FORM 1473
1 NOV 65

UNCLASSIFIED

Security Classification

14.

KEY WORDS

LINK A

LINK B

LINK C

ROLE

WT

ROLE

WT

ROLE

WT

Condensation
Ice Nuclei
Ice Fog Crystals
Precipitation
Formation
Radiation Cooling